Geochemical and Isotopic Tracing of Paleozoic Groundwater Flow in Breached Anticlines: A Case Study at Lower Kane Cave, Bighorn Basin, Wyoming

by

Melissa Edwards Pearson, B.A.

Thesis

Presented to the Faculty of the Graduate School
of The University of Texas at Austin
in Partial Fulfillment
of the Requirements
for the Degree of

Master of Science in Geological Sciences

The University of Texas at Austin

August, 2004

Geochemical and Isotopic Tracing of Paleozoic Groundwater Flow

in Breached Anticlines:

A Case Study at Lower Kane Cave, Bighorn Basin, Wyoming

APPROVED BY

SUPERVISING COMMITTEE:

(supervisor) Philip C. Bennett

Libby A. Stern

John M. Sharp, Jr.

For John.

ACKNOWLEDGEMENTS

This research project has taught me an incredible amount about hydrogeology, the crazy world of caves, and especially about myself. Very little research is carried out in isolation, so I want to extend my sincere gratitude and appreciation to all the folks in every arena who have helped me through this project and through my graduate school experience.

I want to thank my advisor, Phil Bennett, for introducing me to the world of Lower Kane Cave, for enabling this project, and for teaching me to ask good questions. I also want to thank the rest of the Lower Kane Cave Crew, especially Annette Engel, Libby Stern, Katrina Mabin and John Deans, for support in all aspects of this endeavor - from collecting samples to interpreting data to schlepping gear across the tracks. This research could not have happened without water samples, and I would like to thank the folks who provided me access to the sampling sites necessary for this project: the staff of the BLM, Bighorn National Forest, and Cowley Municpal water supply, and the well owners who allowed me to traipse onto their land, and provided invaluable information.

I would also like to extend my appreciation to all the members of the UT Geology Community who assisted me in analyzing my samples and interpreting the data, in particular Jack Sharp, Jay Banner, John Lansdown, Todd Housh and Larry Mack. And an especial shout out to my fellow Hydro students – Suzanne Pierce, Tania (Wallace) Campbell, Lance Christian and Terrence Garner for immeasureable support and assistance.

Finally I want to send my boundless thanks to my family for their unending support, and especially to my husband, who makes it all worthwhile.

August 2004

Geochemical and Isotopic Tracing of Paleozoic Groundwater Flow

in Breached Anticlines:

A Case Study at Lower Kane Cave, Bighorn Basin, Wyoming

by

Melissa Edwards Pearson, M.S.Geo.Sci.

The University of Texas at Austin, 2004

SUPERVISOR: Philip C. Bennett

Lower Kane Cave is forming in the upper Mississippian Madison Limestone by sulfuric acid speleogenesis. The cave is located along the axial trace of the Little Sheep Mountain anticline where the Paleozoic units have been exposed in a canyon cut by the Bighorn River. The Madison Limestone comprises the upper section of the Madison aquifer, which serves as an important regional aquifer for water supply and petroleum production in much of Wyoming, Montana and the Dakotas. Compared to other Madison springs and wells in the region, the cave springs are characterized by a higher concentration of TDS, SO_4 and H_2S, differences which likely contribute to the localization of cave formation. This study used geochemical and strontium isotope data to determine signatures for the Madison aquifer and other Paleozoic aquifers of the Bighorn Basin to constrain the origin of groundwater to Lower Kane Cave.

Mississippian Madison aquifer waters are characterized by lower [Sr] and higher $^{87}Sr/^{86}Sr$ (between 0.70891 – 0.70925), than groundwater in the overlying Pennsylvanian Amsden and Tensleep and Permian Phosphoria aquifers, which have $^{87}Sr/^{86}Sr$ values between 0.70789 – 0.70856. These values are slightly greater than established marine values of $^{87}Sr/^{86}Sr$ for the respective depositional

periods. Coupled with the increased concentrations of TDS, SO_4 and H_2S, the distinctly radiogenic $^{87}Sr/^{86}Sr$ ratios of 0.71001 to 0.71012 measured at the cave springs suggest that the springs of Lower Kane Cave are the result of mixing between Madison waters and a thermal, saline, radiogenic endmember. Data from the Thermopolis Hot Springs in the southern Bighorn Basin support the existence of such a water within the lower Paleozoic section in the Bighorn Basin of Wyoming, suggesting that similar flow systems operate at the Thermopolis and Little Sheep Mountain anticlines, and potentially at Sheep Mountain anticline as well. These results further demonstrate the importance of structural controls on groundwater flow in the Bighorn Basin, and have implications for our understanding of cave localization and fracture controlled flow at anticlines within the Bighorn Basin, as well as at similar zones of foreland compression in other areas.

TABLE OF CONTENTS

TABLE OF CONTENTS (continued)

FIGURES

TABLES

1. INTRODUCTION

Located in the northeast corner of the Bighorn Basin, Lower Kane Cave is forming in the upper portion of the Mississippian Madison Limestone, where the Bighorn River cuts a canyon through Little Sheep Mountain. The Mississippian Madison Limestone is the upper portion of the Madison aquifer, which also consists of the saturated portions of the Ordovician Bighorn Dolomite and the Devonian Jefferson Formation. Generally confined except in exposed outcrop regions (Cooley, 1986; Doremus, 1986; Libra et al. 1981), the Madison aquifer is an important regional aquifer for water and petroleum production throughout large portions of Montana, Wyoming, South Dakota and North Dakota. While groundwater in the Madison aquifer typically evolves towards more saline waters, often with significant sulfide content (Plummer et al., 1990), this trend is generally observed at greater distances from the recharge zones. In the Bighorn Basin such waters are only observed in the central portion of the basin (Crawford, 1964; Lowry and Lines, 1972; Libra et al., 1981; Doremus, 1986), and the thermal, sulfidic waters that discharge to the springs in Lower Kane Cave are unusual for the Madison aquifer along the eastern margins of basin.

Interest in the source of water to the springs of Lower Kane Cave derives from the role of these waters in the cave's unusual method of formation. While most caves are thought to form from the phreatic infiltration of CO_2 into the groundwater and the subsequent dissolution of limestone by carbonic acid, a subset of caves form by the action of acids brought in by deep-seated fluids. In particular, certain caves form via a "replacement-dissolution" process, where hydrogen sulfide (H_2S) oxidizes to sulfuric acid that first replaces the limestone with gypsum before dissolving out the cave (Egemeier, 1973; 1981). A relative ease of accessibility for caves of this type makes Lower Kane Cave an ideal location for the current on-site research focusing on the role in speleogenesis of

the extensive sulfur-utilizing bacteria inhabiting the cave streams (Engel et al., 2003).

The source of the H_2S containing groundwater powering the cave dissolution and ecosystem remains unknown, however. This study utilizes geochemical and strontium isotope data for Paleozoic aquifer waters of the Bighorn Basin to investigate the origins of groundwater discharging to springs in Lower Kane Cave. Lower Kane Cave serves as a representative site for understanding groundwater flow to the breached anticlines of the Bighorn Basin, and the structural controls on the localization of cave formation. The results of this study may also apply to similar structural features in other areas of foreland compression.

The springs of Lower Kane Cave are characterized by their slightly thermal character (~21°C) and increased total dissolved solid (TDS) and H_2S content compared to the fresher, oxygenated Madison aquifer waters of Salamander spring in Little Sheep Mountain and assorted wells in the area. This suggests that water from an aquifer other than the Madison may provide the H_2S to the cave streams. Water from the overlying Permian Phosphoria formation contains high sulfide concentrations (Crawford, 1940; Lawson and Smith, 1966), and Doremus (1986) proposed that inter-formational mixing between waters of the Phosphoria and Madison aquifers is responsible for the observed chemistry of the Lower Kane Cave springs. Alternatively, hydrocarbon reservoirs are located in the Paleozoic section from the Ordovician through to the Permian, and thus bacterial reduction of sulfate (SO_4) to H_sS coupled to hydrocarbon oxidation may occur within the Madison aquifer.

Previous geochemical investigations of Paleozoic groundwater in the Bighorn Basin are inconclusive in identifying the source of water to Lower Kane Cave. The addition of isotopic data, particularly strontium (Sr) and oxygen (O),

in this study enables an improved characterization of the Paleozoic aquifers, and allows for a more thorough analysis of potential evolutionary pathways for Paleozoic groundwater. This project advances our understanding of the source of groundwater to Lower Kane Cave, and, by extension, sheds light on the flow of groundwater within the fractured zone of a breached anticline and the control of cave localization at these sites. In particular, this study addresses the following questions:

1) What are the geochemical and Sr isotope characteristics of the Paleozoic aquifers, in particular the Madison aquifer?
2) Are the four spring / cave systems in Little Sheep Mountain related, either to one another or to the Paleozoic groundwater systems of the Bighorn Basin?
3) Is the geochemical composition at Lower Kane Cave the result of groundwater evolution within the Madison aquifer, or does it result from inter-formational mixing?
4) Is the origin of Lower Kane Cave spring water a mixture of Phosphoria and Madison water, as proposed by Doremus (1986)?
5) What is the source of dissolved H_2S at Lower Kane Cave?
6) Are similar groundwater systems operating at Sheep Mountain and Thermopolis , the other breached anticlines of the Bighorn Basin?

2. HYDROGEOLOGIC SETTING

Located in the axis of the Little Sheep Mountain anticline, in the northeast corner of the Bighorn Basin, Lower Kane Cave lies southeast of the town of Lovell and just upstream of the Bighorn Canyon National Recreation Area (Figure 2.1). The Bighorn Basin is a large, northwest-trending intermontane basin situated in the north central portion of Wyoming and bordered by the Absaroka Mountains to the west, the Owl Creek Mountains to the south, the Bighorn Mountains to the east and the Pryor Mountains to the north. While the basin is semi-arid, with mean precipitation of less than 254 mm in it's central parts, rainfall is much greater in the surrounding mountains - averaging 1500 mm in the mountains near Yellowstone on the northwestern edge of the Basin (Zelt et al., 1999). Elevations in the floor of the Bighorn Basin center range from 1220 – 1830 m in elevation, while the Bighorn Mountains reach elevations of over 3960 m. Agriculture and oil and gas production are the main economies in the area (Zelt et al., 1999).

2.1 Hydrostratigraphy

The Bighorn Basin includes up to 6400 m of sedimentary fill encompassing deposition from the Cambrian through to the present (Thomas, 1965). Figure 2.2 presents a general stratigraphic section for the Bighorn Basin in the region of Little Sheep Mountain. Based on potentiometric surfaces and differences in common oil reservoirs (Stone, 1967), fluid flow within the basin subsurface is split into three main aquifer groups: the confined Paleozoic aquifers, overlying Upper Cretaceous / Lower Tertiary aquifers, and unconfined, surficial deposits of Upper Tertiary and Quaternary age. The two confined systems are well separated by the thick Cretaceous Thermopolis and Mowry Shales, even in areas of significant structural offset and fracturing (Lawson and Smith, 1966;

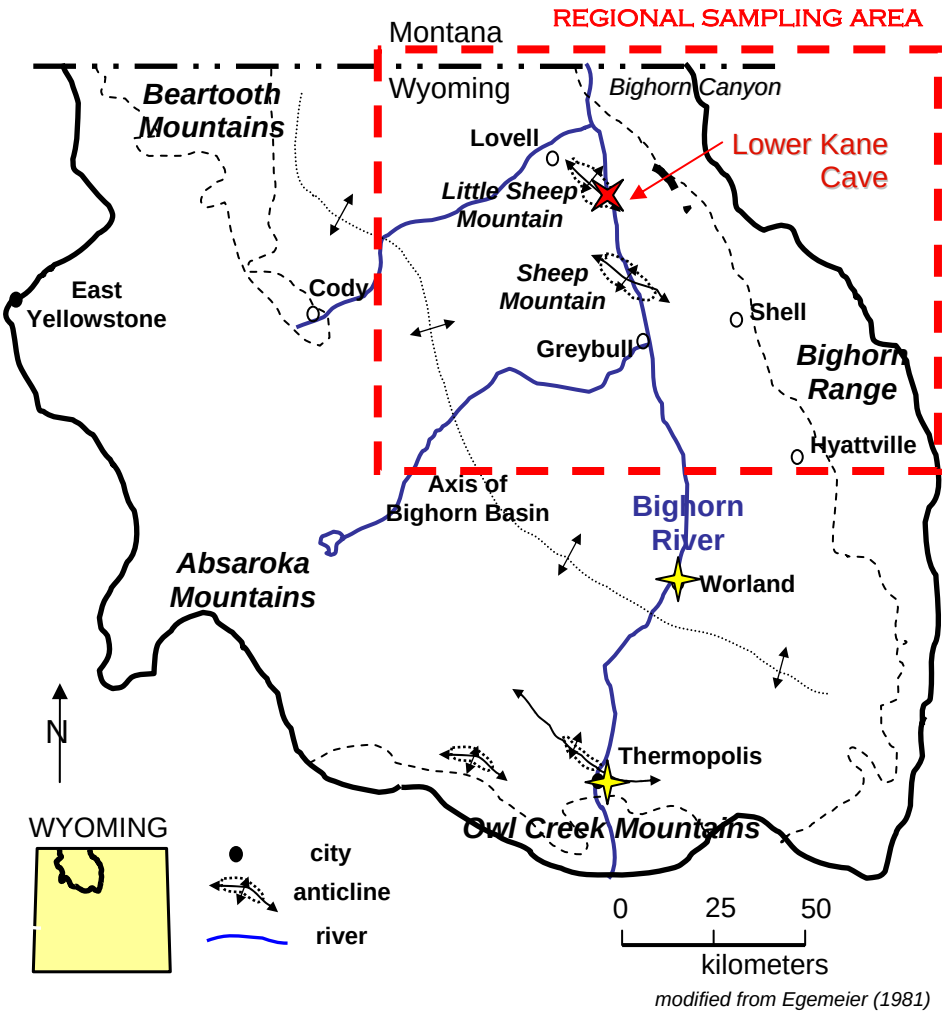

Figure 2.1: Study Area within the Bighorn Basin, showing the location of Lower Kane Cave (marked with a red star) and selected important structural features. The regional sampling area demarcated in red is shown in Figure 3.1 with the locations of Sr sampling sites marked. The yellow stars mark sampling sites at Thermopolis (this study) and Worland (Frost and Toner, in press) that lie outside the regional study area.

Age	Unit	Thickness	Lithology	Aquifer
Quaternary	Quaternary Undivided	0-100	Alluvium	
Cretaceous	Mowry Shale	330	Shale	
	Thermopolis Shale	400-500	Shale	
	Cloverly Fm	80-250	Siltstone	
Jurassic	Morrison Fm	370-560	Siltstone	
	Sundance Fm	370	Siltstone	
	Gypsum Spring Fm	130-200	Gypsum	
Triassic	Chugwater Fm and Dinwoody Fm Undivided	500-600	Siltstone	
Permian	Phosphoria Fm	80-240	Limestone, Shale	Phosphoria / Tensleep
Pennsylvanian	Tensleep Ss	80-150	Sandstone	
	Amsden Fm	160-220	Shale	
Mississippian	Madison Limestone	630-850	Limestone with paleokast zone in upper half	Madison
Devonian	Jefferson Fm	200	Limestone with shale units	
Ordovician	Bighorn Dolomite	300-410	Dolomite	
Cambrian	Gallatin Fm	200-530	Shale with interbedded limestone and sandstone units	
	Gros Ventre Fm	500-600		
	Flathead Ss	0-300	Sandstone	Flathead
Precambrian	Precambrian Undivided		Igneous and Metamorphic	

Figure 2.2: Stratigraphic Section of the Bighorn Basin. Modified from Doremus (1986).

Stone, 1967). As Lower Kane Cave is situated in the upper Mississippian Madison Limestone of the Madison aquifer, this study focused exclusively on the Paleozoic aquifers.

The Flathead, Madison, and Tensleep aquifers are generally considered to be the three principal Paleozoic aquifers in the Bighorn Basin. Minor aquifers include the Phosphoria and Amsden Formations.

The basal Flathead aquifer consists of the Cambrian Flathead Sandstone, a relatively clean, predominantly quartzitic sandstone (Rioux, 1958). This formation lies directly on the Precambrian basement and ranges in thickness up to 90m. The Flathead Sandstone is absent in parts of the eastern basin where the formation thins over Precambrian highs (Stone, 1967). Wells in the Flathead sandstone generally produce high yields (up to 126 L/s (Lowry and Lines, 1972)) of relatively fresh water. However, this aquifer is not extensively used in the Bighorn Basin because of economic constraints imposed by the depth to groundwater. The Flathead Sandstone is the only Paleozoic aquifer that is not a known hydrocarbon reservoir within the Bighorn Basin. The thick siltstones and shales of the Cambrian Gros Ventre Formation and Gallatin Limestone separate the Flathead aquifer from the overlying water bearing strata.

The Madison aquifer consists of the saturated thickness of the Mississippian Madison Limestone, as well as the Ordovician Bighorn Dolomite and the Devonian Jefferson Formation. Silurian deposition is absent in this area. The three formations comprise a thick section (up to 430 m of predominantly limestone and dolomite). Although referred to as the Madison Limestone, the Madison formation has in fact been extensively dolomitized (Plummer et al., 1990). Potentiometric head and geochemical similarities between water from different stratigraphic sections supports vertical integration between the three formations (Cooley, 1986; Libra et al. et al., 1981; Lowry and Lines, 1972).

Madison aquifer wells are generally high yield wells (up to 190 L/s (Lowry and Lines, 1972)) that produce fresh water along the margin of the basin, with decreasing quality basinward (Doremus, 1986; Libra et al. et al., 1981). Madison wells supply the municipal water needs of a number of towns in the basin, including Cowley, Greybull, Shell, Hyattville, and Worland. The Madison aquifer is a major oil producing formation in the Bighorn Basin (Stone, 1967).

The Tensleep Sandstone is a major oil producing formation in the Bighorn Basin (Stone, 1967). In the area of Little Sheep Mountain, the formation consists of between 34 and 50 m of more than 50% sandstone, with significant amounts of shale and carbonates (Agatston, 1954; Rioux, 1958).

The shales of the lower to middle section of the Amsden Formation act as a leaky confining unit between the Madison and Tensleep aquifers. A measured section of the Amsden shales at Little Sheep Mountain contained 25 m of strata (Rioux, 1958). The basal sandstone unit of the Amsden is a minor water producer, and is sometimes included in classifications as part of the Madison aquifer, while water producing dolomite layers in the upper section are sometime included with the Tensleep.

The Phosphoria Formation varies throughout the Bighorn Basin both in name and composition. In the study region, Permian depositional environments ranged between a marine carbonate facies in the west (often referred to as the Park City Formation) and an evaporite facies to the east (the Goose Egg Formation) (Agatson, 1954). The Phosphoria in the area of Little Sheep Mountain is the intertongued border between these two depositional facies (Rioux, 1958). In certain areas, similar potentiometric heads between the Tensleep and Phosphoria Formations suggest that these units are hydrologically connected. However, this connection depends on the absence of low-permeability interbedded shales within the Phosphoria (Doremus, 1986). Although

permeability values are not known, Rioux (1958) measured 21 m of shale in a section of the Phosphoria Formation at Little Sheep Mountain, with an additional 17 m of shale mixed with sandstone.

2.2 Structural Controls on Groundwater Flow

The structure of the Bighorn Basin is the result of compressional shortening that occurred during the Laramide orogeny (Snoke, 1993; Boyd, 1993; Picard 1993). The Laramide thrusting produced the Precambrian-cored mountain ranges that surround the basin and numerous anticlines that parallel the major mountain ranges along the interior basin margin (Hennier and Spang, 1983; Huntoon, 1993). Reverse thrust faults core the majority, if not all, of these anticlines, and can result in major stratigraphic offset, as much as 305 m in the case of Little Sheep Mountain (Jastram, 1999). These anticlines provide the major topographic relief within the basin, up to 500m of relief at Little Sheep Mountain and Sheep Mountain. The Bighorn River, cutting deep canyons into the Paleozoic rocks, has breached three of these anticlines (Little Sheep Mountain, Sheep Mountain and Thermopolis, Figure 2.1). Buried anticlines provide the primary oil traps in the Bighorn Basin (Stone, 1967).

Laramide structural overprinting controls groundwater flow in the Paleozoic aquifers of the Bighorn Basin, and secondary permeability caused by faulting, fracturing, and solution is the dominant contributor to flow (Bredehoeft et al., 1992; Huntoon, 1993). Principal permeability tensors orient parallel to the axis of basin anticlines, as preferential flow occurs in the extensional crest of the anticlines, while the compressional areas and core faults are generally considered to act as barriers to flow (Huntoon, 1993). Recharge to the Paleozoic aquifers from outcrop areas in the surrounding mountain ranges occurs only along

homoclinal portions of the mountain front, as it is severed where large thrust faults extensively offset the aquifer units (Doremus, 1986; Huntoon, 1985, 1993).

Potentiometric head data suggest that throughout most of the Bighorn Basin the Flathead, Madison and Tensleep aquifers are hydrologically distinct (Western Water Consultants, 1982; Doremus, 1986; Huntoon, 1993); however, areas of intense structural deformation produced fractures that allow for vertical movement of groundwater between formations (Cooley, 1986; Huntoon, 1993). The intense fracturing at anticlines serving as oil reservoirs in the Bighorn Basin has produced unified Paleozoic oil reservoirs at these locations (Stone, 1967). Additionally, Cooley (1986) cites numerous instances where groundwater at springs or in wells is believed to source from an underlying aquifer. Since older units outcrop at higher elevations in the mountains, the potentiometric gradient in regions of vertical fracturing should move water upward from the older, underlying aquifers into the younger units.

Potentiometric maps of the northeast Bighorn Basin show three potential recharge areas (Doremus, 1986; Western Water Consultants, 1982) that could source the Madison aquifer in the area of Little Sheep Mountain (Figure 2.3). These recharge areas are the Pryor Mountains to the north and the Bighorn Mountains to the west and southwest of Little Sheep Mountain. Approximately 23 km of aquifer severing related to offset along the Five Springs Thrust Fault (Doremus, 1986) separate the potential recharge areas in the Bighorn Mountains.

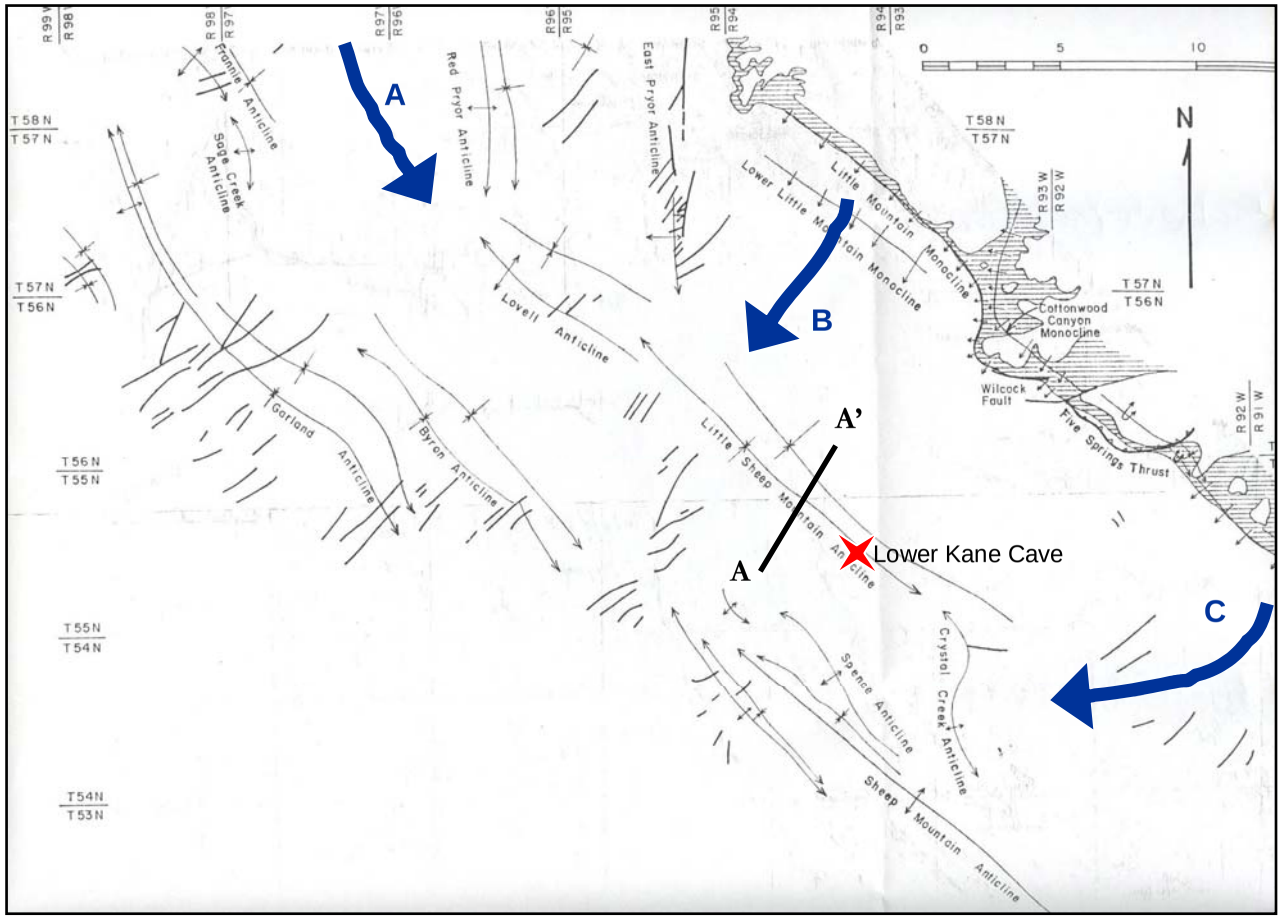

Figure 2.3: Potential Recharge areas for groundwater flow to Lower Kane Cave mapped on based on the potentiometric surface map of Doremus (1986). The base structural contour map is from Doremus (1986). The cross section A-A' through Little Sheep Mountain is shown in Figure 6.1.

3. METHODS

Paleozoic groundwater samples were collected from the springs of Little Sheep Mountain and the surrounding area around Lower Kane, with additional sampling at Thermopolis Hot Springs in the southern Bighorn Basin. Data collected include field parameters (temperature, pH, conductivity, dissolved oxygen, H_2S), alkalinity, major ion concentrations, select trace element concentrations, and isotopes of oxygen and strontium. The geochemical and Sr isotope data were used to assess potential models of the origin of Lower Kane Cave spring water. Geochemical data from previous studies of the Paleozoic aquifers in the northeast Bighorn Basin (Lowry and Lines, 1972; Libra et al. et al., 1981; Doremus, 1986.), along with strontium data for a few points (Frost and Toner, 2004), were utilized in the interpretation of the study results.

3.1 Identification of Sampling Sites

Extensive sampling of the springs and streams of Lower Kane Cave from 6 field trips between June, 2000 and June, 2003 provides the baseline data for this project. Three other springs in the canyon through Little Sheep Mountain – Hellespont Cave, Salamander Spring and PBS Spring - provided additional local samples. Regional samples from the Paleozoic aquifers, including the Ordovician - Mississippian Madison aquifer (11 samples), Pennsylvanian - Permian aquifers (4 samples) and the Cambrian Flathead aquifer (1 sample), were collected in July 2002 and June 2003. A sample was also collected in July 2002 from the Big Spring at Thermopolis Hot Springs State Park, which is located in the southern Bighorn Basin. Sampling locations are shown on the map in Figure 3.1, and marked by a letter and number. These site ID's are referenced in the text, and a list of locations and selected notes for the sampling sites is provided in Appendix A.

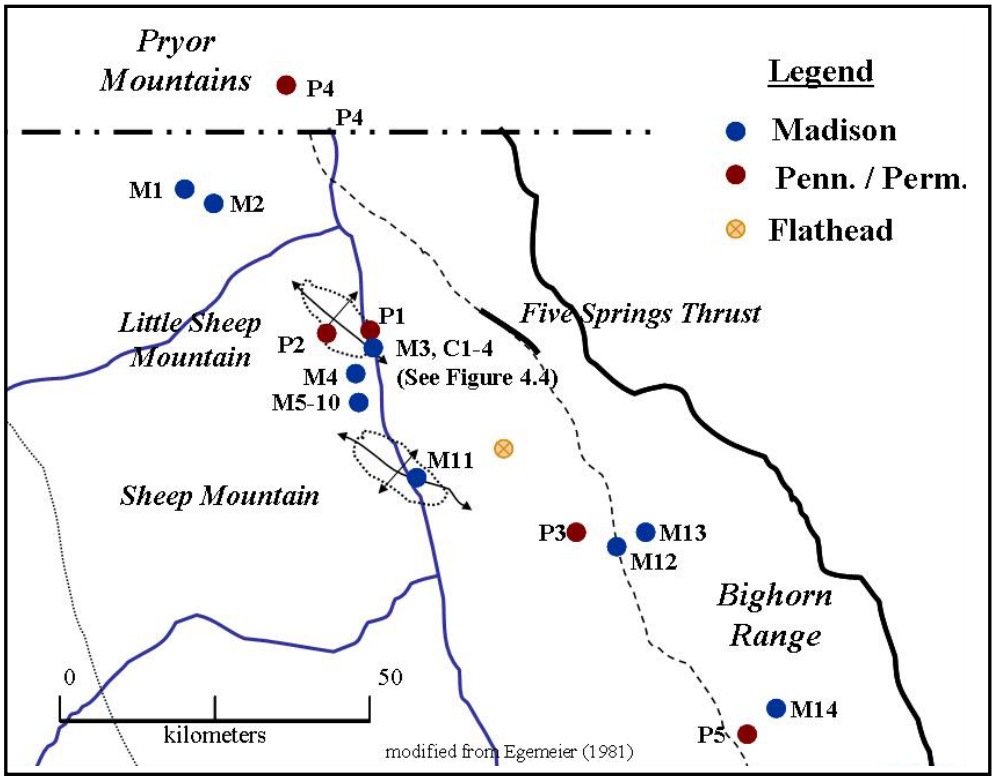

Figure 3.1: Locations of sampling sites in this study. The site identification numbers are given in the text, and referenced with descriptions and actual locations in Appendix A. Sampling sites for the samples from Thermopolis and the Worland Municipal Well (M11) are not shown on this map as they fall outside the map scale, however the towns of Thermopolis and Worland are shown in Figure 2.1.

Potential sampling sites were located through searches of the published literature and available databases, in particular the work of Doremus (1986), Lowry and Lines (1972), the Wyoming state water database, the Wyoming Oil and Gas Conservation Commission website, and through the assistance of BLM and National Park staff. Locations of interest for sampling were determined based on general proximity to Lower Kane Cave, location along potential flow paths, appropriate age of the geologic unit, and the availability of access.

The depth and variable water quality of the Paleozoic aquifers in this region, combined with a low population density, results in infrequent use of these aquifers for water supply purposes. Thus, potential sampling sites in the region are limited by a scarcity of wells drilled into these units. For the water supply wells that do exist, landowners generally provided ready access to their wells. However, the majority of Paleozoic wells in the region exist for purposes of hydrocarbon recovery, and we were able to obtain access to only two of these sites. Produced water samples were collected at the Spence oil field, however, the Crystal Creek oil field was not producing at the time of this study.

The results of this study are compared with published geochemical data for the Paleozoic aquifers, data which are generally not reproduced here. Exceptions include select data from a groundwater study by Frost and Toner (2004), which provide the only other available Sr analyses for groundwater in the northeast Bighorn Basin.

3.2 Sample Collection

The water samples collected came from springs or from actively pumped wells. Wells were allowed to flow prior to sampling in order to ensure flushing of the valve head. Field parameters for temperature, pH, ORP, conductivity, and TDS were collected at the time of sampling using a Myron Ultrameter 6P. Volatile components (hydrogen sulfide, iron, dissolved oxygen) were measured colormetrically, and frequently an additional measurement of dissolved oxygen was collected with an Oakton DO Meter. Water samples for subsequent laboratory analyses were collected in prewashed and rinsed plastic bottles, which were rinsed three times with sample before filling. Samples were generally syringe filtered to 0.22μm, while spring orifice samples from Kane Cave were collected with the aid of a peristaltic pump. Field alkalinity were determined on filtered samples by titration with 0.1N H_2SO_4. Samples for cation and strontium analysis were collected into acid-washed bottles. Sr samples were collected from the last aliquot through the filters. Reagent grade HNO_3 was added dropwise to bring the samples to approximately 1% HNO_3 for the cation samples, and .3% HNO_3 for the Sr samples. Samples were kept in a refrigerator at the field site, and transported on ice to the laboratory. In June 2003, two 1L samples of the Upper Spring of Lower Kane Cave were collected into pre-cleaned brown amber bottles for ^{14}C analysis, and shipped on ice to The University of Arizona Radiocarbon Laboratory.

Oil-field produced waters were collected into five gallon plastic jugs and allowed to separate for 48 hours before analysis. Water samples were collected by drawing water from below the oil interface through a short piece (approximately 8 inches) of plastic tubing attached to a syringe. Field parameters and hydrogen sulfide levels were collected at this time. Bacterial activity over

this period of time may have impacted the composition of the waters, in particular via the conversion of sulfate to hydrogen sulfide.

Whole rock samples for Sr analysis were collected in the Little Sheep Mountain Canyon, and three of these samples have been analyzed: the Madison limestone outcrop ~5m upstream of the entrance to Lower Kane Cave, the Madison Limestone outcrop at the entrance to Salamander Spring, and the upper most carbonate unit of the Phosphoria Formation, from outcrop above PBS spring. Additional whole rock data from the Madison Limestone, Madison Paleokarst, and Tensleep Sandstone in the Hyattville area are taken from the work of Frost and Toner (2004).

3.3 Analytical Analysis

Laboratory analyses discussed in this study include alkalinity, major ion chemistry, uranium, $\delta^{18}O$, and $^{87}Sr/^{86}Sr$. Additionally, one sample of Upper Spring in Lower Kane Cave was analyzed for ^{14}C. Analyses of all components, except ^{14}C, were performed at The University of Texas at Austin facilities. Alkalinity and anion data were collected in the lab of Dr. Phil Bennett. Laboratory alkalinities were obtained utilizing an auto-titrator. Anion analyses were measured by ion-chromatography on a Waters IC-PAK Anion High Capacity column, with Waters 484 UV and 430 Conductivity detectors. Cation and trace metal concentrations were assessed by a Micromass Platform ICP-MS, which is part of a departmental facility. The $\delta^{18}O$ data, provided by Dr. Libby Stern, are reported with respect to SMOW.

Strontium separation chemistry was carried out in the clean lab of Dr. Jay Banner. Water samples for Sr analysis were aliquoted into 300μg amounts, which underwent standard lab protocols for Sr separation by column chemistry. Whole rock samples were powdered in an agate mortar and pestle that was first pre-

cleaned and then pre-contaminated with sample. Literature values for the Sr content of carbonates from Faure (1998) were used to transfer approximately 300μg of whole rock powder to an acid-cleaned Teflon container; the powder was redissolved in 0.1N HNO3 and then taken through the same procedure as the water samples. Strontium isotope ratios were determined from 300ng/ml solution on the departmental Magnetic Sector, multi-collector ICP-MS. $^{87}Sr/^{86}Sr$ analyses of the NBS 987 strontium carbonate sample standard varied by day of analysis within the range of 0.710199 and 0.710250, but reported ratios have been adjusted relative to a value of 0.710250 for this standard. A full list of Sr analysis data, including Rb correction, standard corrections, and blank analysis are provided in Appendix C.

3.4 Strontium Isotope Systematics

Strontium (Sr) serves as a valuable groundwater tracer because it provides isotopic as well as elemental concentration data. These data are particularly useful when traditional geochemical parameters can not distinguish between two chemically similar waters. In the past decade, Sr tracers have assisted in general studies of groundwater evolution through water-rock interaction in both saline (Banner et al., 1989; Chaudhuri et al., 1987) and freshwater systems (Banner and Musgrove, 1994; Armstrong and Sturchio, 1997; Hogan et al., 2000; Land et al., 2000). Additionally, Sr data can be used specifically to address the determination of flowpaths and to assess the viability of inter-formational mixing models (Katz and Bullen, 1996; Dogramaci and Herczeg, 2002; Frost et al., 2002).

Isotopic ratios of Sr are useful as groundwater tracers due to the radiogenic properties of ^{87}Sr. Natural Sr consists of 4 isotopes: the non-radiogenic isotopes of ^{84}Sr, ^{86}Sr and ^{88}Sr, and the radiogenic isotope ^{87}Sr that is produced from the radioactive decay of ^{87}Rubidium (Rb) (with a half-life of 4.8 x

10^{10} years, (Faure, 1998)). Thus the ratio in a rock of ^{87}Sr to its non-radioactive sisters depends on the initial Sr ratio, the ratio of Rb to Sr, and the amount of time available for decay to occur. This measurement is given as $^{87}Sr/^{86}Sr$ because the similarity in abundance of these two isotopes, at roughly 7% and 10% respectively, maximizes the accuracy of the mass spectrometer measurements.

Since Rb and Sr have distinct chemical characteristics, they partition differently into various minerals. Sr is an alkaline earth, with similar chemical properties to calcium, while Rb is an alkali metal, and shares the chemical properties of K. Thus, Ca minerals, such as carbonates, will contain significant amounts of Sr, and K bearing minerals, such as the micas and K-feldspars, will incorporate Rb. Processes that separate Ca and K will therefore determine the initial ratio of Rb to Sr in a rock. Over long periods of time as ^{87}Rb decays to ^{87}Sr, the $^{87}Sr/^{86}Sr$ ratio of all rocks will increase. However, the rate of this increase depends on this initial ratio of Rb to Sr. For example, the change in initial $^{87}Sr/^{86}Sr$ is negligible in rocks where [Sr] >> [Rb], while radiogenic decay significantly alters the $^{87}Sr/^{86}Sr$ of rocks with initial [Rb] >> [Sr]. Thus, differences in the relative incorporation of Rb and Sr results in wide variations in the $^{87}Sr/^{86}Sr$ ratio of various earth materials.

Because the isotopic ratio of Sr is not fractionated to any measurable extent by biological or chemical activity, the $^{87}Sr/^{86}Sr$ ratio of hydrologic systems reflects only the ratio of the initial recharge water and any subsequent modifications caused by interactions with the aquifer host rock. With time, groundwater will equilibrate in Sr content and isotopic ratio with the host rock through which it flows, thus acquiring the Sr "signature" of a particular rock unit.

Due to the exclusion of K by carbonate minerals, the $^{87}Sr/^{86}Sr$ of marine carbonates is generally low, between 0.7067 and 0.7093, and should reflect the Sr ratio of the ocean water at the time the rock formed (Faure, 1998). Oceanic

values for $^{87}Sr/^{86}Sr$ have been determined as far back as the Cambrian (Montanez and Banner, 2000), although the established range of marine values for a given period is larger for greater ages due to the increasing problems caused by diagenesis and error in age determination in older rocks. Barring contamination by K-containing siliciclastic components, the $^{87}Sr/^{86}Sr$ value for carbonates should remain relatively fixed at the level of the ocean from which it formed. The concentration of Sr in these rocks can be high, however, as Sr readily replaces Ca in the carbonate matrix. Alternatively, siliciclastic rocks, which contain high levels of K, continually acquire ^{87}Sr from the decay of ^{87}Rb, and thus evolve over time to more and more radiogenic values of $^{87}Sr/^{86}Sr$. However, for similar reasons the actual concentration of Sr in these rocks is generally low.

A particularly useful feature of Sr data is that a mixture of two waters results in a linear relationship when $^{87}Sr/^{86}Sr$ is plotted against the reciprocal of the Sr concentration (1/[Sr]). Thus, the Sr signature of groundwater, in conjunction with geochemical evidence, can identify particular water types. It can also provide a simple method to assess potential mixing origins of groundwater and help determine the necessary fractions of given endmembers necessary to generate a mixed sample. If we know the $^{87}Sr/^{86}Sr$ ratio and Sr concentration of the endmembers, we can calculate the values of these parameters for a given mixture utilizing the following equations (based on Faure, 1986):

$$[Sr]_{mix} = f[Sr]_A + (1-f)[Sr]_B \tag{3.1}$$

and

$$\left(\frac{^{87}Sr}{^{total}Sr}\right)_{mix} = \frac{f\left(^{87}Sr/^{total}Sr\right)_A[Sr]_A + (1-f)\left(^{87}Sr/^{total}Sr\right)_B[Sr]_B}{f[Sr]_A + (1-f)[Sr]_B} \tag{3.2}$$

Where f is the fraction of the mixture from endmember A; [Sr] is the Sr concentration in the mix, endmember A, or endmember B, respectively; and

($^{87}Sr/^{total}Sr$) is the ratio of ^{87}Sr to total Sr in the mixture, endmember A or endmember B.

If the difference in $^{87}Sr/^{86}Sr$ between the two endmembers is less than 10%, than ^{86}Sr is nearly proportional to $^{total}Sr$, and equation (2) simplifies to:

$$\left(\frac{^{87}Sr}{^{86}Sr}\right)_{mix} = \frac{f\left(^{87}Sr/^{86}Sr\right)_A[Sr]_A + (1-f)\left(^{87}Sr/^{86}Sr\right)_B[Sr]_B}{f[Sr]_A + (1-f)[Sr]_B} \qquad (3.3)$$

Thus strontium data can be used to assess the viability of mixing hypotheses.

4. DESCRIPTION OF SAMPLING SITES

4.1 Madison Aquifer

The Madison wells sampled for this study are generally open to a large portion of the Madison Limestone, and one of the Greybull Municipal wells is also drilled into approximately the upper 90m of the Bighorn Dolomite (Bob Graham**,** Greybull Town Water Supply Manager**,** personal communication). Wells sampled for this study include municipal water supply wells for the towns of Cowley (M2) and Greybull (M8 and M9), the Spence oil field wells (M5 to M10), which maintains a surface water discharge permit, a stock well (M1), and the supply well for the Georgia Pacific (GP) plant (M4). Most Madison wells were sampled from valves at or near the well head. The well at the GP plant is separated from the well head by approximately 60m of underground piping, and the Cowley Municipal Well was sampled at a stock tank that draws water from the main distribution line about 0.5km from the well head. Additional data for a spring in Sheep Mountain (M11) and the municipal supply wells for the towns of Hyattville (M15) and Worland (M15) were obtained from Frost and Toner (2004). The spring at Sheep Mountain is of particular interest, as the structure of Sheep Mountain is equivalent to that of Little Sheep Mountain, and we expect to see similar structural controls on groundwater flow at both locations.

Madison water samples are located on both sides of the Bighorn River, but the wells and springs north of Sheep Mountain are located on the western side of the river, the same side as Lower Kane Cave, while the spring at Sheep Mountain and the wells to the south are located on the eastern side of the river. The Madison Limestone is a confined aquifer throughout most of this region except where the Little Sheep and Sheep Mountains anticlines have brought it close enough to the surface to be breached by the Bighorn River (Lowry and Lines, 1972; Libra et al., 1981; Doremus, 1986). Therefore the Bighorn River should

function as a local discharge point, without serving as a regional groundwater divide. To the north, however, the Bighorn River Canyon has down cut to the Cambrian formations, severing aquifer connection in that area.

4.2 Pennsylvanian / Permian Aquifers

Relatively few water wells in the study area have been drilled into the Pennsylvanian and Permian section. The yield and quality of these waters make the Madison aquifer preferable for water supply purposes. The majority of wells drilled into these units were originally drilled for hydrocarbon exploration, and "dry" wells are generally abandoned. One such non-producing well outside the town of Greybull (location 52-91-20bcd, "Red Gulch Sooner") was turned over to the BLM, and had been recently filled in at the time of this study (Bob Graham, personal communication).

In this study, groundwater samples from any portion of the Amsden, Tensleep, and Phosphoria Formations are collectively classified as belonging to the Pennsylvanian and Permian aquifers, as the wells co-produce water from multiple formations. The available samples analyzed in this study are shown as P1 – P5 in Figure 3.1. Two of these samples come from wells, two from springs, and one from a surface stream sourced by a spring. PBS Spring (P1) is discussed in the preceding section on Little Sheep Mountain. The Clay Well (P2) is listed as a Tensleep well (Shirley Bye-Jechs, BLM office, personal communication) and is currently leased by the BLM as a stock well. The Greybull Cemetery Well (P3) was originally intended to source the Madison aquifer and serve as a Municipal supply well for the town of Greybull. However, the well was improperly drilled, and the 240m thick producing zone instead draws primarily from about 210m of the Pennsylvanian through Permian sections, breaching the upper 33m or so of the Madison Limestone (Bob Graham, personal communication). Due to the average

thickness of the Amsden Formation (52 m) and Tensleep Sandstone (30–50 m) in the area (Agatston, 1954; Rioux, 1958), this well likely draws water primarily from the Amsden Formation, Tensleep Sandstone, and the basal portion of the Phosphoria Formation. Due to the poor quality of the water in these formations, the well water is unsuitable for human consumption and is used as a stock supply well. Since valves at the well head were sealed off, the only available sampling site at the Greybull Cemetary well was the high pressure spray discharging from a leaking seal. While this should not impact the more stable constituents, we did not observe the presence of any volatile components, as they are likely outgassed in the spray.

Sample P5 was analyzed by Frost and Toner (2004) and comes from a spring in the Tensleep Sandstone outside Hyattville. For purposes of this study, this sample is classified with the Pennsylvanian / Permian aquifers as it discharges from the Tensleep Sandstone. However, as discussed below, the chemistry and Sr signature of this spring is different from that of the other Pennsylvanian / Permian water samples, suggesting either a different evolutionary path or a different source for this water.

Site P4 is from a stream in the Bighorn National Recreation Area near Hillsboro. The stream sampled emerges from a thickly vegetated seepage zone below a red shale unit that is believed to be the equivalent of the Horseshoe Shale Member of the Amsden Formation that serves as a leaky confining layer between the Madison Limestone and the overlying Tensleep Sandstone. We include this sample in our study for purposes of completeness and as a sampling point available to future researchers, but use sample P4 in our interpretation of the groundwater within the Paleozoic system cautiously for three reasons: 1) its location on the eastern side of the Pryor Mountain region places it in a potentially different flow system, 2) uncertainty exists about the source formation from

which the seep derives, and 3) evidence exists for surface contamination – the site is located in a ravine below the road through the park, and the presence of low-molecular weight organic carbon compounds was detected in sample from this site.

4.3 Other Aquifers

Samples from the Precambrian Flathead Sandstone and Thermopolis Hot Springs analyzed for this study are considered independently of other samples, as they consist of a sole aquifer sample (in the case of the Flathead Sandstone), or cannot be classified to any particular Paleozoic aquifer (in the case of Thermopolis).

The Flathead Sandstone contains a large supply of fair to good quality water; however, very few wells are drilled into this formation. Due to the great depth of the aquifer and associated high pressures, it is cheaper to drill and maintain water wells into the Madison aquifer. The Flathead well sampled for this study is located southeast of Lower Kane Cave on the eastern side of the Bighorn River. This is a deep well, drawing water from an interval of 1359 to 1366 m, that was originally drilled for natural gas exploration and yields 28 L/s of water at nearly 24bars of pressure at the surface (Steve Helbrun, well owner, personal communication). The well is currently in use as an agricultural well. Such exploratory wells are rare, however, as the Flathead aquifer has not been shown to produce hydrocarbons.

Thermopolis Hot Springs State Park is located in the south end of the Bighorn Basin, and consists of a number of hot springs discharging from the undifferentiated Paleozoic aquifers (Jarvis, 1986; Spencer, 1986), although the springs have been suggested to source from the deeply buried Madison aquifer (Spencer, 1986). This study sampled the Big Spring (referred to in this study as

the “Thermopolis” sample). Although these springs are at a great distance from Lower Kane Cave, they are of interest as they are thermal, sulfidic springs discharging from within an anticline breached by the Bighorn River. These springs therefore display similar characteristics to the springs of Lower Kane Cave, and may result from similar groundwater flow systems.

4.4 Little Sheep Mountain Springs

Lower Kane Cave is a linear feature approximately 325 meters in total length, without branching passages. Figure 4.1 presents a plan view map of Lower Kane Cave showing the location of the cave springs discussed below. The cave geology and morphology has been well described in the works of Egemeier (1973; 1981). More recent studies have investigated the bacterial ecosystem within the cave and its role in speleogenesis (Engel et al., 2003; 2004). An additional dry cave, Upper Kane Cave, is located almost directly above Lower Kane Cave and parallel to it. This cave is no longer active, but is believed to have formed from the same mechanism as Lower Kane Cave during an earlier period of higher regional water table.

The cave is forming along a fracture trace in the anticlinal crest that parallels the axis of Little Sheep Mountain. The cave cuts across breccias of Mississippian paleokarst, which are more resistant to dissolution than the host limestone. These paleokarst features are believed to be barriers rather than conduits to flow (Sando, 1988). Three main springs – Fissure (C1), Upper (C2) and Lower (C3) springs - discharge water carrying H_2S into Lower Kane Cave from linear fractures in the cave floor. The tubular structure of Lower Kane Cave enlarges at these three sites. Lower Spring and Upper Spring are shown in Figures 4.2 and 4.3, respectively.

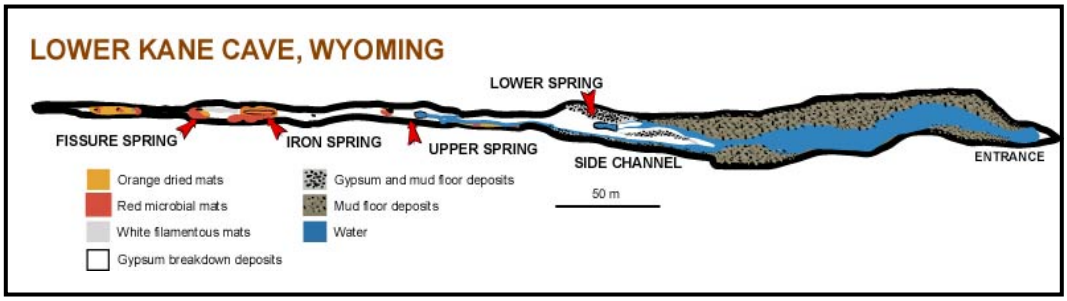

Figure 4.1: Plan view map of Lower Kane Cave showing the locations of springs and bacterial mats, as well as gypsum and mud deposits. The main springs feeding the cave system and the springs of interest in this study are Fissure Spring, Upper Spring and Lower Spring.

Figure 4.2: Looking downstream from the orifice at Lower Spring, Lower Kane Cave. Note the white bacterial mats in the outflow channel from the orifice. Similar mats are significantly larger and more extensive downstream of the Upper Spring orifice. Photo courtesy of A. Engel, 2001.

Figure 4.3: Performing a salt dilution trace at the outflow channel just downstream of the Upper Spring orifice. Note the linear fracture running through the ceiling in the upper right side of the picture. The thick bacterial mats start at roughly the location of the yellow stake visible in the bottom of the picture. The gas masks are worn for protection from any organic sulfur gases and the high levels of radon gas. Photo courtesy of A. Engel, 2001.

A dilution trace measurement conducted in August 2002 gauged Upper Spring at a discharge of 6.9 L/s. Long term temporal variations in discharge are apparently minimal, as this value is consistent with weir measurements by Egemeier in the 1970's (Egemeier 1973). However, variations in flow have been observed at Fissure Spring, and appear to be the result of small head fluctuations. This spring has been observed in both dry (1970; 1971; 1975; March, 2001) and flowing (1969; December, 2001; August, 2002) conditions (Egemeier, 1981; Annette Summers Engel, personal communication; this study). Between June 5 and June 8, 2003 the head at Fissure Spring was observed to rise from a few inches below the lip of the spring orifice to flowing conditions. These changes in head do not appear associated with fluctuations in the discharge of the Bighorn River, which decreased over this same period. Any seasonal or barometric correlations have not been established. These slight fluctuations in head do not appear to result in significant changes to the groundwater chemistry at the cave springs.

Two additional small water features, Hidden Spring and Iron Spring, also contribute to the Lower Kane Cave stream. Hidden Spring emerges from a collapse pile, and flows through mud deposited by the Bighorn River near the cave entrance. This spring has not been extensively analyzed as the flow appears small and the collapse feature prevents access to the spring orifice. Preliminary sampling, however, suggests that this water shares the characteristics of the main springs. A sample from the Iron Spring in August 2001 had no detectable H_2S, and increased concentrations of SO_4 and Ca (40% and 29% increases, respectively, data not shown). This sample also has significantly more Fe than the other springs, which supports orange mats of iron oxidizing bacteria. The other constituents, however, are similar between the springs. Iron spring emerges from the south side of a large gypsum pile located along the northern side of the

cave between Lower and Upper Springs, and the changes in chemistry observed in this sample are likely the result of underflow from Fissure spring interacting with the collapse pile of gypsum. Similar underflow, without the dramatic iron content, is observed at the channels which emerge from a gypsum pile at the location of Lower Spring (underflow channels that are distinct from the actual spring orifice). These springs were dry at the start of the June 2003 field session, but were observed to resume flow when the water level at Fissure spring once again rose over the lip of the spring orifice.

The natural entrance to Lower Kane Cave has been partly blocked by debris from the construction of the Burlington Northern Railroad, and the cave discharge enters into this rock pile at the cave entrance. Although this point is only around 5 meters from the Bighorn River, three separate dye traces of the cave exit point have failed to provide visual evidence of cave discharge entering the river. However, an extensive zone of seepage points is found along a roughly 15 meter stretch of the mud bank of the Bighorn River outside the entrance to Lower Kane Cave and is a likely path for discharge.

The canyon through Little Sheep Mountain contains 3 spring / cave systems in addition to Lower Kane Cave, as shown in Figure 4.4. Views of Little Sheep Mountain are given in Figures 4.5 and 4.6. Three of these caves (Lower Kane Cave, Hellespont Cave (C4), and Salamander Cave (M3)) discharge from the Upper Madison Limestone, while PBS Spring (P1) discharges from the upper carbonate layer of the Phosphoria Formation. No other springs have been observed within the canyon, although the fracture system discharging at the caves probably also provides water directly to the bed of the Bighorn River. All the sites except Hellespont Cave are located on the western bank of the Bighorn River. Salamander Cave discharges a high yield (85L/s) of water directly to the Bighorn River. Hellespont Cave discharges from a short distance above the river

level at the time of study, and yields a similar volume of water (6.7L/s) as the Lower Kane Cave springs. PBS spring is located on the northern edge of the canyon, just south of the surface expression of the reverse fault that cores Little Sheep Mountain. The yield from this spring is unknown, but appears to be less than that of the caves. Surficial offset along this fault displaces Jurassic units against Triassic strata to the northeast, and dies out to the southeast (Jastram, 1999). The Madison caves are all located near the axis of the anticline. Of the three Madison caves, only Lower Kane Cave provides relatively easy access: Hellespont Cave requires specialized breathing equipment due to high H_2S levels, and the entrance to Salamander Cave is partially submerged and blocked by collapse features. PBS spring discharges from a large breakdown pile, and it is unknown whether a cave exists beneath the breakdown.

Access to these caves is provided either by river or by foot along the Burlington Northern tracks on the western bank of the canyon. In analyzing these samples, Salamander Spring and PBS Spring are included in the groupings for the Ordovician / Mississippian and Pennsylvanian / Permian aquifer systems, respectively. Due to similarities in chemistry and Sr signature that distinguish them from the other Madison samples, Lower Kane and Hellespont Caves are considered separately.

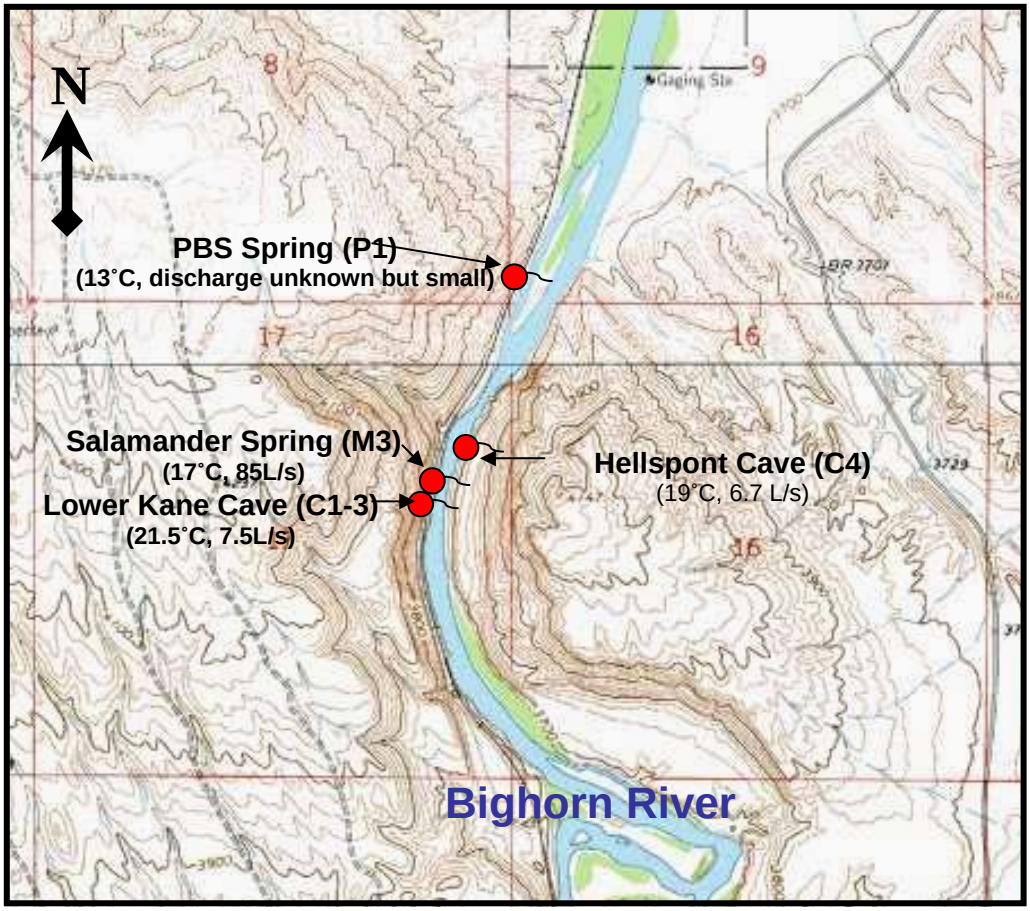

Figure 4.4: Topographic map of the canyon through Little Sheep Mountain showing the location of springs and caves. The squares outlined in red on the map and numbered are sections in the Township and Range location system, and are a mile square. Temperature data from this study, discharge data from Egemeier (1981).

Figure 4.5: Research group walking south along the Burlington Northern tracks into Little Sheep Mountain. PBS Spring emerges from the thicket of trees directly to the left of the walkers. The uppermost carbonate layer of the Phosphoria Limestone is exposed in outcrop on the right of the picture, while the Paleozoic section from Permian down to the upper Madison is exposed on the left canyon wall. Photo courtesy of A. Engel, 2001.

Figure 4.6: A view of the Bighorn River through Little Sheep Mountain, facing north. The research group is scrambling down the debris slope from the railroad tracks. The entrance to the cave is directly to the left of the bush behind the figure in red. The entrance to Salamander Spring is very near to the green bushes in the back of the picture. Photo courtesy of Nova Productions, 2001.

5 ANALYTICAL RESULTS

Data for field parameters, major ion analysis, select trace element and SI values for the water samples in this study are listed in Tables 5.1 and 5.5. All geochemical data for the samples from this study are compiled in Appendix B. Data shown include samples analyzed in this study, as well as select literature values from Doremus (1986), Egemeier (1981) and Toner (1999). Table 5.6 lists average values and data ranges for field parameters and major constituents for Lower Kane Cave and its main springs. Available oxygen isotope data is listed in Table 5.2. Graphical representations of the geochemical facies of the water samples are presented in Figures 5.1, 5.2, 5.4 and 5.5. Temporal changes in the chemistry of the Lower Kane and Hellspont Cave springs are shown in Figures 5.6, 5.7 and 5.8 Results of strontium analyses for water samples and whole rock digestions are presented in Tables 5.3 and 5.4. These results are also presented in graphical form in Figure 5.3, which plots the inverse of Sr concentration against the isotope ratio.

5.1 Madison Aquifer

Groundwater from the Paleozoic aquifers sampled in this study range from fresh to brackish, with all measured conductivities below 3100µS. The Madison waters are all fresh water, with conductivities between 400 - 1200µS, and a median conductivity of 500µS. As shown in the Piper diagram in Figure 5.1 and Stiff diagrams in Figure 5.2, the dominant chemistry of groundwater in the Madison aquifer is generally Ca-Mg-HCO_3 type, however there is significant spread along the HCO_3 to SO_4 axis of the piper diagram. In particular, wells from the GP plant (M4) and Spence Oil wells #11 and #12 (M5 and M6) show a marked increase in sulfate concentrations, from approximately 40 ppm to between 200 – 320 ppm. At the GP well this increase in SO_4 and conductivity is

accompanied by a decrease in dissolved oxygen concentration. Oxygen contents were not measured at the Spence oil field due to the presence of hydrocarbon. Within the samples from these aquifers, an increase in conductivity is associated with an increase in SO_4, both in absolute concentration and in percentage of dissolved ions. Oxygen isotope data for Madison aquifer samples fall within a range of $\delta^{18}O$ values from -19.0 to -19.9‰ (Table 5.2). Uranium is widespread in all samples in the Bighorn Basin, and in the Madison samples ranges from low levels, below 1 ppb, up to 50 ppb.

Madison water samples from 11 sites range in Sr concentration between 0.22 ppm and 2.24 ppm, and vary in Sr signature between 0.70891 and 0.70925. The two samples which contain the most Sr also have the lowest values of $^{87}Sr/^{86}Sr$. Two sites were sampled in both 2002 and 2003 and show temporal consistency, with variations in $^{87}Sr/^{86}Sr$ of only 0.00001 (Table 5.3, Figure 5.3). Frost and Toner (2004) list a ^{13}C-corrected, ^{14}C age-date of 8,655 ± 355 years for the Hyattville Municipal well.

5.2 Pennsylvanian / Permian Aquifers

Water from the Pennsylvanian / Permian aquifers are generally on the fresh side of brackish, with conductivities of 1150 - 3100μS. As shown in Figures 5.1 and 5.2, the Pennsylvanian / Permian waters are generally Ca-Mg-SO_4 type. Data on oxygen isotopes is only available for two of the Pennsylvanian / Permian samples, P1 and P2, and these are more and less depleted than the Madison samples, at $\delta^{18}O$ values of -18.5 and -21.8‰ (Table 5.2), respectively. Samples from the Pennsylvanian and Permian aquifers also contain high levels of uranium, between 4 and 53 ppb.

Four of the five waters from the Pennsylvanian / Permian aquifers (P2 – P5) are less radiogenic and more concentrated in Sr than water from the Madison

aquifer. These waters contained between 2.20 and 8.34 ppm of Sr and ranged in $^{87}Sr/^{86}Sr$ between 0.70789 to 0.70856. Although separated geographically, the two well waters, P2 and P3, are particularly similar in Sr space, differing by only 0.00009 in $^{87}Sr/^{86}Sr$. With 0.42 ppm of Sr with a $^{87}Sr/^{86}Sr$ of 0.71220, water from the Tensleep spring (P5) measured by Frost and Toner (2004) contains significantly less Sr of a more radiogenic character than the other waters of the Pennsylvanian / Permian aquifers (Table 5.3, Figure 5.3).

5.3 Other Paleozoic Waters

The Flathead Sandstone sample is fresh, with a conductivity of 713µS, Na-HCO_3-SO_4 in type, and thermal, at 31˚C. The sample from the Flathead Sandstone contains 0.12 ppm of Sr at a $^{87}Sr/^{86}Sr$ ratio of 0.71601.

Water from Thermopolis is Ca-Mg-SO_4 type. Due to sampling constraints, field parameters were not obtained for the Thermopolis sample collected for this study. However, literature values list the spring as thermal, with an average temp of 56˚C, and brackish (TDS of 1920 – 2249) with H_2S levels of 4.5 ppm (Jarvis, 1986; Nickens et al., 1996). The sample from Thermopolis Hot springs contains 2.82 ppm of Sr with a $^{87}Sr/^{86}Sr$ ratio of 0.71558. The $\delta^{18}O$ of the Thermopolis sample is -18.7‰. Both the Thermopolis and Flathead samples contain less than 1ppb of uranium.

	#	Site ID	T C	pH	DO ppm	Cond uS	H2S	Cl ppm	HCO3 ppm	SO4 ppm	Na ppm	Ca ppm	Mg ppm	CBE	Si ppm	Fe ppm	U ppb	SI Gypsum	SI Calcite
MISSISSIPPIAN	1	M1	14.5	7.4	7.25	436	bdl	1.5	203	40	1	48	22	-1	3	0	12	-2	-0.15
	2	M2	17.2	7.47	4.88	421	bdl	1.3	214	39	1	48	24	0	4	0	5	-2.11	-0.11
	3	M2	17.2	7.38	-	408	bdl	1.4	214	47	2	53	21	-2	4	0	5	-2.12	-0.18
	4	M3	-	7.55	3.2	505	bdl	1.4	183	316	4	112	57	3	4	0	15	-1.76	0.08
	5	M3	17.2	7.59	3.31	483	bdl	1.5	239	55	4.3	53	24	-3	4	0	16	-1.75	0.02
	6	M3	17.4	7.52	-	466	bdl	*3.8*	*201*	*86*	*4*	*55*	*21*	*-6*	4	0.01	17	-1.73	0.03
	7	M4	17.5	7.23	-	864	0.1	2.3	183	83	5	57	21	-1	5	0.19	49	-1.06	-0.16
	8	M11	-	-	-	-	-	2.3	202	81	4	63	25	3	-	-	-	-	-
	9	M5	-	-	-	865	-	2.8	237	43	4.3	51	23	-3	4	0.01	0	-	-
	10	M6	-	7.1	-	1204	14	1.7	233	50	4	51	25	-2	4	0.04	0	-	-
	11	M7	-	-	-	473	22	9.8	369	204	21	99	43	-5	4	0.02	21	-	-
	12	M9	-	-	-	687	55	8.3	358	388	57	163	47	0	5	0.03	0	-	-
	13	M10	-	-	-	719	58	*11.9*	*418*	*36*	*23*	*100*	*40*	*9*	5	0.02	0	-	-
	14	M8	-	-	-	492	4	2.8	456	36	8	95	45	3	4	0.01	4	-	-
	15	M12	17.7	7.56	5.41	422	8	1.8	241	63	5	61	28	2	4	0	3	-2.39	0.07
	16	M13	15.4	7.57	4.38	463	bdl	1.7	285	31	6	61	30	3	4	0	2	-2	0.04
	17	M14	-	-	-	-	-	1.3	243	21	3	49	25	2	-	-	-	-	-
	18	M15	-	-	-	-	-	0.8	228	13	2.6	39	22	-2	-	-	-	-	-
PENN./PERMIAN	19	P1	13.2	7.17	0.93	2233	5	33.3	241	1041	134	233	129	1	7	0.03	14	-0.48	-0.02
	20	P1	-	7.31	-	2441	0.6	*47.8*	*238*	*1137*	*10*	*255*	*114*	*-14*	6	0.01	12	-0.4	0.15
	21	P2	17.8	7.04	-	3091	bdl	12.3	169	1788	82	428	261	5	1	8.08	9	-0.17	-0.07
	22	P3	11.3	7.59	8.74	1159	bdl	2.8	195	479	11	181	45	-2	6	0	4	-0.73	0.3
	23	P4	15.7	7.73	4.68	2548	bdl	9.4	62	1445	26	407	128	-1	4	0.16	53	-0.18	0.18
	24	P5	-	-	-	-	-	0.7	280	11	2.7	56	20	-2	-	-	-	-	-
OTH.	25	Therm.	*56*	-	-	-	*4.5*	247	622	568	191	301	66	0	15	0.01	0	-	-
	26	Flat.	31.2	8.58	0.06	713	0.1	22.2	154	146	146	7	1	3	6	0	0	-2.41	0.16

Table 5.1: Selected data for water samples from the Paleozoic aquifers. Italicized samples are from Frost and Toner (2004).

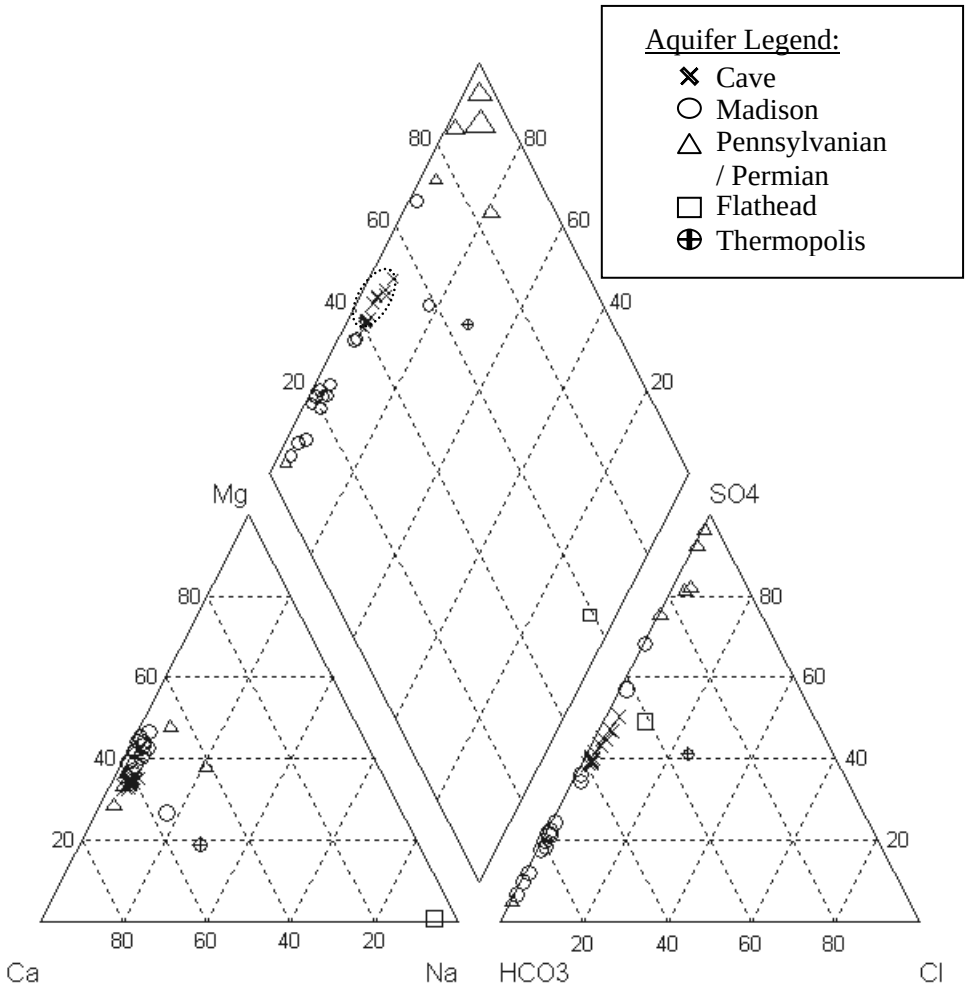

Figure 5.1: Piper Diagram of samples from the Paleozoic aquifers of the Bighorn Basin. Sample sizes are plotted in proportion to the samples concentration of SO_4. In general, Madison waters are Ca-Mg-HCO_3 in type, while waters of the Pennsylvanian / Permian are more concentrated and Ca-Mg-SO_4 type. The dashed oval in the piper diagram encircles all samples from Lower Kane Cave. Na and Cl are only significant contributors to the dissolved ions in the Thermopolis and Flathead samples.

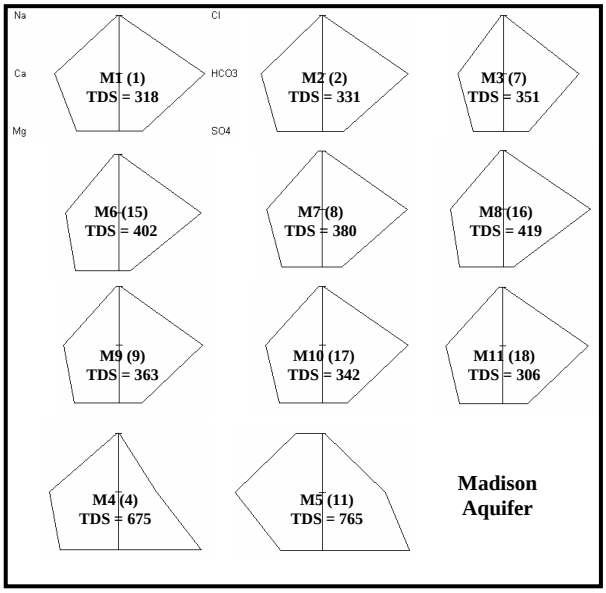

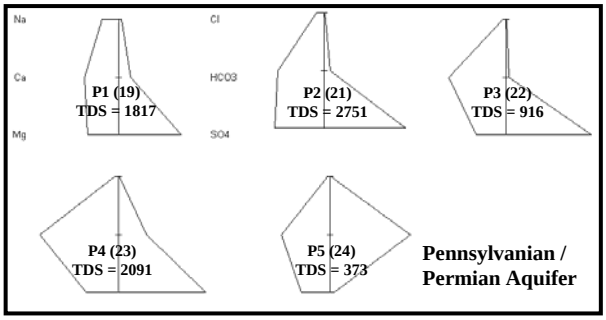

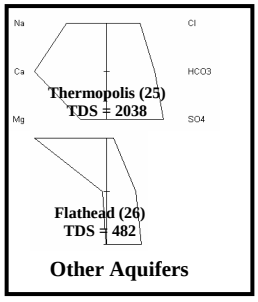

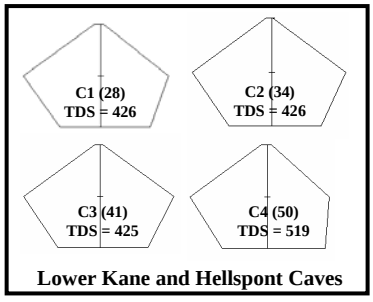

Figure 5.2: Stiff Diagrams of waters from the Paleozoic aquifers of the Bighorn Basin. Diagram labels correspond to locations in Figure 3.1. Stiff diagrams represent the geochemistry of a water sample by displaying concentration amounts relative to the distance from the center line, cations to the left and anions to the right. Amounts of the various consitutents are given in mg/l, however these images are scaled to the total dissolved solid of the individual samples. The TDS values for the samples are shown along with their Sr site idea and samples identification number (in parenthesis). TDS values were calculated from the sum of the major constituents to provide a consistent measure between samples from different studies. The legend on sample M1 applies to all the diagrams shown.

Sample ID #	Site ID	d18O
PALEOZOIC AQUIFERS		
Mississippian		
2	M2	-19.0
4	M4	-19.6
6	M3	-19.6
7	M3	-19.9
9	M12	-19.6
10	M5	-19.7
11	M6	-19.6
12	M9	-19.7
13	M10	-19.9
14	M7	-19.3
Penn. / Permian		
19	P1	-18.5
20	P1	-18.5
21	P2	-21.8
Themopolis		
25	-	-18.7
LOWER KANE CAVE		
Fissure Spring		
28	C1	-19.8
30	C1	-19.5
31	"	-19.8
Upper Spring		
34	C2	-19.6
36	"	-19.5
38	"	-20.0
Lower Spring		
42	C3	-19.7
44	"	-19.5
46	"	-20.0
HELLSPONT CAVE		
50	C4	-19.6
51	"	-19.7
52	"	-20.1
53	"	-20.1

Table 5.2: Available oxygen isotope data for samples from this study. Sample ID# refers to the analysis number in Appendix B.

Analysis #	Sr Site ID	Location	Sr (ppm)	$^{87}Sr/^{86}Sr$
27	C1	Fissure Spring	0.77	0.71007
33	C2	Upper Spring	0.72	0.71010
34	*"*	*Upper Spring*	*0.71*	*0.71003*
37	*"*	*Upper Spring*	*0.76*	*0.71012*
41	C3	Lower Spring	0.73	0.71001
50	C4	Hellspont Cave	0.96	0.71015
3	M1	Crosby Well	0.22	0.70891
2	M2	Cowley Municipal Well	0.22	0.70895
1	*"*	*Cowley Municipal Well*	*0.23*	*0.70894*
8	M3	Salamander Spring	0.49	0.70924
7	*"*	*Salamander Spring*	*0.50*	*0.70925*
4	M4	GP Gypsum Plant	1.41	0.70856
12	M6	Spence Oil Well #12	2.24	0.70840
16	M8	Spence Oil Well #74	0.74	0.70900
9	M11*	Sheep Mountain Spring	0.87	0.70926
17	M12	Shell Well #2	0.46	0.70909
10	M13	Shell Well #3	0.47	0.70905
5	M14*	Hyattville Municipal Well	0.495	0.70873
18	M15*	Worland Municipal Well	0.284	0.70941
19	P1	PBS	2.96	0.70825
21	P2	Clay Well	6.42	0.70847
23	P3	Greybull Cemetery	8.34	0.70856
22	P4	Hillsboro Stream	2.20	0.70789
24	P5*	Tensleep Spring	0.42	0.71220
26	Flathead	Mayland-Leavitt Well	0.12	0.71601
25	Thermopolis	Thermopolis	2.82	0.71558

Table 5.3: Strontium data for water samples. The Sr site ID refers to the locations in Figure 3.1. The analysis # references the complete water chemistry listed in Appendix B. A * next to the Sr site ID designates a sample from Frost and Toner (in press), all other samples were collected as part of this study. Samples in italics are duplicates of the same site that are not plotted in Figure 5.4.

Source	Location	Geology	87Sr/86Sr
This study	Outcrop above PBS spring	Phosphoria Lm	0.70722
This study	Lower Kane Cave entrance	Madison Lm	0.70804
This study	Salamander entrance	Madison Lm	0.70797
Frost and Toner (in press)	-	Madison Lm	0.70809
Frost and Toner (in press)	-	Madison Paleokarst	0.70875
Frost and Toner (in press)	-	Tensleep Ss	0.71123

Table 5.4: Strontium data for analyses of whole rock samples. Samples from this study come from outcrops of the Phosphoria and Madison Limestones in the Little Sheep Mountain Canyon. Samples from Frost and Toner (in press) come from locations near the town of Hyattville, Wyoming.

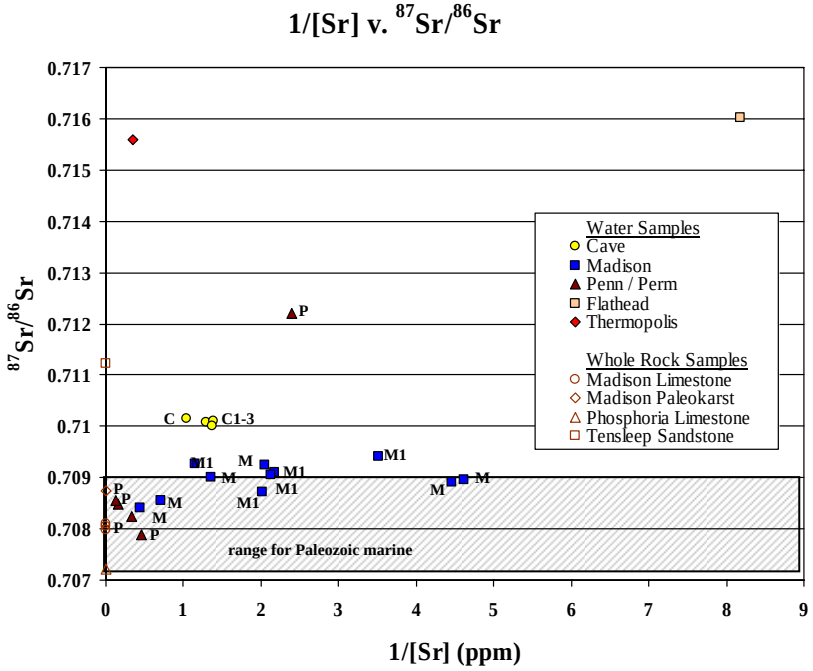

Figure 5.3: Sr data for waters of the Paleozoic aquifer, northeast Bighorn Basin. Data point labels refer to the sampling locations shown in Figure 3.1. Error bars are not shown, as the sampling error of less than +/-0.00002 is smaller than the data points. The full range of $^{87}Sr/^{86}Sr$ for marine Paleozoic carbonates is shown above. The breakdown of this range according to depositional era is as follows: Ordovician: 0.7078 – 0.7089; Devonian: 0.7078 – 0/7088; Mississippian, 0.7075 – 0.7083; Pennsylvanian: 0.7080 – 0.7082; Permian: 0.7067 – 0.7081 (Faure, 1986, Figure 11.2).

5.4 Little Sheep Mountain Springs

Lower Kane Cave

Water samples from Lower Kane Cave are Ca-Mg-HCO_3-SO_4 in type, with consistent temperature, pH, conductivity and major ion chemistry between springs. The waters are relatively fresh, with conductivity values averaging 569μS, and circum-neutral pH averaging 7.2. The waters of the cave springs are thermal, averaging 21.5˚C, and reducing, with measured concentrations of hydrogen sulfide up to 1.1ppm. A Piper diagram of the waters of Lower Kane Cave is shown in Figure 5.4. Schoeller diagrams of the groundwater chemistry of the Lower Kane Cave springs, as well as the other springs of Little Sheep Mountain, are presented in Figure 5.5. Figure 5.2 presents Stiff diagrams for the samples analyzed for Sr data. The Ca/Mg ratios of the cave waters are constant at 1.8 +/- 0.1. Data from Lower Kane Cave and Hellespont Cave are listed in Table 5.5, while the range and averages for field parameters and major ion analyses for Lower Kane Cave and Hellespont Cave are shown in Table 5.6.

All Lower Kane Cave waters sampled have $^{87}Sr/^{86}Sr$ values between 0.71001 and 0.71012 and Sr concentrations between 0.71 and 0.77 ppm. This sample set includes 6 total data points split between Fissure Spring (1 sample), Upper Spring (3 samples), and Lower Spring (2 samples). Values of $\delta^{18}O$ for Lower Kane Cave spring waters ranged between -19.5 and -20.0‰. The spring water from Upper Spring analyzed for ^{14}C returned values for $\delta^{13}C$ of -8.33‰ with respect to VPDB, with 37.31 +/- .21 PMC, yielding an estimated age of 7,920 ± 45 years (Mitzi DeMartino, The University of Arizona, personal communication). Lower Kane Cave is characterized by a high level of radioactivity: radon levels in the cave atmosphere were detectable by a handheld

radiation detector, and dissolved uranium is present in the groundwater at an average concentration of 27ppb, with a high concentration measured at 45ppb.

The chemistry of the cave springs shows only minor variations over the field sessions between 2000 and 2003. However, the spring samples from earlier studies at Lower Kane Cave by Egemeier (1981) and Doremus (1986) (analysis #'s 32, 39, 40, 47, 48 and 49 in Appendix B) are more concentrated in all major constituents other than bicarbonate, containing 25-30% more Ca and Mg, 65% more SO_4 (Figure 5.6), and over 200% more Cl. The waters sampled by Egemeier are also more thermal than modern values, averaging 23.5˚C (Figure 5.7). However the 1981 measurement of Lower Kane Cave by Doremus (1986) lists a modern value of 21˚C. These studies also measured spring H_2S levels of 5ppm, a significant increase over present day values (Figure 5.8).

Hellespont Cave

Hellespont Cave waters are also Ca-Mg-HCO_3-SO_4 in type. With an average conductivity of 690µS, the Hellespont spring is more concentrated in the major elements (by 25-100%) than the springs of Lower Kane Cave. Bicarbonate is an exception, with similar levels at both Hellespont and Lower Kane Caves. Hellespont Cave is also slightly less thermal than Lower Kane Cave, at an average temperature of 18.2˚C. Due to access constraints at Hellespont Cave, the sample from July, 2002 was collected outside the cave entrance just upstream of the discharge point into the Bighorn River. This sample is excluded from the average temperature calculation, as solar heating may be responsible for raising the temperature of this sample to 19.1˚C. Hellespont Cave waters measured by Egemeier (1981) contain higher major ion concentrations than modern waters (Figure 5.6), although by a slightly smaller margin than at Lower Kane Cave. At 19.5˚C, the waters listed in Egemeier (1981) are also 1.3˚C more thermal than

modern waters (Figure 5.7), and, at 13ppm, contain significantly higher concentrations of H_2S (Figure 5.8). The spring water from Hellespont Cave analyzed for strontium data contained 0.96 ppm of Sr with a $^{87}Sr/^{86}Sr$ value of 0.71015. At an average concentration of 1.03 ppm for all samples, Hellespont Cave spring water consistently contains 30% more Sr than the Lower Kane Cave springs. The measured $\delta^{18}O$ values at Hellespont Cave are comparable to those at Lower Kane Cave. However, the uranium content of the spring waters is approximately 1/3 of that measured in Lower Kane Cave spring water.

Salamander Cave

Although located in the same stratigraphic unit of the Madison Limestone as Lower Kane Cave, the water discharging from Salamander Cave is chemically distinct. Salamander Spring waters are Ca-Mg-HCO_3 type, with conductivity values averaging 480µS. All constituents are more dilute than the waters of Lower Kane Cave, and SO_4 comprises a lower percentage of the total solutes. Salamander waters are well oxygenated, with no measurable H_2S content. A measured $\delta^{18}O$ value of -19.5‰ is within the range of Madison waters. Salamander spring water contains 0.50 ppm of Sr with a $^{87}Sr/^{86}Sr$ value of 0.70925. Uranium levels are lower than at Lower Kane Cave, although still relatively high at 9ppb. The chemistry and Sr signature for Salamander spring water places this spring within the measured range for the Madison aquifer.

PBS Spring

PBS Spring is separated both geographically and stratigraphically from Lower Kane Cave, discharging from the upper limestone unit of the Phosphoria Formation. Compared to Lower Kane Cave, PBS waters are significantly more concentrated, particularly in Na, Cl and SO_4, with measured conductivity values

between 2200 - 2450μS. PBS Spring waters are reducing, with high concentrations of H_2S at 5 ppm. At 13.2˚C, PBS spring is significantly cooler than waters of the underlying Madison Limestone, and the $\delta^{18}O$ value of -18.5‰ for PBS spring water is less depleted than at Lower Kane Cave or for the Madison aquifer as a whole. PBS spring water contains 2.96 ppm of Sr with a $^{87}Sr/^{86}Sr$ value of 0.70825. The chemistry and strontium signature of PBS spring water places this spring within the range for the samples from the Pennsylvanian / Permian aquifers.

	#	Date	T	pH	DO	Cond	H_2S	Cl	HCO3	SO4	Na	Ca	Mg	CBE	Si	Fe	U	SI	
			˚C		ppm	µS	ppm	ppm	ppm	ppm	ppm	ppm	ppm	%	ppm	ppm	ppb	Gypsum	Calcite
Fissure Spring	27	Jun-03	-	-	-	569	0.7	4.4	201	116	6.8	76	24	1	5	0.02	23	-1.54	0.03
	28	Aug-02	21.6	7.4	-	561	0.8	4.0	201	110	7.0	73	27	3	6	0.05	29	-1.54	0.05
	30	Aug-01	22	7.3	0	580	0.4	4.4	209	115	5.8	68	23	-5	5	0.03	24	-1.57	-0.09
	31	Aug-00	21.3	-	-	-	0	5.4	214	156	7.1	89	27	-1	6	0	-	-	-
	32	Jun-70	23.5	6.8	0	695	5	14.5	195	319	10	140	34	-1	17	0	-	-0.97	-0.38
Upper Spring	33	Jun-03	22.12	7.4	0.05	562	-	4.3	206	107	6.5	73	24	1	4	0	24	-1.58	0.05
	34	Jul-02	21.9	7.4	-	547	0.9	4.4	202	108	7.3	74	27	4	5	0.03	26	-1.52	0.12
	35	Dec-01	20.4	7.0	0.4	524	-	5.3	212	143	5.7	76	26	-5	5	0	45	-1.45	-0.41
	36	Jul-01	21.3	7.4	0	577	1.1	5.3	211	110	5.9	70	23	-3	5	1.23	20	-1.58	0.01
	38	Aug-00	-	-	-	-	0.6	5.2	215	122	7.7	77	27	1	6	0.01	-	-	-
	39	Jun-70	24	7.0	0	550	6	12.3	213	182	11	90	29	-2	0	0	-	-1.32	-0.27
	40	Jun-70	23.5	6.9	0	550	6	12.5	218	189	11	97	31	-1	0	0	-	-1.28	-0.34
Lower Spring	41	Jun-03	21.5	7.2	-	562	0.8	4.3	209	107	6.1	72	24	0	4	0	23	-1.58	-0.14
	42	Jul-02	21.7	7.3	-	615	0.8	4.7	207	110	7.2	74	28	3	5	0.02	25	-1.52	-0.05
	46	Aug-00	22.8	6.9	2.7	-	0.5	5.1	213	124	7.1	82	28	3	6	0.01	-	-	-
	47	Jun-70	23.5	7.3	0	*525*	5	12.5	218	195	11	96	32	-1	0	0	-	-1.28	0
	48	Jun-70	23.5	7.1	0	*525*	5	12	218	218	11	104	31	-2	0	0	-	-1.21	-0.12
	49	May-81	21	7.8	-	-	-	11.2	218	198	10.5	104	29	-1	-	-	-	-	-
Hellspont	50	Jul-02	19.1	7.4	-	663	0.4	9.0	214	161	9.0	90	32	2	6	0.01	10	-1.36	0.05
	52	Aug-00	18.1	7.4	-	-	0.6	12.0	212	188	10.0	92	32	-2	5	0	-	-1.29	0.03
	53	Aug-00	18.2	7.2	-	-	1.2	11.0	217	189	11.0	99	34	1	5	0	-	-1.27	-0.09
	54	Jun-70	19.5	7.3	0	-	8	19	236	275	15	122	32	-4	16	0	-	-1.07	0.05
	55	Jun-70	19.5	7.1	0	-	13	19	236	269	16	119	39	-1	16	0	-	-1.09	-0.11

Table 5.5: Field paramaeter and elemental data for samples from Lower Kane and Hellspont Cave. Only samples with complete major ion chemistry and charge balance < 5% are included. See Appendix B for a complete compilation of all data for samlpes collected for this study, the # column refers the analysis # in this appendix. Samples collected in 1970 are from Egemeier (1981), while sample #49 from 1981 is from Doremus (1986).

Lower Kane	Temp. (˚C)	pH	Cond. (µS)	F ppm	Cl ppm	HCO3 ppm	SO4 ppm	Ca ppm	Mg ppm	Na ppm	K ppm
Fissure Spring											
Average	**21.2**	**7.3**	**580**	**0.8**	**5**	**208**	**129**	**72**	**25**	**6.6**	**1.6**
Range	19.9 - 22	7.2 - 7.4	561-611	0.5 - 1.1	4 - 5	201 - 214	115 - 156	68 – 76	23 - 27	5.8 - 7.1	0.3 - 2.3
# samples	4	4	4	3	3	3	3	3	3	3	3
Upper Spring											
Average	**21.7**	**7.2**	**553**	**0.9**	**5**	**212**	**121**	**74**	**25**	**6.5**	**1.4**
Range	20.4 - 22.1	6.9 - 7.4	524-577	0.6 - 1.0	4 - 6	205 - 215	107 - 143	70 – 77	23 - 27	5.7 - 7.7	0.3 - 2.0
# samples	5	5	4	4	5	5	5	5	5	4	3
Lower Spring											
Average	**21.5**	**7.2**	**557**	**0.8**	**5**	**210**	**119**	**76**	**27**	**6.6**	**2.1**
Range	20.2 - 22.8	6.9 - 7.6	539-615	0.8 - 0.9	4 - 6	209 - 213	107 - 125	72 - 82	24 – 28	6.1 - 7.1	1.9 - 2.2
# samples	6	6	4	2	3	3	3	3	3	2	2
Hellspont Cave											
Average	**18.4**	**7.3**	**690**	**1.1**	**10**	**214**	**180**	**94**	**33**	**9.8**	**2.8**
Range	18.1 - 19.1	7.2 - 7.4	663-718	0.9 - 1.3	9 - 12	212 - 217	161 - 189	90 - 99	32 - 34	8.6 - 10.5	2.5 - 3.0
# samples	4	4	2	3	3	3	3	3	3	3	3

Table 5.6: Table of water chemistries for the discharge from the springs at Lower Kane Cave over field sessions between August 2000 and June 2003. This table lists composite values averaging over the whole cave, as well as values broken out by individual spring. Data for Hellspont Cave is included in the table as groundwater chemistries are similar between the two cave, and Hellspont is believed to derive in part from the same source of groundwater as Lower Kane Cave. Major ion data included in this table utilizes only those samples with charge balance error <5%.

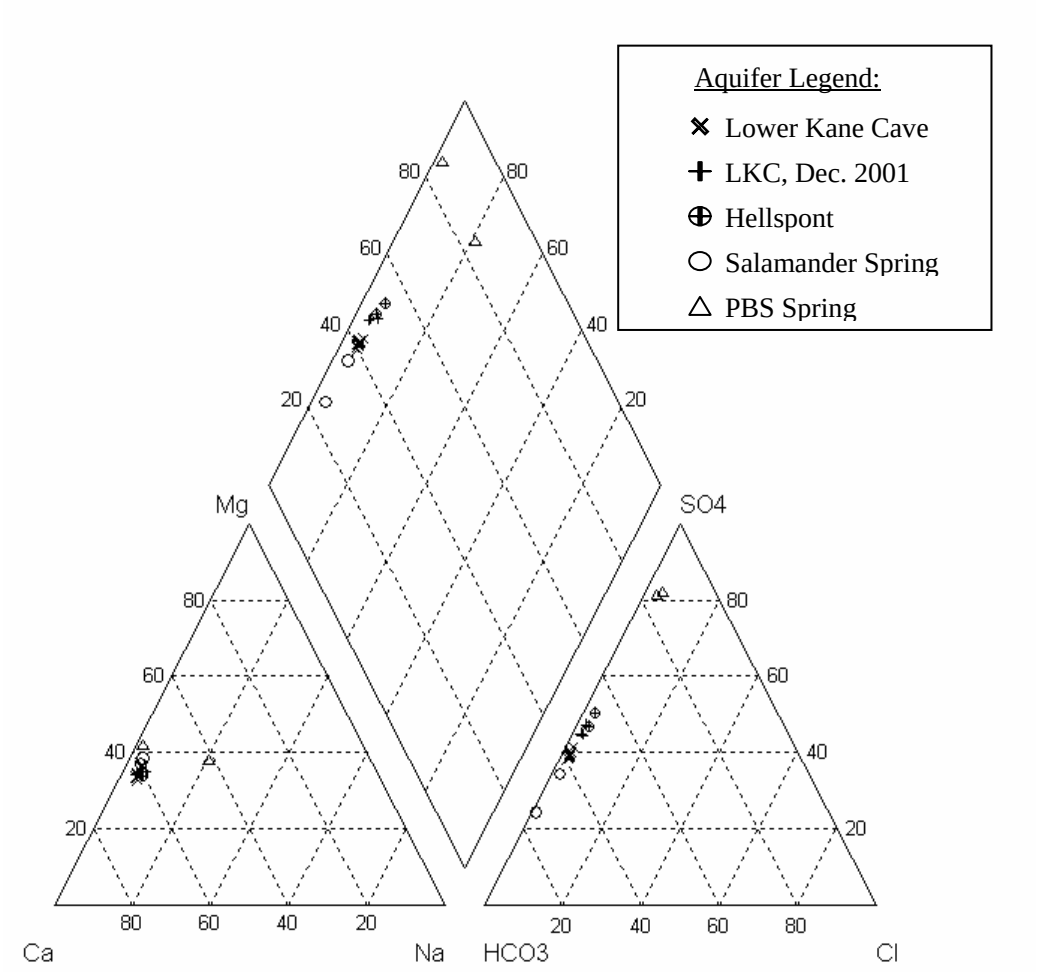

Figure 5.4: Piper Diagram of samples from the springs of Little Sheep Mountain. Note that the majority of the Lower Kane Cave data points cluster tightly together, but the samples from December, 2001 are shifted toward increased SO_4, in the direction of the samples from Hellspont Cave. For clarity, the Lower Kane Cave samples from the study by Egemeier are not shown, however the samples would plot in the range of the Hellspont samples.

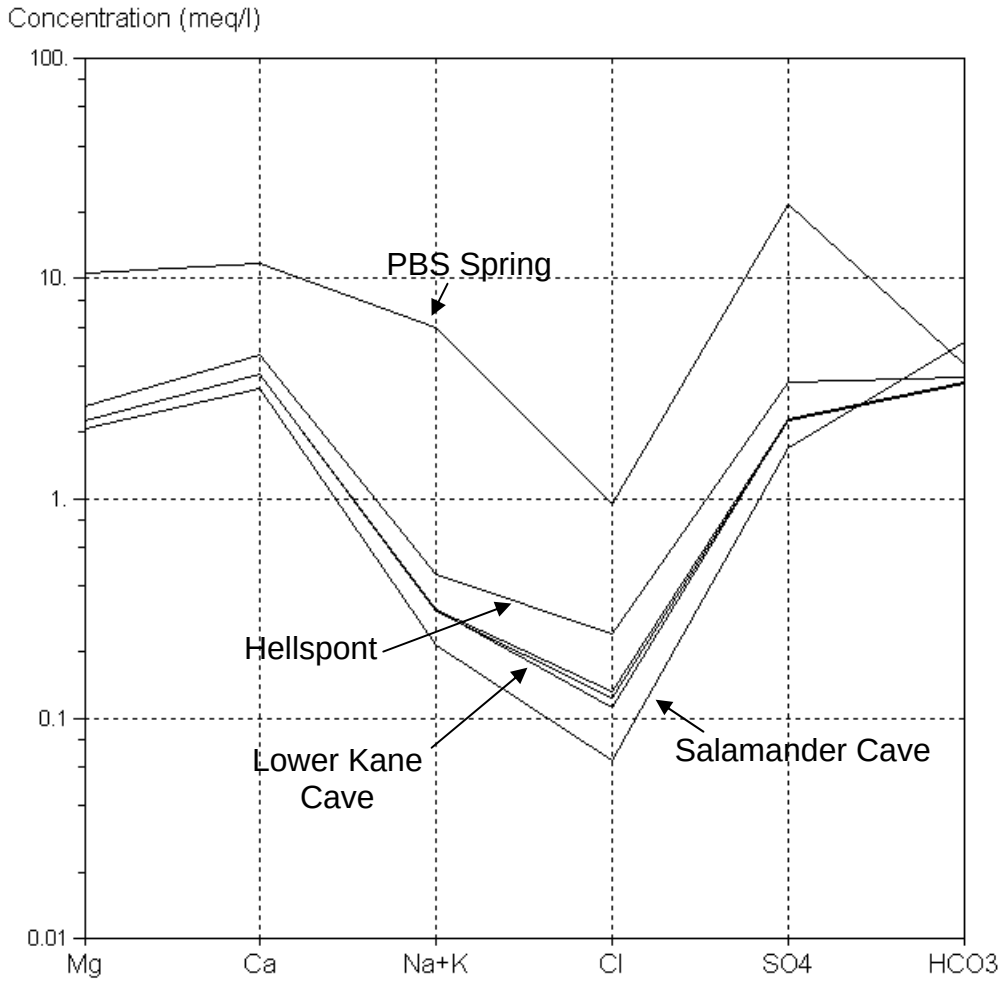

Figure 5.5: Schoeller Diagram illustrating the chemical characteristics of waters from the springs in Little Sheep Mountain. The three springs of Lower Kane Cave display very similar water chemistry in terms of absolute concentration and distribution of constituents.

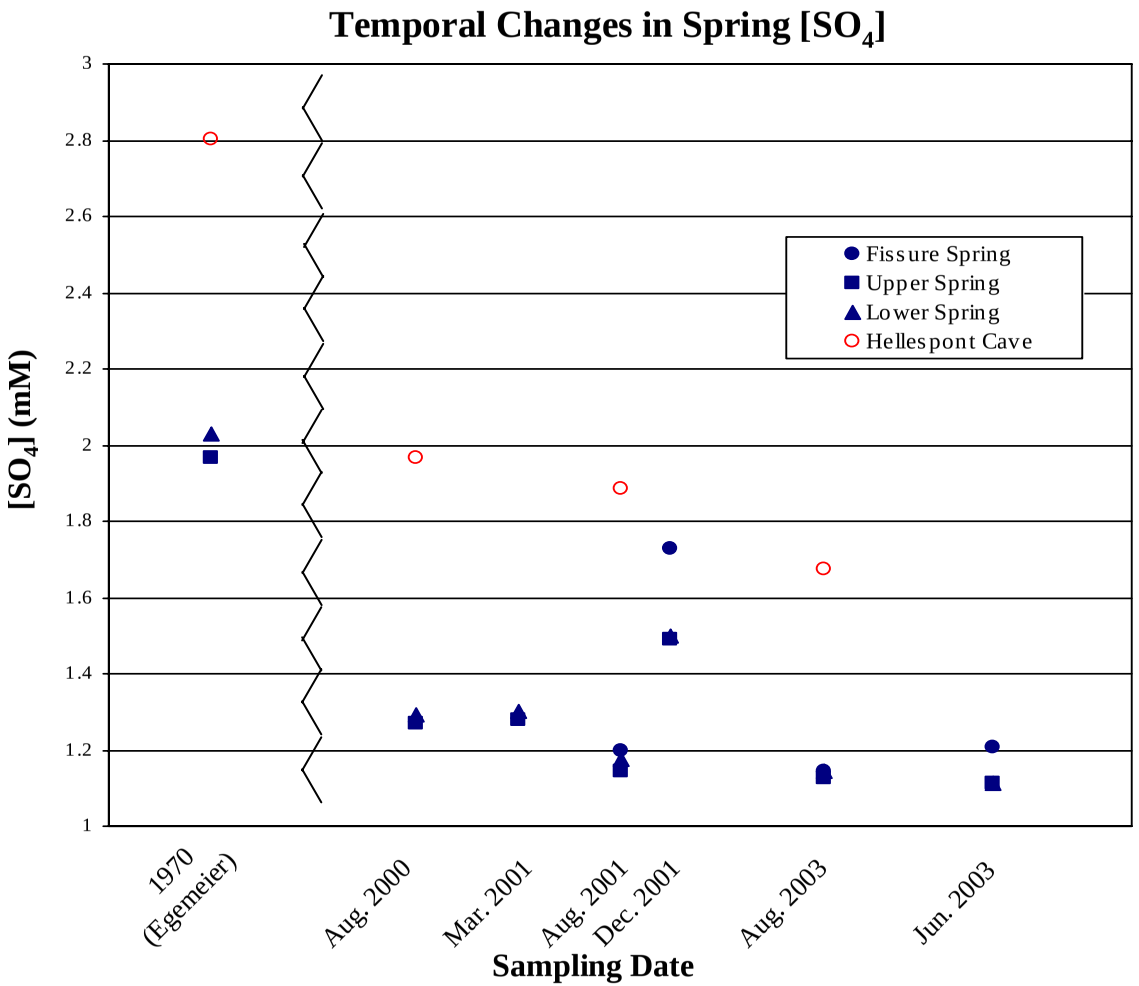

Figure 5.6: Temporal Changes in dissolved SO_4 in the cave spring water at Lower Kane and Hellespont Caves. Fissure, Upper and Lower springs (shown with blue symbols) are all in Lower Kane Cave.

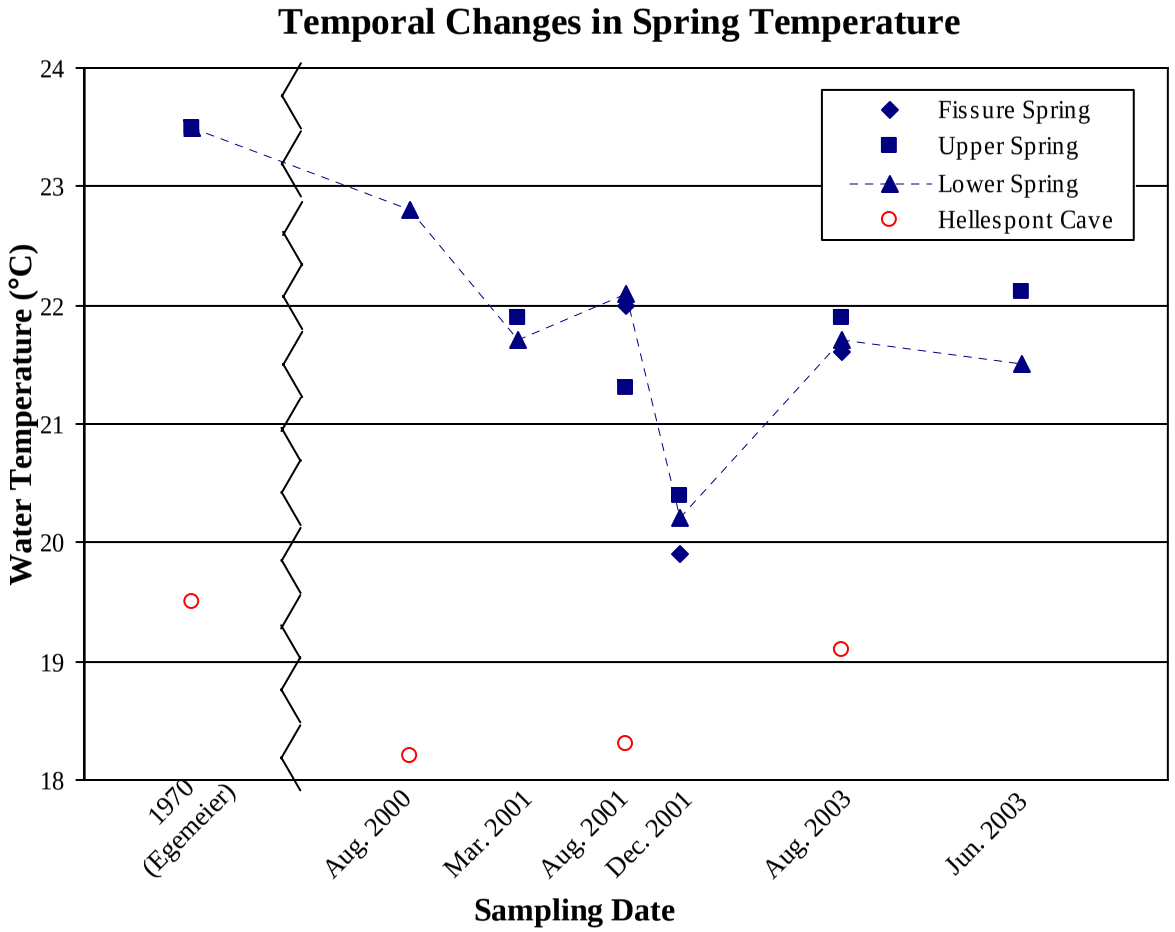

Figure 5.6: Temporal Changes in the water temperature of cave springs in Lower Kane and Hellespont Caves. Fissure, Upper and Lower springs (shown with blue symbols) are all in Lower Kane Cave. The dashed line connects data points from Lower spring and represents the general trend over time.

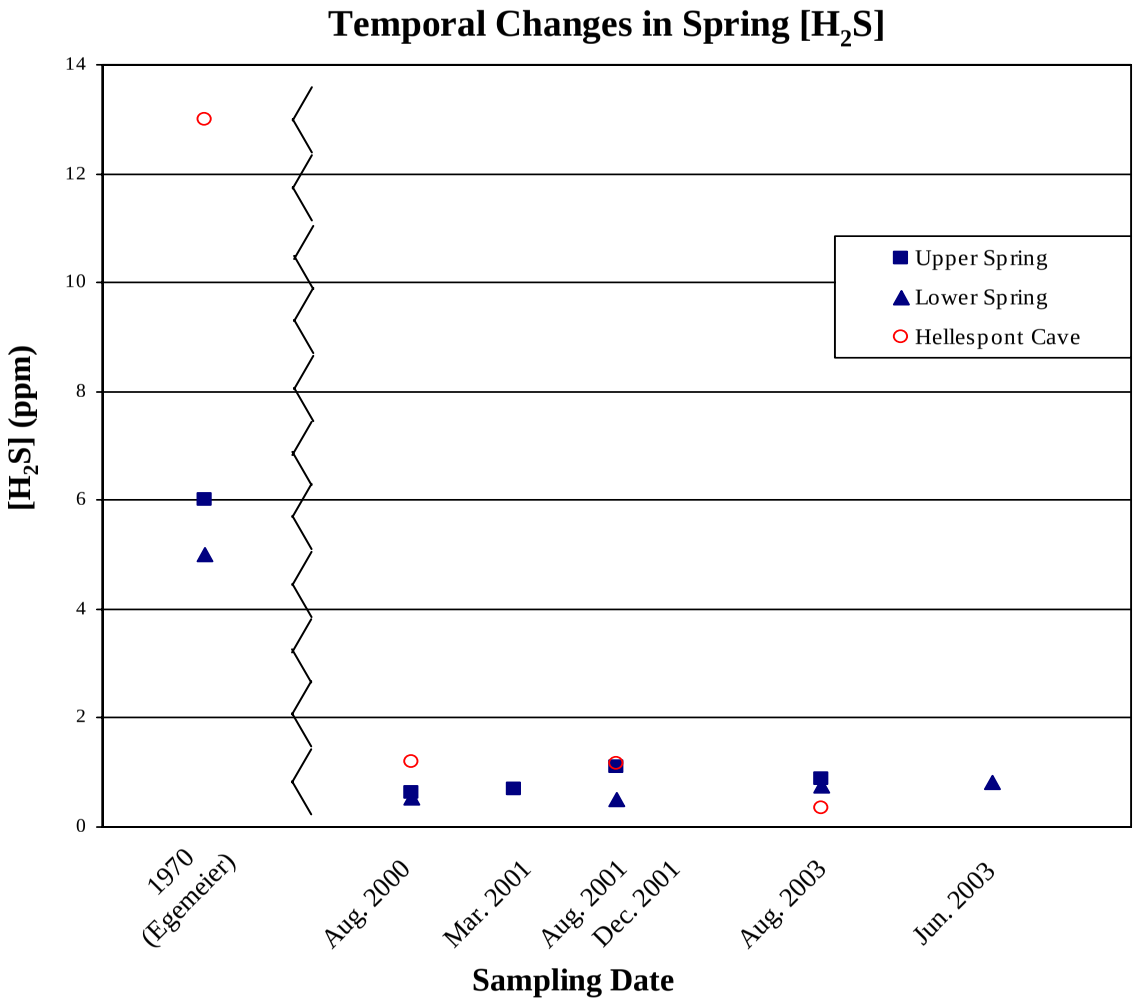

Figure 5.8: Temporal Changes in dissolved H_2S in the cave spring water at Lower Kane and Hellespont Caves. Fissure, Upper and Lower springs (shown with blue symbols) are all in Lower Kane Cave.

6. DISCUSSION

The geochemical and Sr characteristics of the waters analyzed in this study provide an in depth characterization and interpretation of the Paleozoic aquifers, particularly the Madison. Lower Kane and Hellespont Cave are discussed separately from the Madison aquifer, as the chemical and Sr data suggests a partial non-Madison origin for these waters. The data from this study are used in an interpretation of potential radiogenic Sr and evolutionary flow paths that could explain the observed chemistry of the Lower Kane Cave springs.

6.1 Characterization of Paleozoic Groundwater

Madison Aquifer

The geochemical results for the Madison aquifer show a consistent chemical facies of well oxygenated, Ca-Mg-HCO_3 type waters over a large spatial area along the eastern margin of the Bighorn Basin. Consistency between Stiff diagrams for the Madison aquifer water samples shown in Figure 5.2 suggest that this pattern is characteristic of Madison waters along the eastern margin of the Bighorn Basin.

Samples M4-6 are an exception to the Madison trend, with Stiff diagram patterns intermediate between those of the Madison aquifer and the overlying Pennsylvanian / Permian aquifers. The two oil field waters (M5 and M6) are produced from older wells that were drilled in 1946 and 1957, respectively. Casing in these wells has deteriorated over time, and the owner believes that leakage from the overlying units is entering these wells (Milo Johnson, personal communication). This hypothesis is supported by the standard Madison chemistry and Stiff patterns for water from two nearby wells in the same oil field (M7 and M8) that were drilled and cased in 2001. Thus the observed variation in

geochemical and Sr isotopic signatures between the general Madison waters and samples M4-6 likely represents evidence of leakage from overlying units.

The geochemical results presented here agree with previous work in the Paleozoic aquifers of the Bighorn Basin (Lowry and Lines, 1972; Libra et al. et al., 1981; Doremus, 1986) that found similar type waters in the Madison aquifer on the basin's northeast margin. Results from previous studies in the southern Bighorn Basin (Jarvis, 1986; Spencer, 1986) as well as in the Madison aquifer of eastern Wyoming, Montana and the Dakotas (Busby et al., 1991; Plummer, 1990) also parallel these results, and span the range of chemistries observed here.

Previous studies also showed significant increases in salinity and changes in the chemical facies, including noteworthy relative increases in SO_4 and Cl concentrations, in Madison aquifer samples from oil fields in the more central areas of the basin. Many of the more saline Madison waters samples in the literature come from early work by Crawford (1940, 1964) on oil-field waters of the Bighorn Basin. Oil-field reservoirs of the Bighorn Basin are generally located in subsurface, reverse-fault cored anticlines of similar structure to those breached by the Bighorn River. The extensive faulting and fracturing in these structures has led to the development of common Paleozoic oil reservoirs, and thus extensive intermingling of groundwater between formations (Stone, 1967). Such inter-formational mixing may be augmented by the operation of hydrocarbon extraction and injection wells. Thus, these saline water samples, although drawn from wells cased in the Madison matrix, may represent a composite Paleozoic geochemistry, rather than that of just the Madison aquifer. Alternatively, these waters may indicate the existence of a saline Madison water in the Basin center that is distinct from the fresh waters on the basin margins, most likely due to differences in residence times within the aquifer.

The majority of Madison aquifer samples have $\delta^{18}O$ values that fall between -19.6 and -19.9‰, with a higher value of -19.3‰ measured at the Spence oil field well #74. Water from the Cowley Municipal well is slightly higher than the main trend, with a $\delta^{18}O$ value of -19.0‰. This well is located northwest of the cave, and is most likely recharged from the Pryor Mountains to the North (Western Water Consultants, 1982; see Figure 2.3). This $\delta^{18}O$ value may indicate that recharge in the Pryor Mountains occurs at slightly lower elevations as compared to the Bighorn Mountains, and therefore oxygen isotope data may be able to distinguish between recharge areas in the Pryor and Bighorn Mountains. More oxygen isotope data from samples along the Pryor Mountain recharge pathway are necessary to determine this.

While the samples from the Madison aquifer were taken from a large spatial area and vary in Sr concentration over a range from 0.22 to 2.24 ppm, values for $^{87}Sr/^{86}Sr$ are limited to a range between 0.70840 and 0.70925, a variation of 0.00101. The range in Sr isotope data for "pure" Madison aquifer water may be even narrower than this, as the incorporation of water from overlying units that impact major ion chemistry may also contribute higher Sr concentrations and lower values of $^{87}Sr/^{86}Sr$. The Madison waters (M4 and M6) that contain increased conductivity and SO_4 concentrations also possess the lowest $^{87}Sr/^{86}Sr$ and highest Sr concentrations of all the Madison samples (Figure 5.3; Sr isotope data is unavailable for location M5). If water from overlying aquifers is indeed leaking into these wells and contributing significant amounts of less radiogenic Sr, then the true range in Sr signature for Madison waters is actually less concentrated in Sr, with an increased base level of $^{87}Sr/^{86}Sr$. Excluding these two samples for evidence of contamination reduces the range of [Sr] to between 0.22 and 0.74, and the total variation in $^{87}Sr/^{86}Sr$ for Madison waters to 0.00068 ($^{87}Sr/^{86}Sr$ ratios between 0.70873 – 0.70941).

In addition to the two samples mentioned above, three Madison samples (M3, M7 and M11) possess values of $^{87}Sr/^{86}Sr$ that are slightly higher than the main trend for Madison waters (Figure 5.3). In the case of M11 (the Worland Municipal well (Frost and Toner, 2004)), this larger $^{87}Sr/^{86}Sr$ is accompanied by a low concentration of Sr. The waters at both site M3 (Salamander Spring) and M7 (Sheep Mountain spring) discharge from springs in the heart of breached anticlines: Little Sheep and Sheep Mountain, respectively. The slight increase in $^{87}Sr/^{86}Sr$ at these springs may result from the input of a small amount of a deep seated water with more radiogenic Sr in these locations, a hypothesis discussed further in the sections on the origin of groundwater to Lower Kane Cave.

Even including the samples with slightly higher ratios, the Sr signature of Madison waters appears fairly constant over a large range of Sr concentrations. This suggests that the groundwater equilibrates fairly rapidly with Sr content of the host rock, such that continued dissolution of carbonates, while increasing the total amount of dissolved Sr, does not further impact the $^{87}Sr/^{86}Sr$ ratio. The small observed range in $^{87}Sr/^{86}Sr$ of these samples is likely due to the fact that, although hydrologically connected, the Madison aquifer is not homogeneous throughout the entire Ordovician to Mississippian saturated thickness or across the area of study, and the assorted Madison wells case individual subsections of the aquifer.

The $^{87}Sr/^{86}Sr$ ratios for the Madison aquifer are consistently more radiogenic than published marine carbonate values for the Mississippian, and are also higher than measured whole rock values from regional Madison Limestone samples. This radiogenic Sr appears to be widespread throughout the aquifer, and could be due to one or a combination of the following factors:

1) *The incorporation of siliciclastic material within the Madison rock units.* While the Madison Limestone is predominantly a carbonate unit, small amounts of siliciclastic material are present. In particular, large amounts of

clay materials from the Pennsylvanian have filled in collapse features in the paleokarst zone of the upper Madison (Sando, 1988). The siliciclastic components of such units are expected to possess higher $^{87}Sr/^{86}Sr$ ratios due to a greater Rb content and the long period of time since deposition.

2) *Alteration in the host rock due to diagenesis during periods of karstification and subsequent burial, in particular along paths of preferential flow, such that the matrix the groundwater currently interacts with possesses a more radiogenic Sr signature*. Secondary permeability is considered to be the predominant control on groundwater flow in the Madison aquifer (Huntoon, 1993; Libra et al. et al., 1981), thus travel along fractures and dissolution pathways are the likely conduits for groundwater flow, and may contribute a disproportionate amount of water to wells. Groundwater-rock interactions along these paths over the approximately 60 Ma since the Laramide Orogeny may have created alteration zones of increased radiogenic Sr content along the margins of these pathways. While such alterations in the Sr isotope signature were not observed in the whole rock samples analyzed for this study, the presence of bright colored, fine grained secondary minerals in outcrop above Lower Kane Cave provides evidence of hydrothermal alteration (L. Stern, personal communication). A more systematic assessment of formation chemical heterogeneity within the Madison would therefore be necessary to discount this hypothesis.

3) *A significant portion of the groundwater in the Madison aquifer derives from the underlying Bighorn Dolomite, which has a higher $^{87}Sr/^{86}Sr$ ratio.* The $^{87}Sr/^{86}Sr$ of Ordovician marine carbonates are more radiogenic than those from the Mississippian, and the Madison aquifer waters fall at and slightly above the high end of this range. Whole rock analysis of the Bighorn

Dolomite would help clarify this issue by definining the actual $^{87}Sr/^{86}Sr$ ratios for this formation.

The incorporation of siliciclastic material within the Madison aquifer host material is the most probable explanation for the increased $^{87}Sr/^{86}Sr$ values observed in Madison aquifer waters. This hypothesis is supported by the more radiogenic $^{87}Sr/^{86}Sr$ signature of the paleokarst whole rock sample, analyzed by Frost and Toner (2004), as compared to the limestone samples from the Madison analyzed in this study. Additionally, the Devonian Jefferson provides a potential source of siliciclastic components within the aquifer. However, the other possibilities can not be the ignored. Whatever the reason for the radiogenic Sr in the Madison aquifer, it appears to be widespread, and consistent across the basin. Additionally, if the variations in $^{87}Sr/^{86}Sr$ observed at select Madison locations in this study are indeed due to contributions from other formations, than changes in chemistry and Sr characteristics may provide a diagnostic tool for assessing leakage within Madison wells of the Bighorn Basin.

Pennsylvanian / Permian Aquifers

Due to the scarcity of sampling sites, the Pennsylvanian and Permian aquifers – the major Tensleep Sandstone aquifer and the minor Amsden and Phosphoria Formation aquifers – are not as well characterized as the Madison aquifer. However, the waters collected agree with results from earlier studies (Lowry and Lines, 1972; Libra et al. et al., 1981; Doremus, 1986). As expected, these waters are Ca-Mg-HCO_3-SO_4 type, and generally contain significantly more dissolved solutes than Madison waters.

Four of the five waters (P1-P4) from the Pennsylvanian and Permian aquifers are uniformly high in SO_4 and TDS. Not only are all major constituents more concentrated in these waters when compared to Madison waters, but, as

shown in Figures 5.2 and 5.4, the relative proportions of ions in the samples are different, with SO_4 representing the dominant ion in solution for all four samples. The Ca/Mg ratio is higher at the Greybull Cemetary well, but lower at PBS Spring and the Clay Well.

The Tensleep spring water (P5) sampled by Frost and Toner (2004), provides the exception to the generally poor quality of water from the Pennsylvanian / Permian aquifers. Unlike the other four samples, this spring is fresh, Ca-Mg-HCO_3 in type, with only minor amounts of SO_4. Although waters of the Tensleep aquifer are often considered to be generally poor in quality (Doremus, 1986; Libra et al. et al., 1981; Lowry and Lines, 1972), in some areas, such as the region near Tensleep, Wyoming, the Tensleep Sandstone contains high quality water with TDS values similar to those in the Madison (Cooley, 1986). Since the Tensleep is often co-produced with waters from the overlying Phosphoria Formation and underlying Amsden Formation, both of which contain poor quality water that is high in sulfate (Cooley, 1986), it is unclear if the development of poor quality water in Tensleep wells is the result of groundwater evolution within the formation itself, or as the result of incorporation of water from the Amsden and Phosphoria Formations, either within the aquifer or at the location of the well. The Tensleep spring may indicate that the poor quality of many Tensleep waters, such as at the Clay Well, actually result from incorporation of water from the Amsden or Phosphoria Formations. Alternatively, the fresh quality of this spring may be the result of its location near the recharge zone, such that the groundwater is early in its evolutionary path, and has not yet reacted extensively with the host matrix.

Both the Clay well (P2) and the Greybull Cemetary well (P3) posess high iron concentrations, with 8 ppm of iron measured in water from the P2. Although measured iron content at P3, on the order of 40ppb, was far less, waters from this

well are known to contain high amounts of iron (Bob Graham, personal communication). Evidence for this is visible in the red coating, likely an iron oxide, that covers the well head and ground around this site. The measured concentrations of iron at this site are possibly low as the result of sampling from a high pressure, aerated spray.

With a $\delta^{18}O$ value of -18.5‰, the oxygen isotope data for the sample from PBS spring is less depleted than the Madison waters, while water from P2 is more depleted, with a $\delta^{18}O$ value of -21.8‰. Oxygen data is not available for the other Pennsylvanian and Permian samples. The greater range of $\delta^{18}O$ values in these non-Madison waters suggests that these waters are likely the result of a less homogenized aquifer system, and may indicate variations in recharge areas for the two sites. More $\delta^{18}O$ data from the Pennsylvanian / Permian aquifers is necessary to evaluate potential trends or implications for groundwater flow within this hydrostratigraphic section.

Excluding water from the Tensleep spring (P5), samples from the Pennsylvanian / Permian aquifers are characterized by relatively high Sr concentration, and relatively low $^{87}Sr/^{86}Sr$ values. The two well waters (P2 and P3), although separated by about 18 miles, plot close to one another in Sr space. Both these wells sample groundwater from a thick stratigraphic section. Stiff diagrams for these two waters are similar in shape, as variations in the Ca/Mg ratio represent the primary chemical difference between the two waters. The similarity of the Sr signature between the two samples suggests the possibility that a particular unit or units within the hydrostratigraphic section sampled by both wells is the primary contributor of Sr to the groundwater at these wells. Thus, although the Pennsylvanian and Permian sedimentary sequence is heterogeneous, particular units that provide the main contribution to flow within this section may

dominate the water chemistry and Sr signature of water from wells that sample large hydrostratigraphic sections.

Since Ca containing rocks are the principal mineral source of Sr, this primary contributors of Sr is likely carbonate and gypsum layers within the Pennsylvanian and Permian section. However, although lower than values for the Madison waters, the $^{87}Sr/^{86}Sr$ ratios at these two wells is higher than the range for Pennsylvanian and Permian marine carbonates, suggesting that siliciclastic components within the host rock do contribute small amounts of Sr to the groundwater in these aquifers.

While the wells are known to draw from a large hydrostratigraphic section, waters from PBS spring (P1) and the Hillsboro stream (P4) emerge from discrete locations. With a $^{87}Sr/^{86}Sr$ of 0.70825, the spring water has a significantly higher $^{87}Sr/^{86}Sr$ than the Phosphoria Limestone whole rock sample from this site, however, the ratio does falls within the marine range for deposition during the early Permian and Pennsylvanian. Assuming low concentrations of Sr in sandstone aquifers, the spring water at PBS spring may result from Tensleep water traveling up along fractures into the Phosphoria Formation, where it dissolves gypsum. This mechanism has been used to explain other wells in the Phosphoria further south in the Bighorn Basin (Cooley, 1986), and could explain the high concentration at this spring of constituents associated with siliciclastic units, in particular the Na far in excess of Cl, while providing the necessary source of high amounts of Sr with a low $^{87}Sr/^{86}Sr$ ratio.

The Hillsboro stream waters had the lowest Sr concentration and $^{87}Sr/^{86}Sr$ ratio of all the samples in this study. The $^{87}Sr/^{86}Sr$ ratio of this water is consistent with marine carbonates deposited during either the Mid-Mississippian or the Permian era. Due to its location in the Pryor Mountains, this sample likely undergoes different evolutionary flowpaths from the samples further south,

which, assuming similar flow paths as in the Madison aquifer, likely recharge from the Bighorn Mountains. Additionally, other changes may have occurred since this sample was collected from a surface stream.

Other Aquifers

The fresh, Na-SO_4-HCO_3 type chemistry of groundwater from the Flathead aquifer is attributed to the clean, quartzitic sandstone composition of the aquifer (Rioux, 1958) and the absence of interaction with carbonate species. While the Flathead aquifer is poorly characterized due to a lack of available sampling sites, the chemistry of this water is distinct from that of the other available sites, with Na/Cl ratios much greater than 1, suggesting a non-halite source of the Na in the water, as expected from a predominantly siliciclastic aquifer.

As anticipated in an old, siliciclastic aquifer, water from the Cambrian Flathead Sandstone is radiogenic, with a $^{87}Sr/^{86}Sr$ of 0.71601. However, because the sandstone contains relatively small amounts of Ca, the Sr concentration in groundwater from the Flathead Sandstone is low, around 0.12ppm. $^{87}Sr/^{86}Sr$ measurements of whole rock samples from the Flathead in Montana are significantly higher than that measured in the groundwater here, with samples of various rock fractions ranging in $^{87}Sr/^{86}Sr$ between 0.7363 and 0.7645 (Chaudhuri, 1969). The likely explanation for this is that a significant portion of the Sr in the groundwater derives from interactions with materials, either during recharge or within the Flathead sandstone itself, that possess lower values of $^{87}Sr/^{86}Sr$.

The Big Spring at Thermopolis Hot Springs State Park is characterized by highly thermal water containing a significant concentration of H_2S and other chemical constituents. Compared to Madison aquifer waters, the spring waters

are more concentrated in all constituents, with a greater relative percentages of total solutes derived from SO_4 and Na, and less from HCO_3 and Mg (Figure 5.2). This water also contains the highest levels of Cl observed in this study. At a $^{87}Sr/^{86}Sr$ of 0.71558 this sample is also very radiogenic. The geochemical and Sr characteristics of the Thermopolis sample distinguish it from the other waters. While studies investigating groundwater flow in the southern Bighorn Basin near Thermopolis have been conducted previously (Jarvis, 1986; Spencer, 1986), the origin of groundwater to the springs has not been definitively established. The extremely radiogenic $^{87}Sr/^{86}Sr$ values for the Thermopolis spring water suggest that the spring can not be interacting predominantly with a carbonate formation, and must be sourcing from a highly radiogenic aquifer. Such radiogenic Sr in groundwater generally derives from siliciclastic formations, and in this case may be the result of contributions from the Precambrian basement or the sandstones and shales of the Cambrian Period.

Lower Kane Cave

Variations in the chemistry of groundwater between the three main springs of Lower Kane Cave (Fissure, Upper and Lower Spring) are negligible, suggesting that the three springs are produced from the same water source and that they all emerge from a single, connected fracture system. Temporal variations in the chemistry of the spring waters have been slight over the sampling period of this study, between March 2000 and July 2003 (see Table 5.6, Figures 5.6, 5.7 and 5.8), however they appear to be part of a longer term trend towards cooler, fresher, less sulfidic water. At an average temperature of 21.5˚C, the waters are distinctly warmer than the average air temperature of 7˚C, and are also warmer than Madison waters in the region. Temperature characteristics of the cave and Paleozoic aquifers are discussed separately below.

The December 2001 field session represents an exception to the recent trend. Samples from this trip are on the order of 1 – 1.5°C cooler than the other field sessions. These samples also contain approximately 30% more SO_4 than the other sampling periods. However, the charge balance errors for these samples are all significantly negative, outside the 5% cutoff. Therefore it is unclear if the observed variation in chemistry is real, or the product of analytical error.

Spring samples collected by Egemeier (1971, 1983) in 1970 are warmer, more sulfidic, and more concentrated in dissolved solids, particularly SO_4 and Cl, than modern values. The sample by Doremus (1986) collected in May 1981 had very similar chemistry to that of the Egemeier samples. However, the temperature of 21°C for this sample is consistent with samples collected today. The springs of Lower Kane Cave are believed to result from inter-formational mixing along the fracture zone, potential endmembers of which are discussed in the following sections, and the observed temporal changes in chemistry most likely reflect a change in the mixing percentages between the 1970's and today, with the samples from the Egemeier study deriving a larger percentage of water from the warm, sulfidic, saline endmember. A theoretical saline endmember was calculated utilizing the temperature and major element concentrations measured at Upper Spring in 1970 (Appendix B analysis #40) and today (Appendix B analysis #34). The mixture was constrained by assigning the endmember a temperature. The temperature of the Thermopolis Hot springs (56˚C) was used as this constraint, as it provides a reasonable temperature for the deep Paleozoic waters of the Bighorn Basin. For this mixture, modern Upper Spring water was used as the fresh endmember, as the fraction of the two endmembers in Upper Spring water from 1970 was calculated with the following equation:

$$T_{1970} = (1\text{-}X)*T_{\text{theoretical endmember}} + X*T_{\text{Modern}} \quad (6.1)$$

	T(°C)	H_2S	Cl	HCO_3	SO_4	Na	K	Ca	Mg	Sr
Upper Spring (2002)	21.9	0.88	4.4	202	108	6	2	74	27	0.7
Upper Spring (1970)	23.5	6	12.5	218	189	11.0	3.0	97	31	1
Theoretical Endmember	56	110	177	542	1834	113	25	572	103	7

Table 6.1: Results of calculations of a theoretical saline endmember at Lower Kane Cave based on temporal changes in water chemistry between 1970 and today. Calculations used in the generation of the theoretical endmember are outlined in the segment on Lower Kane Cave in section 6.1. All concentration data is given in ppm. The Upper Spring samples used in these calculations are Analysis #34 (2002) and #40 (1970) in Appendix B.

Where T is temperature in ˚C. Solving for X gives a value of 0.953. Therefore the concentration of constituent X of the theoretical endmember is given by:

$$[X]_{\text{theoretical endmember}} = ([X]_{1970} - 0.953*[X]_{\text{modern}})/0.047 \quad (6.2)$$

The results of these calculations are shown in Table 6.1. The theoretical endmember calculated has concentrations within 100% of those at Thermopolis, except for SO_4, which is 200% more in the theoretical endmember, and H_2S, which is much greater (110ppm as opposed to 5ppm). However, both the calculated concentrations of the theoretical endmember and the agreement of these calculations with the concentrations at the Thermopolis springs are reasonable. This suggesting that the observed temporal variation in water chemistry at Lower Kane Cave may represent changes in the mixing percentages, and that the waters of the Thermopolis Hot Springs are a realistic representative water for this saline endmember.

Work by Doremus (1986) utilized drill-stem test and other well data to reconstruct changes in the potentiometric surface of the northwest Bighorn Basin caused by petroleum extractions, in particular due to the pumping at the Byron and Garland Fields to the northwest. This work suggested that the pumping for hydrocarbons may be responsible for widespread temporal changes in the potentiometric surface and flowpaths within the Madison aquifer. These changes may explain the observed long term variation in the chemistry of water to Lower Kane Cave, either by altering the amount of a saline endmember moving through the discharge fracture system, or by drawing a fresher Madison endmember to the mixing zone.

The Sr data for the springs are fairly consistent, with maximum variations in the $^{87}Sr/^{86}Sr$ ratio at Upper Spring (3 sample) of 0.00007. However, while these variations in the Sr ratio are small, they are greater than the variation of only 0.00001 between 2002 and 2003 observed at the Cowley Municipal well and

Salamander Cave. Therefore, the small variations observed between 2000 and 2003 in Sr isotope data and major ion chemistry may in fact reflect slight variations in the mixing ratios at Lower Kane Cave. The three springs of Lower Kane Cave are believed to discharge from the same water source, and the slight temporal variations observed in spring chemistry and $^{87}Sr/^{86}Sr$ ratios are likely due to small fluctuations in the actual mixture sourcing the cave.

The depleted oxygen isotope data for Lower Kane Cave (with a range of $\delta^{18}O$ values between -19.5 and -20.0‰) are indicative of recharge at high elevations or during periods of cooler climate. These values are also consistent with a water of predominantly Madison origin. Recharge from the Pryor Mountains to the north is unlikely, as well M2, which falls along the potential flowpath (Figure 2.3, flowpath A) from the Pryor Mountains, contains less depleted $\delta^{18}O$ values. Of the potential flowpaths shown in Figure 2.3, path C from the southeast is the most likely, as sites along this flowpath possess similar $\delta^{18}O$ values and a flowpath from this direction is parallel to the main structural trends in the areas, while flowpath B would cut across these structures. Although the cave discharges from a carbonate aquifer, the waters have 37.3% modern carbon, which give an age estimate of 7,920 ± 45 years. Thus these data support recharge in the nearby Bighorn Mountains, and relatively rapid transit times.

Doremus (1986) postulated that the springs of Lower Kane Cave result from a mixture of waters from the Madison aquifer with those from the overlying Phosphoria and Tensleep Formations. The working hypothesis for this study was that Salamander Spring and PBS Spring might represent the geochemistry of these two endmembers, although clearly the true mixture would require a more thermal endmember, and a mixture of this type would produce water intermediate between the two endmembers in Sr concentration and $^{87}Sr/^{86}Sr$. Waters of this intermediate type are in fact observed in the Madison wells M4 and M5, where

water from the overlying formations leaks into the well casing. However, the data from this study clearly show that the springs of Lower Kane Cave are too radiogenic to result from a simple mixing of this type.

Hellespont Cave

A second sulfidic cave discharging from the Madison aquifer in Little Sheep Mountain, Hellespont Cave differs from Lower Kane Cave in a few important aspects: 1) the cave's location on the east, rather than west, bank of the Bighorn River, 2) it's markedly smaller size, and 3) the absence of an "upper", no longer active, Hellespont cave. The waters from Hellespont Cave are a similar water type to that at Lower Kane Cave, however, the Hellespont waters are more concentrated in dissolved solids, particularly SO_4, Cl and Na, and cooler, at 19°C. The springs in Hellespont Cave also contain slightly more Sr with a slightly higher $^{87}Sr/^{86}Sr$. The oxygen isotope ratios at Hellespont Cave, between -19.6 and -20.1, fall in essentially the same range as Lower Kane Cave.

The similarity in hydrostratigraphic position, oxygen isotopes and Sr signature of these two waters suggests that a similar mechanism may source both caves. However, the differences in chemistry suggest that the mixing proportions are not the same at both caves, and that the actual endmembers likely differ slightly. This is not unexpected, as the fractures that feed these two springs are clearly offset, and are separated by the Bighorn River and the intervening Salamander Spring, which discharges a purer Madison water. Two potential models can explain the observed differences in temperature: 1) water moves more slowly through the fracture system to Hellespont Cave and thus has a greater time to cool, or 2) the Madison aquifer endmember supplying Hellespont Cave is cooler, and likely more concentrated, than the Madison water supplying Lower Kane Cave. Option 2 is the most likely scenario, as it accounts for difference in

both temperature and composition. While both Hellespont and Lower Kane Cave are sulfidic caves located in a breached anticline, the small differences in temperature, chemistry and Sr data between the two sites may provide important insights into the Paleozoic flow system, and the mechanism of cave formation and localization within Little Sheep Mountain.

6.2 Temperature Considerations

The thermal gradient for the Paleozoic aquifers of the Bighorn Basin near Tensleep is 1.45˚C/100 m, or 1.27˚C/100 m when only considering the formations of the Madison aquifer (Cooley, 1986). Assuming a mean annual temperature of 7˚C, this requires a travel depth on the order of 1000 – 1160 m to achieve the water temperatures measured at the Lower Kane Cave springs. Structural contour maps on the surface of the Tensleep show that the Madison Limestone reaches depths of 1220 m in the synclines that border the Little Sheep Mountain anticline (Doremus, 1986). Though located at a similar stratigraphic level to Lower Kane Cave, both Salamander Spring (M3) and the GP well (M4) on the southern flank of Little Sheep Mountain discharge water cooler than that at Lower Kane Cave. This suggests that, when compared to Lower Kane Cave waters, the Madison water at these locations did not travel as deep, traveled up from depth more slowly, or, most likely, that the thermal character and radiogenic signature at Lower Kane Cave both derive from a deep-seated source that does not contribute significantly to sites M3 and M4. Potential sources of thermal water at Lower Kane Cave may be constrained by the source of radiogenic strontium discussed below, but can derive from 1) upwelling along extensional fractures in the crest of the anticline from deeper zones within the Madison aquifer, 2) upwelling from deeper formations underneath the Madison, or 3) movement of thermal

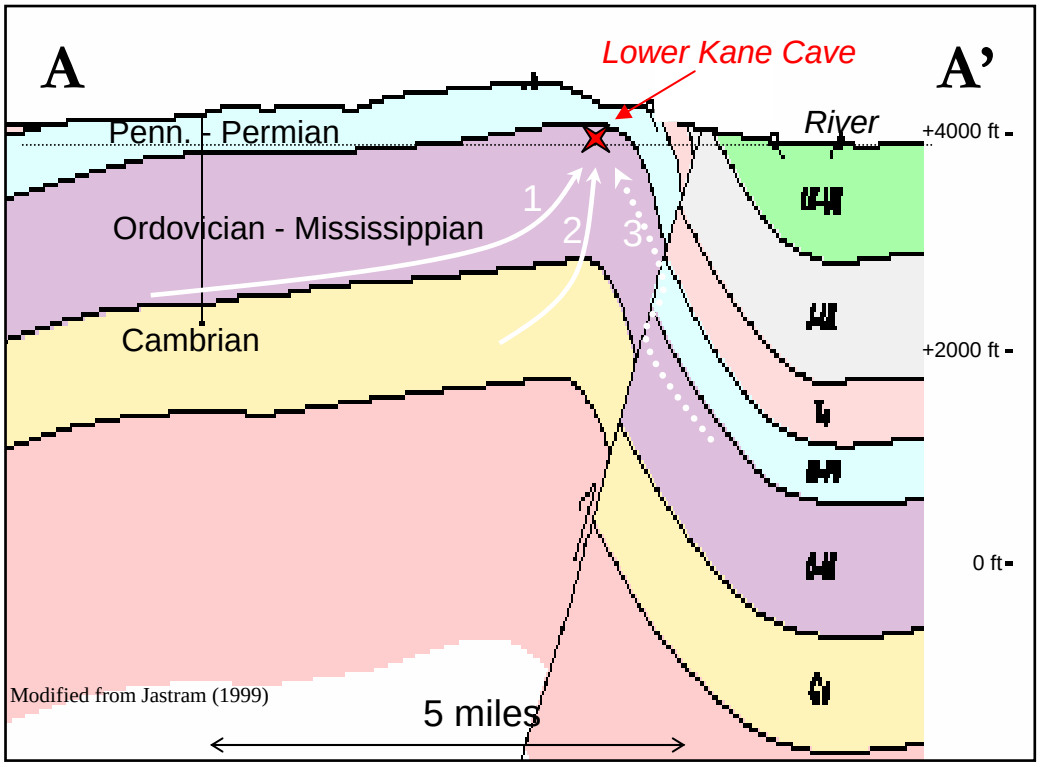

Figure 6.1: Cross section through Little Sheep Mountain from Jastram (1999), shown on the map in Figure 2.3. The cross section is perpendicular to the anticlinal axis to the northwest of Lower Kane Cave. The position of the cave is projected onto the line of the cross section. The arrows represent the two potential sources of thermal water to the cave: 1) upwelling of water from the deeper Madison aquifer along extensional fractures in the axis of the anticline, 2) flow along extensional fractures from the deeper seated Cambrian formations, and 3) flow upward along the coring thrust fault that brings up water from the more deeply buried footwall.

groundwater along the coring fault of Little Sheep Mountain introducing water from the footwall into the Madison aquifer (Figure 6.1).

Chalcedony geothermometer calculations (Henley, 1984, Table 6.2) underestimate actual measured temperatures for all sites except PBS Spring (P1) and the Hillsboro stream (P4), which are slightly cooler (5˚C and 3˚C, respectively) than the calculations. For the other samples, geothermometer temperatures generally underestimate actual temperatures by between 4˚C (at Hellespont Cave (C4)) and 21˚C (at the Cowley Municipal well (M2)). The silica concentration of water from the Clay well is especially low, underestimating the actual temperature by 66˚C. This suggests that the majority of waters from the Paleozoic aquifers in the region of study have not reached equilibrium with silica phases. With predominantly carbonate aquifer lithologies, this is not unexpected. Geothermometer calculations also underestimate the temperature of the Thermopolis spring by 6˚C. Since the silica concentration and temperature data for this calculation were obtained at different times (from the July 2002 sample and literature values, respectively), cautious interpretation of this calculation is required. However, since reported literature values for the temperature of the springs do not show significant variations, this calculation suggests that the waters of Thermopolis have also not reached equilibrium with silica. Alternatively, if actual variations in temperature are indeed responsible for the difference between measured and calculated values, and the waters are in fact at equilibrium, than the data imply that the waters of the springs do not cool as they move upward.

	ID#	Site	Measured T (˚C)	Calculated T (˚C)	Difference (˚C)
Mississippian	1	Cowley Muni. Well	17.2	-4	21
	2	Cowley Muni. Well	17.2	-2	19
	3	Crosby Well	14.5	2	12
	4	GP Gypsum Plant	17.5	0	17
	6	Salamander Spring	17.2	4	14
	7	Salamander Spring	17.4	6	12
	9	Shell Well #3	15.4	1	15
	16	Shell Well #2	17.7	1	16
Penn. / Perm.	19	PBS	13.2	19	-5
	21	Clay Well	17.8	-48	66
	22	Hillsboro Stream	11.3	15	-3
	23	Greybull Cemetery	15.7	3	13
Oth.	*25*	*Thermopolis*	*56*	*50*	*6*
	26	Mayland-Leavitt Well	31.2	17	14
Hellspont Cave	50	Hellspont Cave	19.1	15	4
	51	"	18.3	11	7
	52	"	18.1	8	10
	53	"	18.2	12	6
	*54**	*"*	*19.5*	54	*-34*
	*55**	*"*	*19.5*	54	*-34*
Lower Kane Cave	28	Fissure Spring	21.6	13	9
	29	"	19.9	11	9
	30	"	22	7	15
	31	"	21.3	14	8
	*32**	*"*	*23.5*	57	*-33*
	33	Upper Spring	22.12	4	18
	34	"	21.9	12	10
	35	"	20.4	11	9
	36	"	21.3	7	14
	41	Lower Spring	21.5	3	18
	42	"	21.7	12	10
	43	"	20.2	7	13
	44	"	22.1	8	14
	46	"	22.8	14	9

Table 6.2: Silica geothermometer calculations of formation water using the Chalcedony thermometer from Henley (1984): T (˚C)=[1032/(4.69–log(SiO_2))]–273.15, where the concentration of SiO_2 is in ppm. Italicized data represent calculations using data not collected for this study. The silica concentration for the Thermopolis sample was measured, but the comparison temperature data was taken from the literature. The italicized cave points are all from Egemeier (1981).

6.3 Groundwater Uranium Concentrations

Significant uranium concentrations were observed in the majority of wells sampled, over a range of 0 – 53 ppb. Levels of uranium do not appear correlated to a particular aquifer. Uranium levels were below detection limits for waters from Thermopolis, the Flathead Sandstone, and four of the Madison wells (M5,6,9 and 10) at the Spence oil field, however the rest of the samples all contained noticeable uranium content. At 53 ppb, the Pennsylvanian / Permian Greybull Cemetery well (P3) had the highest uranium content of any sample collected, while the GP well (M4) also contained high levels of Uranium at 49 ppb. Levels of uranium in Lower Kane Cave water are fairly constant, averaging 27 ppb. The levels of uranium in Hellespont cave are about 1/3 that of Lower Kane Cave.

The uranium content of groundwater appears relatively consistent over time at sites sampled over multiple years, such as at Lower Kane and Hellespont caves and the Cowley Municipal well (M2). Spatial variations are significant, however, as the Crosby well (M1) contains 12 ppb uranium, more than twice that at the nearby Cowley Municipal well. This variation is likely the result of either truly heterogeneous distributions of uranium within the Paleozoic formations, or differences between the two wells in the actual cased section within the Madison aquifer.

The presence of high levels of uranium in what are generally reduced waters, in particular at the GP well, is surprising, as uranium is soluble in the oxidized form, and we do not observe increased uranium levels in oxygenated waters. Variations in the uranium content of the Paleozoic aquifers point to interesting distinctions in groundwater evolution, however an explanation for the observed variation remains to be determined.

6.4 Groundwater Evolution in the Paleozoic Aquifers

Using geochemical and isotope (carbon and oxygen) data in PhreeqC, Plummer (1990) and Busby et al. (1991) modeled groundwater flow paths in the Madison, and characterized the evolution of Madison groundwater in the Powder River Basin as predominantly the result of dedolomitization (the dissolution of dolomite and associated precipitation of calcite), accompanied by varying amounts of interaction with organic material and, in a few cases, the dissolution of halite. In this model, increasing total dissolved solid (TDS), SO_4 and, in some cases, H_2S concentrations of the waters indicate increases in residence times.

Assuming Madison waters along the northeast margin of the Bighorn Basin undergo similar evolutionary processes as those described in Plummer (1990) and Busby et al. (1991), the fresh, oxygenated quality of the Madison aquifer groundwater in the study area suggest that these waters are relatively young in terms of their evolution. While waters of the Madison aquifer in the Bighorn Basin have not generally been age dated, the high percentage of modern carbon in the spring water at Lower Kane Cave suggests that water is indeed traveling relatively rapidly from recharge zones to this location. This percentage of modern carbon yields a ^{13}C-corrected age of 7,920 ± 45 years, a travel time slightly faster than the 8,655 ± 355 years calculated for the Hyattville City Well (Frost and Toner, 2004).

Madison waters sampled for this study display a linear relationship between Mg and Sr concentrations (Figure 6.2). A similar relationship exists between Ca and Sr concentrations (Figure 6.3). In both cases, the highest concentrations of these ions are present in waters from the Spence oil field, suggesting that increased dissolution of host minerals may occur at these sites. As expected, we also observe linear increases in the concentrations of Mg and Ca versus Sr concentrations in the Pennsylvanian / Permian aquifers (data not

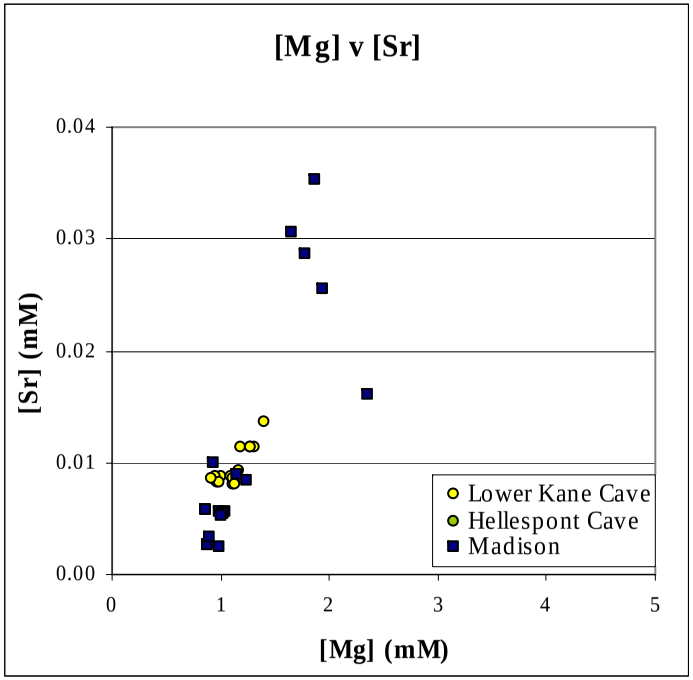

Figure 6.2: Plot of dissolved [Mg] v [Sr] for the Madison aquifer waters and Lower Kane and Hellspont Caves.

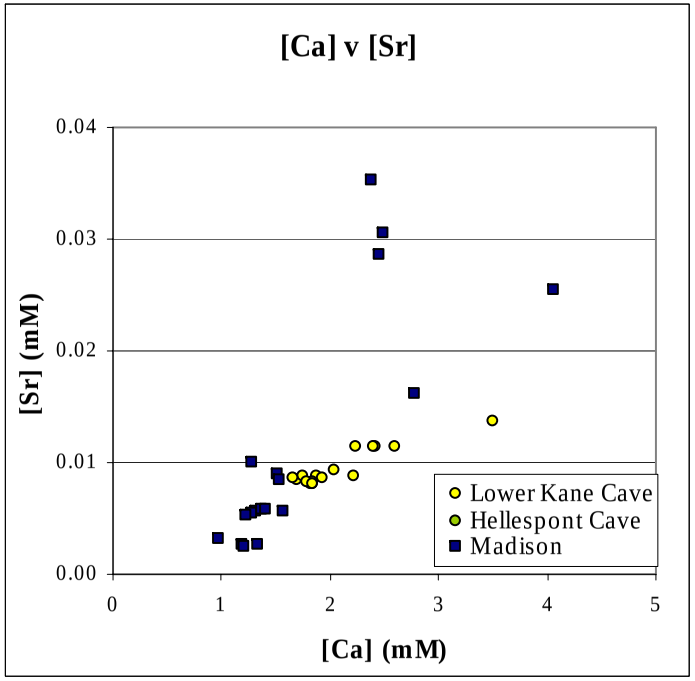

Figure 6.3: Plot of dissolved [Ca] v [Sr] for the Madison aquifer waters and Lower Kane and Hellspont Caves.

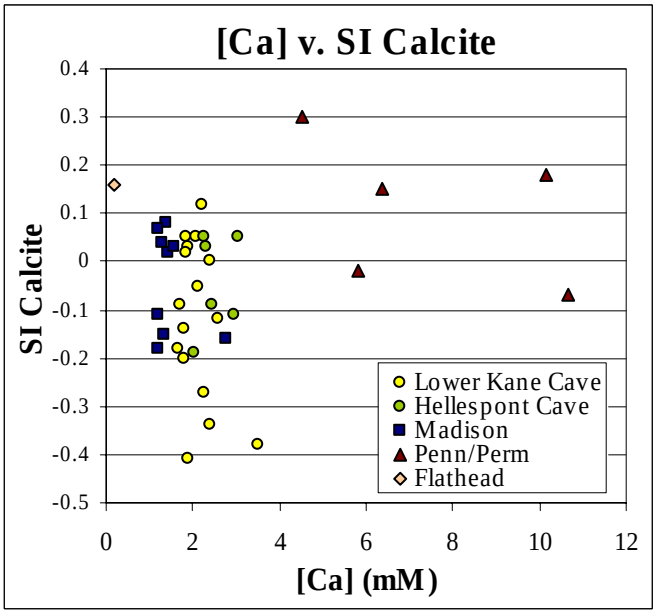

Figure 6.4: Plot of dissolved [Ca] concentration versus the saturation index (SI) for Calcite.

shown.) However, the process of dedolomitization should increase the concentration of Mg and Sr, more than the concentration of Ca, as some amount of Ca will be removed from solution during the precipitation of calcite. Instead, we observe greater increases in Ca concentration, suggesting an additional source is introducing dissolved Ca into the system.

Calcite saturation in the Madison, Lower Kane Cave and Hellspont Cave waters is not correlated to concentrations of dissolved Ca (Figure 6.4). These waters spread in roughly vertical lines to both oversaturated and undersaturated conditions, although the range in SI, between approximately -0.4 and 0.1 favors the undersaturated condition. Waters from the Pennsylvanian / Permian aquifers contain higher concentrations of dissolved Ca, with a trend toward more saturated conditions. The waters display a similar relationship to Dolomite SI (data not shown).

Since the lithology of the Madison aquifer is dominated by the carbonate formations of the Madison Limestone and Bighorn Dolomite, it is expected that the chemistry of groundwater in this aquifer will reflect interaction with these materials. Carbonate dissolution occurs by the following reaction:

$$Ca_XMg_{(1-X)}CO_3 + CO_2 + H_2O = XCa^{2+} + (1-X)Mg^{2+} + 2HCO_3^- \qquad (6.3)$$

This reaction results in a net increase in solution of 2 moles of HCO_3 for every mole of dissolved Ca and Mg ion. Thus if the major ion chemistry of a groundwater is controlled by interaction with carbonates, when concentrations of HCO_3 are plotted against the sum of concentrations of Ca and Mg, the data should plot along a 2:1 line. As shown in Figure 6.5, the waters from the Madison aquifer are arrayed along and slightly above the 2:1 line for pure carbonate interaction, which also suggests the input of additional dissolved Ca.

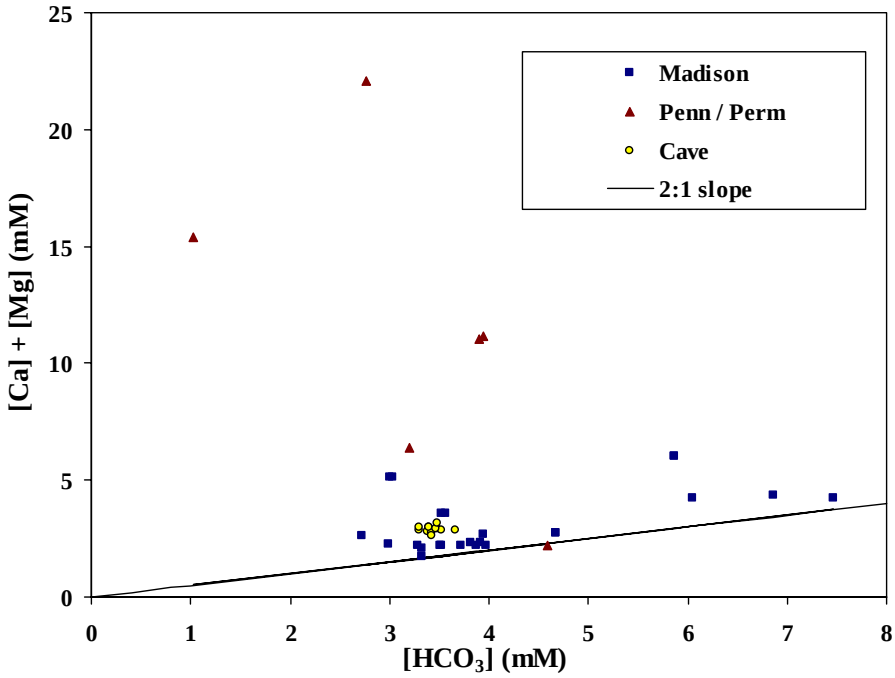

Figure 6.5: Plot of Paleozoic aquifer water samples to assess groundwater evolution, in particular interaction with carbonates. Groundwater evolution purely through dissolution of carbonate releases twice the concentration of HCO_3 in to the groundwater as the sum of the Ca and Mg concentrations. Therefore groundwater interacting just with carbonates will fall along the 2:1 line when the molar concentration of HCO_3 is plotted against the sum of Ca and Mg concentrations. Samples that plot above this line are acquiring additional cations from another source.

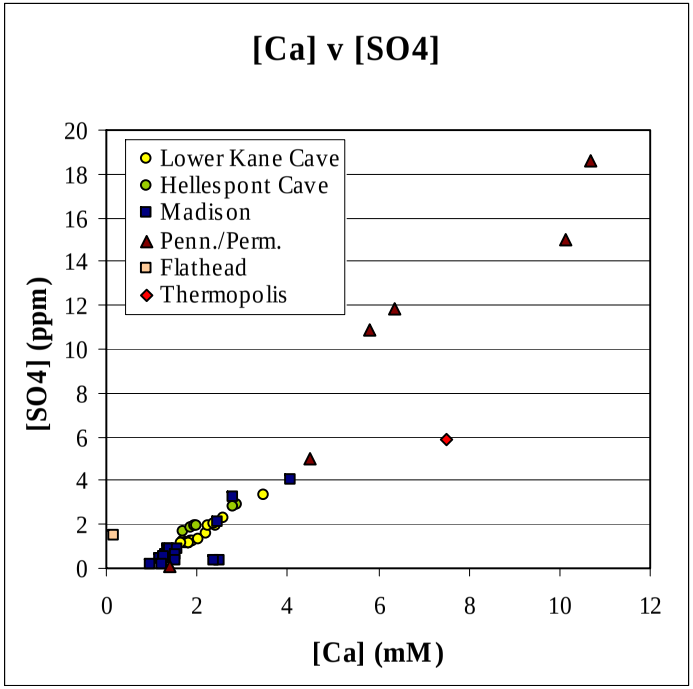

Figure 6.6a: Plot of dissolved [Ca] versus [SO_4]concentrations for the Paleozoic groundwater of the northeast Bighorn Basin.

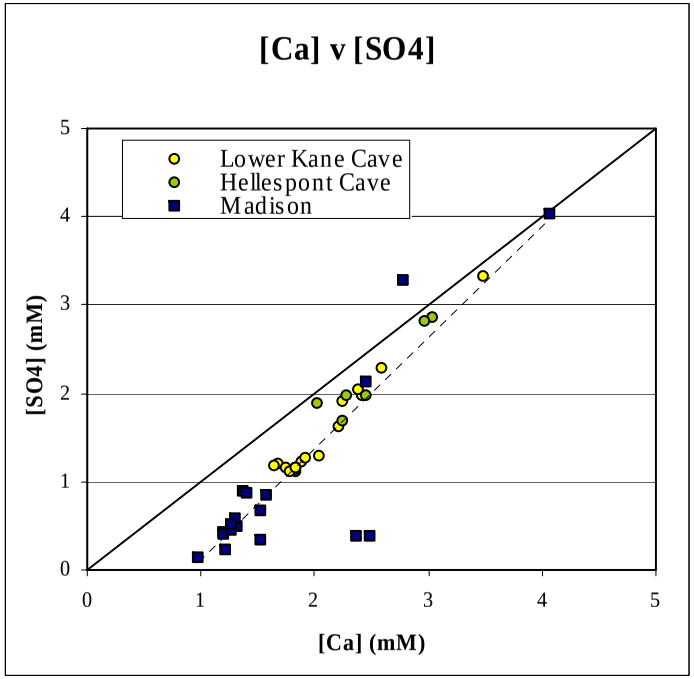

Figure 6.6a: Plot of dissolved [Ca] versus [SO_4]concentrations for waters from the Madison aquifer and Lower Kane and Hellespont Cave. The dashed line plots the trendline through the data, while the solid line represents a 1:1 relationship.

A plot of dissolved Ca versus SO_4 conentrations (Figure 6.6) suggests a potential source of the additional Ca in solution. The strong linear relationship between these two ions suggests the influence of the dissolution of gypsum or anhydrite. Such a reaction will provides an additional source of dissolved Calcium ions, as shown in the reaction for anhydrite below:

$$CaSO_4 = Ca^{2+} + SO_4^{2-} \quad (6.4)$$

As this reaction results in equal concentrations of Ca and SO_4, subtracting the SO_4 concentration from the sum of the Ca and Mg concentrations will back out the effect of gypsum or anhydrite dissolution, and waters should again plot on a 2:1 line. When the effects of interaction with gypsum are accounted (Figure 6.7), the data fall roughly along the 2:1 line.

Though not sampled as part of this study, the more concentrated Madison waters from the basin center (data from Doremus, 1986; Libra et al. et al., 1981; Lowry and Lines, 1972) plot far above the 2:1 line in both cases (Figure 6.8). These waters are therefore not simply the result of greater dissolution of carbonates and anhydrite / gypsum, evidence that further supports the idea that Madison waters of the central Bighorn Basin are distinct from Madison waters on the eastern margin of the basin.

Assuming that the majority of water to Lower Kane Cave derives from the Madison aquifer, we expect the spring water to display a carbonate type chemistry. The Cave waters display similarly characteristics to the Madison aquifer in this regard (Figure 6.5), clustering just above the 2:1 line for pure carbonate reaction. When SO_4 measurements are included (Figure 6.7), however, the samples spread out below the line in a rough line with a slight negative slope. The cause of SO_4 in excess of that contributed by gypsum is unknown.

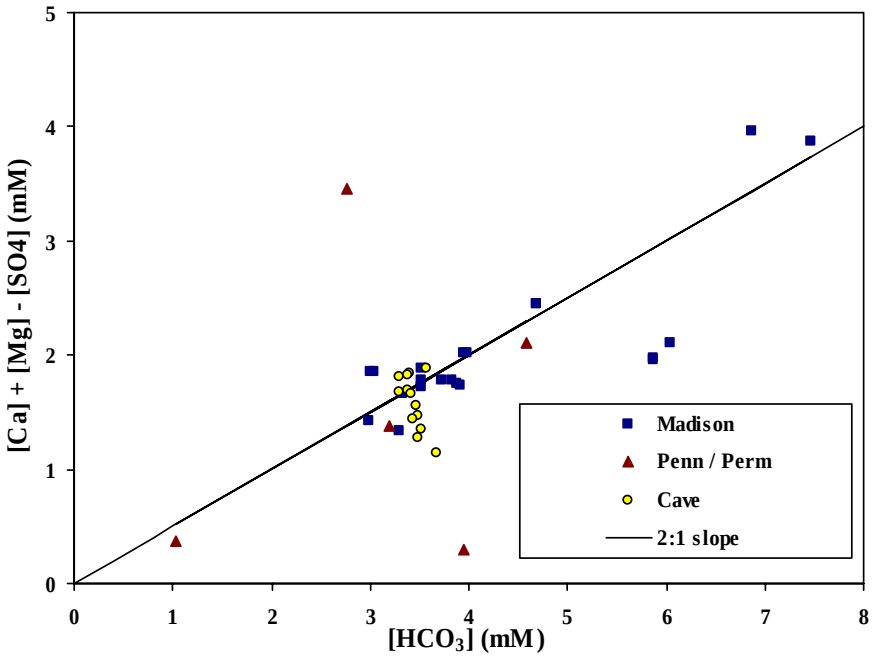

Figure 6.7: Plot of Paleozoic aquifer water samples to assess the influence of gypsum or anhydrite dissolution These minerals ($CaSO_4$, with or without associated water molecules) provide a common source of additional Ca in solution. If groundwaters are undergoing this process, subtracting the concentration of SO_4 from the sum of Ca and Mg accounts for this dissolution, and waters that interact only with carbonates and gypsum or anhydrite will again plot on the 2:1 line.

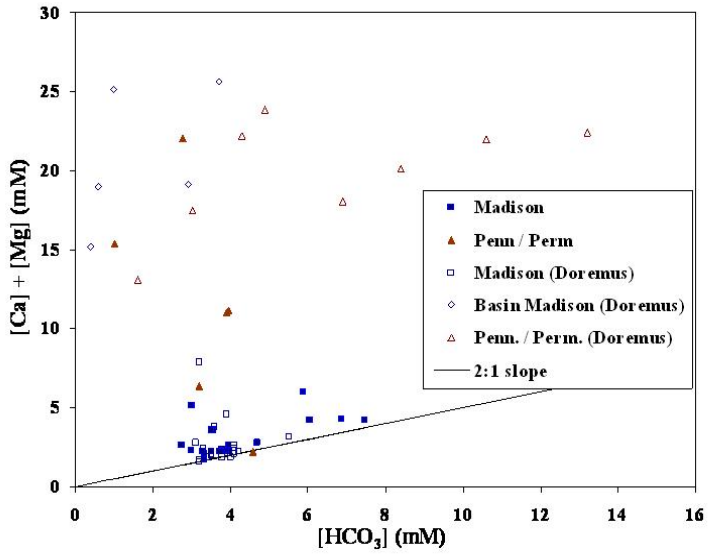

Figure 6.8a

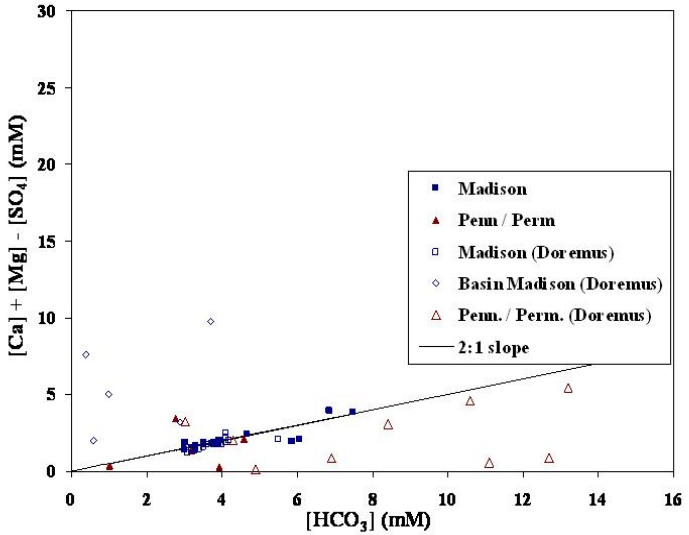

Figure 6.8b

Figure 6.8a and b: The majority of Madison aquifer water samples from both this study and the work of Doremus (1986) fall along the line of carbonate interaction when the influence of gypsum is accounted for. However, Madison aquifer samples from Doremus that are more central in the basin do not follow this trend, and instead fall above the line, as shown in Figure 3.b. Samples form the Pennsylvanian and Permian aquifer contain very high levels of SO_4, which cause the water samples to fall far above the line in Figure 7.3a, but far below the line in Figure 7.3b.

When looked at in terms of interactions with carbonates, groundwater from the Pennsylvanian / Permian aquifers is more varied than the waters of the Madison aquifer. When only reactions with carbonates are considered (Equation 6.3) and the concentration of HCO_3^- is plotted against the sum of the Mg and Ca concentrations, all waters except for the Tensleep Spring (P5) plot far above the pure carbonate dissolution line (Figure 6.5). When the presence of gypsum is accounted for (Equation 6.4), the waters from the Greybull Cemetary (P3) and the Hillsboro Stream (P4) also fall on the carbonate interaction line (Figure 6.7). However, water from the Clay well (P2) remains above the line, while the water from PBS spring (P1) falls far below the line, such that the spring has an excess of sulfate beyond that accounted for by gypsum or anhydrite dissolution. The actual sampling point at PBS Spring is downstream from the spring orifice, which is buried under a breakdown pile. Therefore the excess SO_4 in this water may result from the oxidation of dissolved H_2S. These variations in chemistry suggest the heterogeneity of the Pennsylvanian / Permian aquifer system. The data also suggest the importance of sulfate interactions within these aquifers, and support significant interactions with additional non-carbonate minerals, at least along certain flowpaths within the aquifers.

A plot of Ca concentrations versus the SI for gypsum (Figure 6.9) further suggests the importance of gypsum dissolution in the Paleozoic aquifers. The waters samples in this study fall along a logarithmic line heading from dilute, undersaturated waters towards saturation with gypsum. The fact that the waters from the Pennsylvanian / Permian aquifer line up near the logarithmic line through the Madison waters would generally suggest that these wateres represent stages along a single reaction pathway, as opposed to waters from separate aquifers. The geochemical modeling software PhreeqC Interactive was used to model the evolution of an Upper Spring water interacting with gypsum in

equilibrium with calcite (Figure 6.10). The input file for this model is given in Appendix D. The results of this model generate a line just below the groundwaters of the Pennsylvanian / Permian aquifer.

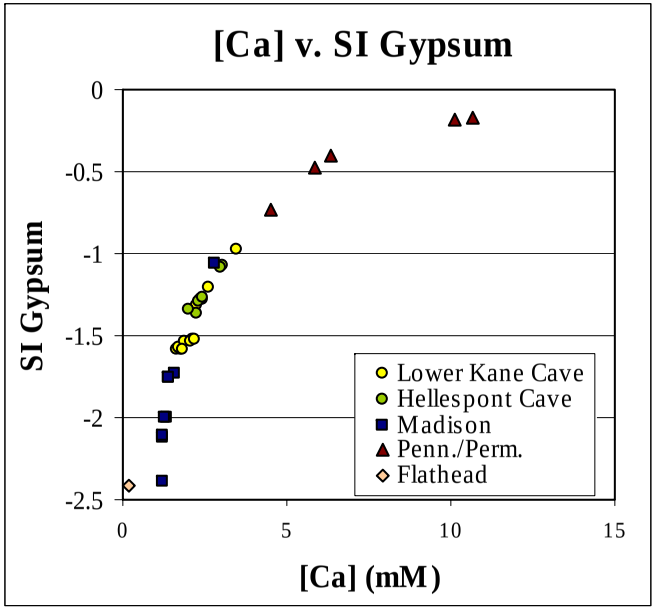

Figure 6.9: Plot of dissolved Ca concentration versus Gypsum saturation.

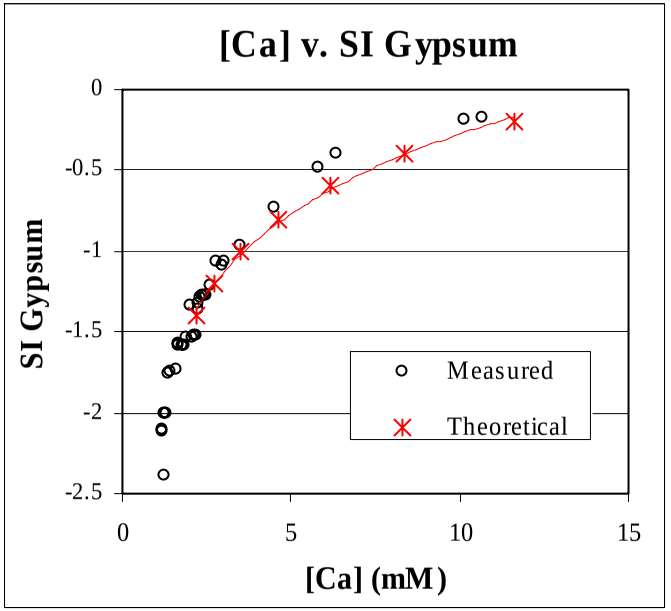

Figure 6.10: PhreeqC modeling of the theoretical evolution of an Upper Spring water (Appendix B analysis #33) towards saturation with gypsum in equilibrium with calcite. The measured values are the data shown in Figure 6.9.

6.5 Potential Sources of Radiogenic Strontium

As mentioned previously, the chemistry of Lower Kane Cave spring water is distinguished from average Madison aquifer water by increased conductivity, more SO_4, and the presence of dissolved H_2S. Perhaps the most important difference observed in this study, however, is the significant increase in the radiogenic Sr of these waters. The data in Figure 5.3 show three samples with more radiogenic Sr than the groundwater at Lower Kane Cave: the Flathead Sandstone, the Tensleep Spring (site P5; Frost and Toner, 2004), and the Big Spring at Thermopolis Hot Spring State Park. This section considers the potential for each of the three samples mentioned above to serve as the source of radiogenic Sr to Lower Kane Cave.

Other radiogenic samples from this study and that of Frost and Toner (2004) that are not shown include snow, spring, stream and well samples from the recharge areas in the Bighorn Mountains. These samples are not considered in this study as they are all from mountain sources early in the groundwater evolution flowpaths, and are not representative of evolved formation waters. Additionally, since these are young or recharge waters, they contain extremely low concentrations of Sr and thus could not contribute enough Sr to impact the $^{87}Sr/^{86}Sr$ signature of the Lower Kane Cave waters. While these samples represent early recharge waters, interpretations of groundwater evolution from this data are complicated by uncertainties in the formations of origin for these samples. Data for these samples are provided in appendices A-C under the heading Bighorn Mountain waters for use in future studies.

The groundwater at Lower Kane Cave may not result from a mixture, or may result from a mixture of more than two endmembers. While Lower Kane Cave waters differ in chemistry from Madison aquifer waters, the majority of the Madison samples come from wells which case a large stratigraphic section.

Therefore, although unlikely, it is possible that the Lower Kane Cave and Hellespont Cave waters source from a particular zone deeper within the Madison aquifer that produces more concentrated, radiogenic waters, perhaps from the siliciclastic components in the Devonian Jefferson Formation or the infill of the paleokarst collapse features in the Upper Madison. Additionally, the mixture of waters at Lower Kane Cave may incorporate water from multiple formations. Water from three or more formations may intermingle in the fault and fracture zones of Little Sheep Mountain, a situation which can not be assessed by the two-member mixing model discussed here.

Mixing percentages were determined by normalizing to the $^{87}Sr/^{86}Sr$ of a representative sample from the Upper Spring of Lower Kane Cave (analysis ID #33 in Appendix B) using Equations 3.1 – 3.3. See section 3 for a discussion of Sr isotope use in tracing groundwater mixing. Mass balances of the major elements were calculated with Equation 3.1, and then compared to measured values for the representative sample of Upper Spring water. The results of the calculations are listed in Table 6.3, and mixing lines that utilized the Tensleep spring and Thermopolis Hot Spring samples as radiogenic endmembers are shown in Figure 6.11.

First we consider the sample from the Flathead Sandstone. While radiogenic, the Sr concentration of this water is low enough that a mixing line drawn from this samples through the data for Lower Kane Cave intersects a region of Figure 5.3 that plots a Sr signature not observed in any of the waters assessed in this study. It is possible that longer residence times within the basin produce more concentrated waters in the Flathead Sandstone that would plot in this region and could contribute the necessary radiogenic Sr and thermal characteristics observed at Lower Kane Cave. While the thick Cambrian Gallatin Limestone and Gros Ventre Shale act as effective confining layers throughout

MIX A												
					Anions (ppm)				Cations (ppm)			
	%	fraction	[Sr]	87/86Sr	F	Cl	HCO3	SO4	Na	K	Ca	Mg
P5 (Tensleep)	45	0.45	0.42	0.71220	0.2	1	280	11	3	2	56	20
M7 (Sheep Mtn)	55	0.55	0.87	0.70926	0.6	3	237	43	4	1	51	23
mixture	-	-	0.67	0.71009	0.4	2	256	29	4	2	53	22
% difference	-	-	*-7*	*0*	*-52*	*-56*	*24*	*-73*	*-44*	*-6*	*-27*	*-9*

MIX B												
					Anions (ppm)				Cations (ppm)			
	%	fraction	[Sr]	87/86Sr	F	Cl	HCO3	SO4	Na	K	Ca	Mg
Thermopolis	2.7	0.027	2.82	0.715581	3.4	247	622	568	191	39	301	66
M3 (Salamander)	97.3	0.973	0.49	0.709241	0.5	2	315	81	4	1	63	25
mixture	-	-	0.55	0.710118	0.6	9	324	95	9	2	69	27
% difference	-	-	*-31*	*0*	*-45*	*52*	*36*	*-13*	*30*	*20*	*-6*	*11*

COMPARISON SAMPLE												
					Anions (ppm)				Cations (ppm)			
	%	fraction	[Sr]	87/86Sr	F	Cl	HCO3	SO4	Na	K	Ca	Mg
Upper Spring	100	1	0.72	0.71010	0.84	4	206	107	6	2	73	24

Table 6.3: The results of the strontium mixture calculations discussed in section 6.5.

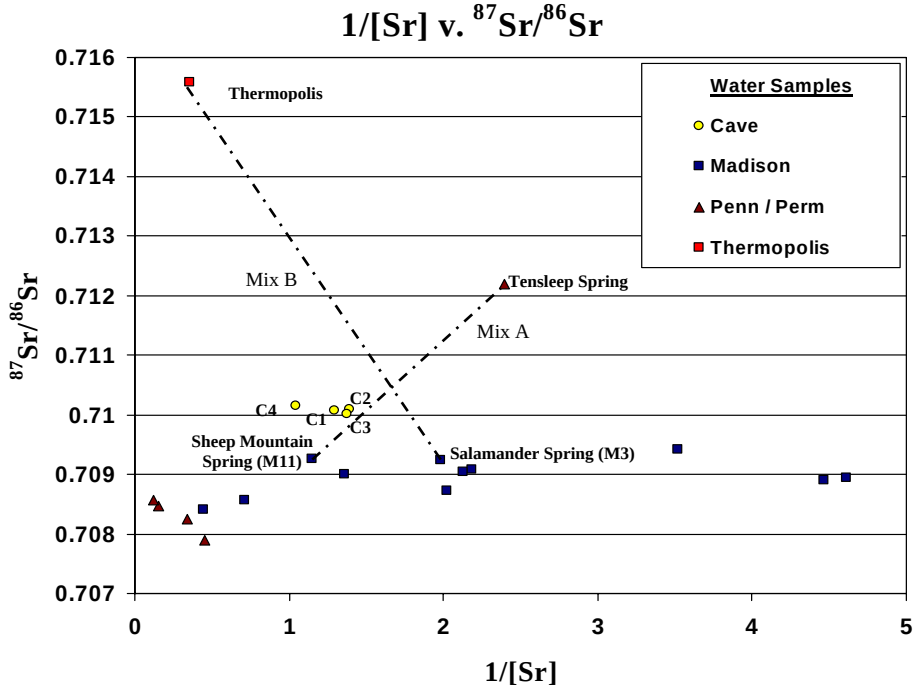

Figure 6.11: Plot of the mixing lines A and B discussed in section 7 that are potential sources of the radiogenic Sr at Lower Kane Cave. Note that the scales of this plot are slightly smaller than in Figure 5.3.

most of the basin, generating up to 244 m of head difference between the Madison and Flathead aquifers, evidence does exists for upward leakage into the Madison in highly fractured regions such as at Little Sheep Mountain (Cooley, 1986.) However, the comprehensive separation between the Flathead and Madison aquifers, combined with the high relative percentages of Na and the absence of H_2S contributing hydrocarbon reservoirs within the Flathead Sandstone make waters of the type assessed an unlikely contributor to the springs at Lower Kane Cave.

The second potential source water considered is the Tensleep Spring (P5) sampled by Frost and Toner (2004). As shown in Figure 6.11, a line, labeled Mix A, drawn from this sample through Lower Kane Cave intersects with the spring sample from Sheep Mountain (M11). While such a mix satisfies the strontium isotope data, concentrations of all the major elements, except bicarbonate, are too low. Additionally, this mixture would requires 45% of the Tensleep endmember, and necessitate the movement of water from an overlying unit to an underlying formation, which opposes the general potentiometric heads in the basin (Cooley, 1984; Doremus, 1986). Therefore Tensleep water as represented by this sample is an unlikely source for the radiogenic Sr in the Lower Kane Cave spring water.

One consideration worth mentioning is that this sample comes from a location close to the recharge area, and Tensleep waters have been shown to evolve to higher TDS values toward the basin center (Doremus, 1986; Libra et al. et al., 1981; Lowry and Lines, 1972; Western Water Consultants, 1982). If water in the Tensleep acquires a radiogenic, siliciclastic signature, such as that of the whole rock Tensleep sandstone (Table 5.4, Figure 5.3), and a high concentration of solutes, then Tensleep water from the footwall of Little Sheep Mountain migrating upward within the Little Sheep Mountain anticline remains a potential source of radiogenic Sr to Lower Kane Cave.

The third potential endmember considered is represented by the Thermopolis spring sample. A mixing line (Mix B in Figure 6.11) connecting this sample to the Salamander Spring sample (M3) roughly approximates the Sr chemistry of Lower Kane Cave, although the Sr concentration in the mix is too low. In this case, the calculated mixture also under represents the concentrations of F, SO4 and Ca. While the Salamander Spring sample was chosen as a reasonable endmember due to its close proximity to Lower Kane Cave, the actual Madison endmember at Lower Kane Cave could easily be more concentrated, which would raise the concentration of major ions in the mixture. While calculated concentrations of Na and Cl are also too high in this model, at 0.94 the ratio of Na:Cl suggests that these solutes derive from the dissolution of halite, the availability of which likely varies greatly throughout the basin subsurface. While a mixture of Thermopolis and Madison waters does not perfectly approximate the springs of Lower Kane Cave, the Thermopolis spring waters clearly demonstrate the existence of a deep-seated, thermal radiogenic saline water in the Paleozoic of the Bighorn Basin, and it is possible that the process that generates the water at Thermopolis produces a similarly radiogenic, thermal water with a variable geochemistry in the area of Little Sheep Mountain. This interpretation is supported by the similarity between the measured values at Thermopolis spring, and thetheoretical values of the saline endmember calculated in section 6.1 (Table 6.1) using the chemistry of Upper Spring water from 1970 and the present along with the temperature of Thermopolis.

Although the mixing models presented here are non-unique, they provide insights into the groundwater system at Lower Kane Cave. Based on geochemical and hydrologic considerations, the most likely mixture to Lower Kane Cave consists of a minor amount of a thermal water concentrated in radiogenic Sr combined with primarily Madison aquifer water; this hypothesis is supported by

the similarity in geochemical and oxygen isotope parameters between local Madison waters and the Lower Kane Cave springs.

The temporal changes in groundwater chemistry at Lower Kane Cave between the early 1970's (Egemeier, 1973, 1981), 1980's (Doremus, 1986) and today suggest that concentrations of H_2S in the cave are linearly related to the temperature and solute concentrations of the water (Figure 5.6, 5.7 and 5.8). While Sr data is not available for these earlier samples, this suggests that the thermal, saline source that introduces radiogenic Sr into the cave also contributes the dissolved H_2S in the spring water.

It is interesting to note that both Lower Kane Cave and Thermopolis Hot Springs produce thermal, sulfidic waters with radiogenic Sr signatures from springs located in basin margin anticlines breached by the Bighorn River. A similar mechanism may provide the thermal, sulfidic, radiogenic water to both Thermopolis Hot Springs and the caves of Little Sheep Mountain, with the springs at Lower Kane and Hellespont Caves diluted by the Madison aquifer water. The sample from Salamander Spring (M3) is also drawn to slightly more radiogenic value of $^{87}Sr/^{86}Sr$ than the average Madison waters, suggesting that a small amount of the thermal, radiogenic water contributes to this spring. The sample from Sheep Mountain (M11), collected by Frost and Toner (2004), came from a high yield spring that discharges 20˚C water and also displays a slightly increased value of $^{87}Sr/^{86}Sr$ relative to the overall Madison trend, which may suggest that a similar mechanism is delivering thermal, radiogenic water to all three anticlines breached by the Bighorn River. The dead Spence Cave located in Sheep Mountain was probably formed by the same sulfuric acid speleogenesis mechanism as at work in Lower Kane Cave, and studies by Doremus (1986) and Egemeier (1981) list additional small springs in the Sheep Mountain canyon that discharge water at 31˚C. If a similar mechanism is indeed sourcing thermal,

radiogenic, sulfidic waters to the breached anticlines of the Bighorn Basin, we hypothesize that the warmer springs in Sheep Mountain should yield water containing more radiogenic Sr, similar to that at Lower Kane Cave.

6.6 Groundwater Evolution Modeling with PhreeqC

Geochemical modeling of groundwater evolution to Lower Kane Cave was carried out using PhreeqC Interactive (Parkhurst and Appelo, 1999). Based on the Sr data, the following three groundwater evolution cases were considered: (1) Salamander Spring evolving to Upper Spring, (2) a mixture of Salamander and PBS springs evolving to Upper Spring, and (3) a mixture of Salamander and Thermopolis springs evolving to Upper Spring. These three geochemical cases were looked at in order to (1) determine the interactions involved in groundwater evolution within the Madison, (2) test geochemically the PBS spring / Madison aquifer mixing model proposed by Doremus (1986), and (3) to assess the geochemical viability of a Thermopolis / Madison mixture. Additionally, as the earlier discussion of the Sr model showed, the Madison endmember at Lower Kane Cave is potentially more concentrated than Salamander Spring, and modeling the scenario in case (1) can help us understand what the potential endmember might look like.

These three cases were looked at using inverse modeling based on the work of Plummer et al. (1990) and using the PhreeqC example 18 as a starting point. Forward models based on the results of a PhreeqC speciation of the Upper Spring water sample (analysis ID #33) and reaction models using the output of the inverse modeling were also carried out. Results of these models are shown in Tables 6.4 – 6.7. The PhreeqC input files for these models are provided in Appendix D.

Phase Mole Transfer per L model solution			
Phase	Solution 1	Solution 2	Solution 3
Dolomite	2.48E-04	1.88E-04	1.88E-04
Calcite	-5.91E-04	-3.60E-04	-3.60E-04
Anhydrite	5.69E-04	3.98E-04	3.98E-04
CH_2O	4.78E-04	5.20E-05	5.21E-05
Goethite	1.14E-05	-	4.48E-07
Pyrite	-1.14E-05	-	-
Halite	6.76E-05	6.76E-05	6.76E-05
Redox Mole Transfers			
Fe(3)	1.14E-04	-	4.48E-07
H(0)	-1.27E-10	-1.27E-10	-1.27E-10
S(-2)	-2.53E-04	-2.60E-05	-2.60E-05

Table 6.4a: Results of an Inverse Model from Salamander Spring to Upper Spring in Lower Kane Cave. Solutions 1-3 are the output from the model. See Appendix D for PhreeqC input file.

	Measured	Reaction	Forward
HCO_3	3.38	3.20	3.98
Ca	1.83	1.62	1.83
Cl	0.12	0.12	0.12
Fe*	0.48	0.00	0.00
Mg	0.97	1.05	1.28
Na	0.28	0.27	0.26
SO_4	1.11	1.26	1.54
PH	7.41	7.53	7.48

Table 6.4b: PhreeqC modeling data for the evolution of groundwater within the Madison from Salamander Spring to the Upper Spring in Lower Kane Cave. This table compares the measured values (all data in mM except Fe, which is in µM) with the output of a reaction model and a forward model. The reaction model utilized the molar amounts from solution 2 above, while the forward model used the SI values from a PhreeqC speciation of Upper Spring sample KCW-J03-05 (Analysis #33 in Appendix B). See Appendix D for the input files for these models.

		Phase Mole Transfer:							Redox Transfer:	
Sal. (%)	PBS (%)	Dolomite	Calcite	Anhydrite	CH_2O	Goethite	Pyrite	Halite	Fe(3)	S(-2)
99.33	0.67	-	-	3.96E-4	4.09E-4	9.76E-5	-9.56E-5	4.64E-5	9.76E-5	-2.16E-4
99.33	0.67	-	-9.86E-5	4.64E-4	5.37E-4	1.32E-4	-1.30E-4	4.63E-5	1.32E-4	-2.84E-4
99.60	0.40	1.25E-5	-	3.70E-4	3.07E-4	7.03E-5	-6.83E-5	5.26E-5	7.03E-5	-1.62E-4
99.83	0.17	1.16E-4	-1.77E-4	3.03E-4	5.20E-5	1.96E-6	-	6.33E-5	1.96E-6	-2.57E-5
99.83	0.17	2.73E-5	-	2.57E-4	5.20E-5	1.96E-6	-	6.33E-5	1.96E-6	-2.57E-5
99.95	0.05	2.88E-5	-	2.70E-4	5.18E-5	-	-	6.45E-5	-	-2.59E-5

Table 6.5: Results of PhreeqC inverse modeling to produce Upper Spring water from a mixture of Salamander and PBS springs. All of the results are almost entirely Salamander water, with very minor contributions from the saline PBS spring. This is a geochemically unviable solution, as such a mixture would not contribute significant amounts of H_2S. Additionally, the Sr data shows that this mixture can definitely not account for the radiongeic Sr observed at Lower Kane Cave. The PhreeqC input file is given in Appendix D.

Sal.	Therm.	**Phase Mole Transfer**							**Redox Transfer**	
(%)	(%)	Dolomite	Calcite	Anhydrite	CH_2O	Goethite	Pyrite	Halite	Fe(3)	S(-2)
99.14	0.86	1.08E-04	-3.00E-04	4.52E-04	4.62E-04	1.11E-04	-1.10E-04	-	1.11E-04	-2.45E-04
99.14	0.86	3.29E-05	-	2.32E-04	4.98E-05	-	-	-	-	-2.49E-05
99.14	0.86	1.08E-04	-1.51E-04	2.75E-04	5.00E-05	9.62E-07	-	-	9.62E-07	-2.49E-05
99.14	0.86	1.08E-04	-1.50E-04	2.74E-04	4.98E-05	-	-	-	-	2.49E-05
99.14	0.86	1.44E-05	-	3.68E-04	3.04E-04	6.87E-05	-6.78E-05	-	6.87E-05	-1.60E-04
99.14	0.86	3.21E-05	-	2.32E-04	5.00E-05	9.62E-07	-	-	9.62E-07	-2.49E-05
94.95	5.05	-	-	1.39E-05	3.91E-05	9.53E-07	-	-3.19E-04	9.53E-07	-1.94E-05
94.94	5.06	-	-	1.38E-05	3.89E-05	-	-	-3.19E-04	-	-1.94E-05
94.85	**5.15**	**2.28E-04**	**-6.20E-05**	**1.62E-05**	**3.86E-05**	**-**	**-**	**-3.26E-04**	**-**	**-1.93E-05**
94.85	5.15	-	-6.82E-06	9.24E-06	3.86E-05	-	-	-3.26E-04	-	-1.93E-05
94.84	5.16	2.73E-05	-6.29E-05	1.54E-05	3.88E-05	9.53E-07	-	-3.27E-04	9.53E-07	-1.93E-05
94.84	5.16	-	-8.31E-06	8.41E-06	3.88E-05	9.53E-07	-	-3.27E-04	9.53E-07	-1.93E-05
94.69	5.31	-	-	-	3.84E-05	9.52E-07	-	-3.83E-04	9.52E-07	-1.91E-05
94.68	5.32	-	-	-	3.82E-05	-	-	-3.40E-04	-	-1.91E-05
94.68	5.32	-	-8.07E-06	-	3.84E-05	9.52E-07	-	-3.40E-04	9.52E-07	-1.91E-05
94.68	5.32	-	-6.56E-06	-	3.82E-05	-	-	-3.40E-04	-	-1.91E-05
94.67	5.33	2.41E-05	-5.47E-05	3.81E-05	-	-	-	-3.40E-04	-	-1.91E-05
94.46	5.34	2.39E-05	-5.59E-05	-	3.83E-05	9.52E-07	-3.41E-04	-	9.52E-07	-1.91E-05

Table 6.6: Results of a PhreeqC inverse model to derive Lower Kane Cave Upper Spring water from a mixture of Salamander and Thermopolis springs. The reaction model for this pathway utilized the solution in bold type. The PhreeqC input file is given in Appendix D.

	Measured	Reaction	Forward
HCO3	3.38	3.62	3.98
Ca	1.83	1.53	1.82
Cl	0.12	0.41	0.10
Fe*	0.48	0.00	0.00
Mg	0.97	1.19	1.18
Na	0.28	0.62	0.31
SO4	1.11	1.14	1.36
pH	7.41	7.48	7.45

Table 6.7: PhreeqC modeling of a mixture of Salamander and Thermopolis spring water to achieve the water chemistry of Upper Spring in Lower Kane Cave. This table compares the measured values (all data in mM except Fe, which is in µM) with the output of a reaction model and a forward model. The reaction model utilized the molar amounts from the bold solution in Table 7.5, while the forward model used SI values from a PhreeqC speciation of an Upper Spring sample (analysis # 33). See Appendix D for the input files for these models.

Inverse modeling of Salamander Spring as the representative Madison endmember at Lower Kane Cave suggests that groundwater rock interactions with anhydrite, calcite, dolomite and halite could account for the differences in the water chemistries between the two sites. These results, presented in Table 6.4a, agree with similar outcomes for Madison aquifer evolution in the work of Plummer et al. (1990). Forward and reaction models for this reaction pathway are presented in Table 6.4b, and produce very similar water chemistry to that actually measured at Upper Spring. As discussed in the earlier section on strontium isotope systematics, longer time periods for groundwater-rock interaction are expected to bring the waters closer to equilibrium with the $^{87}Sr/^{86}Sr$ of the host rock. Since the $^{87}Sr/^{86}Sr$ ratios observed in the waters of Lower Kane Cave (see Figure 5.3) clearly do not come from Madison carbonates and do not fit the greater Madison aquifer trend, these ratios demonstrate that at least some alternative source must provide the radiogenic Sr to the cave spring waters, and the Lower Kane Cave waters can not result simply from further evolution of groundwater within the Madison aquifer. However, understanding the chemical evolution of groundwater within the Madison is important, as the Sr mixing lines presented in Figure 6.11 suggest that the actual Madison endmember at Lower Kane Cave is likely more evolved than that at Salamander Spring. A line drawn on Figure 6.11 from the Thermopolis data through the cluster of data from Lower Kane Cave would produce a theoretical Madison aquifer water at approximately a $^{87}Sr/^{86}Sr$ ratio of 0.709 and [Sr] of 0.64ppm, well within the observed ranges for these parameters.

The results of geochemical inverse modeling of a mixture of Salamander Spring and PBS waters (Table 6.5) show that, while such a mixture could generate the observed chemistry, it would incorporate only very small amounts (<1%) of the water from PBS spring. While this satisfied the geochemical data,

the Sr isotope data presented above demonstrate that the $^{87}Sr/^{86}Sr$ ratio of the Phosphoria waters are in fact less radiogenic than Madison waters. Since the geochemical and geologic data strongly support a Madison source for the majority of the Lower Kane Cave spring water, PBS spring water is excluded as a potential endmember, as it does not provide radiogenic Sr. While we can not exclude the presence of a radiogenic, siliciclastic unit within the Pennsylvanian and Permian strata that overly the Madison aquifer, water from such a formation is highly unlikely to contain sufficient concentrations of the very radiogenic Sr necessary to generate the observed $^{87}Sr/^{86}Sr$ of Lower Kane Cave with a less than 1% contribution to the mixture. Therefore the available geochemical evidence, in conjunction with potentiometric surfaces that should move water vertically upward, suggest that the hypothesis presented by Doremus (1986) is incorrect, and water from these overlying formations is an unlikely contributor to the waters of Lower Kane Cave.

The available geochemical and Sr data suggest that the Thermopolis Hot Springs sample may represent a deep seated, saline, radiogenic endmember that, when mixed with Madison aquifer water, could produce the water chemistry observed at Lower Kane Cave. The results of mass balance models of this mixture, listed in Table 6.3, show a reasonable fit for most of the major ions.

The inverse model presented twenty-one possible solutions. Of these, three solutions incorporated 0% of the Thermopolis endmember. Results from the remaining solutions are presented in Table 6.6. These solutions incorporate between 0.9% and 5.3% of the Thermopolis endmember into the mixture, values that are in reasonable agreement with the results of a mixture based solely on Sr data. Additionally, mixing percentage based on Sr data utilizing the theoretical concentrated Madison water calculated above, with a [Sr] of 0.64 ppm and $^{87}Sr/^{86}Sr$ of 0.709, would require a mixture of 95.5% Madison and 4.5%

Thermopolis, in good agreement with the PhreeqC inverse model results. Results of forward modeling (using Upper Spring sample ID #34) and reaction modeling using the bolded model solution in Table 6.6 are in reasonable agreement with measured values. The results of these models are given in Table 6.7. Analysis of the results of PhreeqC modeling suggest that reduction of sulfate at hydrocarbon reservoirs, most likely bacterially mediated, provides a probable source of sulfide for the Lower Kane Cave springs.

Both the geochemical and Sr data suggest that the Thermopolis Hot Spring is a representative sample of a regional, deep-seated, saline and radiogenic endmember that is contributing water to the springs of Lower Kane Cave along the axial fracture system of Little Sheep Mountain, and that this endmember supplies both the radiogenic Sr and dissolved H_2S to the Lower Kane Cave springs.

7. CONCLUSIONS

The results of this study show that the Paleozoic aquifers have distinct chemical and Sr isotopic signatures. In general the $^{87}Sr/^{86}Sr$ ratios of Madison aquifer water are more radiogenic than the expected values for marine carbonates of the Mississippian. The water values are also more radiogenic than whole rock samples of the host Madison limestone, which fall within the expected range of $^{87}Sr/^{86}Sr$. Madison paleokarst ratios of $^{87}Sr/^{86}Sr$ are more radiogenic that that of the limestone, suggesting that siliciclastic components and diagenesis are probably responsible for the more radiogenic strontium of the aquifer groundwater.

The data presented here demonstrate that the same groundwater system is discharging at the three main Lower Kane Cave springs, and that the radiogenic Sr and dissolved H_2S both derive from a non-Madison source . A comparison of Sr data between Lower Kane Cave and Hellespont Cave suggest that similar mechanisms supply water to both these cave systems. However, geochemical differences between the caves, in particular the increase in TDS and decrease in temperature at Hellespont Cave relative to the Lower Kane Cave springs, suggest important differences between the two systems. Similar flow systems may also be operating to source the thermal sulfidic springs at Sheep Mountain and Thermopolis, the other Paleozoic anticlines in the Bighorn Basin breached by the Bighorn River. Salamander and PBS springs do not appear to be impacted by inter-formational mixing, and the characteristics of these samples fit with groundwater from the Madison and Pennsylvanian / Permian aquifers, respectively. Thus inter-formational mixing is not occurring to the same extent at all fracture zones within the breached anticline.

Sr isotope data demonstrate that the chemistry of the Lower Kane Cave waters can not result from progressive evolution of groundwater within the

Madison aquifer. Rather, the spring waters are most likely the result of a mixture of predominantly Madison water with that of a saline, thermal, sulfidic water source that contains radiogenic Sr, and provides the dissolved H_2S to the system. The data also show that the overlying Pennsylvanian and Permian aquifers are not the source of the non-Madison endmember to Lower Kane Cave, and thus the mixing model proposed by Doremus (1986) is incorrect. While an exact source for the H_2S, radiogenic Sr, and increased concentrations of major element and thermal character at Lower Kane Cave has not been identified, evidence from the Thermopolis Hot Springs in the southern Bighorn Basin coupled with the potentiometric and thermal gradients in the region of Lower Kane Cave suggests that such a source does exist, and is probably located in the lower portion of the Paleozoic section.

Temporal changes in the chemistry of the springs of Lower Kane Cave suggest that the percentage of the spring water derived from the non-Madison endmember has decreased over time. This variation in the groundwater source is likely the result of potentiometric surface changes caused by extensive extraction of hydrocarbons from oil fields in the area.

The data from this study illuminate important characteristics of the Paleozoic groundwater system in the Bighorn Basin, characteristics that are potentially useful for future water resource investigations in this area. These data suggest that upwelling of thermal, radiogenic waters is occurring along the extensional fracture zone of Little Sheep Mountain, and that similar mechanisms of groundwater flow may be in operation at the other breached anticlines within the Bighorn Basin. Therefore, understanding groundwater flow to Lower Kane Cave can help explain the groundwater system at the springs of Thermopolis Hot Springs State Park, and the structural controls that determine cave locations within breached anticlines.

Additionally, as oil field reservoirs in the Bighorn Basin produce from buried anticlines, insight from Lower Kane Cave into mechanisms of secondary porosity (i.e., cave) development and the role of fractured zones in groundwater flow may also increase our understanding of the basin's petroleum reservoir characteristics. Analysis of the groundwater system in this region may also illuminate groundwater flow in other areas of foreland compression.

APPENDIX A: Legal locations and notes on sampling locations

LEGAL LOCATION[a]	Sr SITE ID	SITE NAME	PRODUCING UNIT	NOTES
MADISON AQUIFER				
58-96-22bc	M1	Crosby Well	Madison Lm	Stock well.
58-96-34cd	M2	Cowley Mun. Well	Madison Lm	Municipal Water supply well.
55-94-17adb	M3	Salamander Spring	Madison Lm	Spring in Madison of Little Sheep Mountain
55-94-28bd	M4	GP Gypsum Plant	Madison Lm	
54-94-4ca	M5	Spence Oil Well #11	Madison Lm	Drilled 1957, 505'
54-94-4cd	M6	Spence Oil Well #12	Madison Lm	Drilled 1946, 550'. Owner believe leaking into casing from overlying units.
54-94-5dd	M7	Spence Oil Well #69	Madison Lm	Drilled 2001, 570'
54-94-9ac	M8	Spence Oil Well #74	Madison Lm	Drilled 2001, 558'
54-94-9ba	M9	Spence Oil Well #32	Madison Lm	Drilled 1976, 490'
54-94-9bb	M10	Spence Oil Well #56	Amsden Fm, Darwin Ss, Madison Lm,	Drilled 1984, 630', plug-back to 607'
54-94-35	M11*	Sheep Mtn	Madison Lm	Sampled one of the larger springs discharging at 20C. Egemeier lists mutliple springs in Sheep Mountain, split between high yiled springs at 20-21C and low yield springs at 34C
53-91-26	M12	Shell Well #2	Madison Lm	Municipal Water supply well. Drilled through Madison, 300' into Bighorn Dolomite. Bottom depth 3379ft, producing interval 2546-2940ft (394' section). Yield 1200gpm.
53-90-19bb	M13	Shell Well #3	Madison Lm, Bighorn Dm	Municipal Water supply well.
49-89-6bd	M14*	Hyattville City Well	Madison Lm	
see note	M15*	Worland City Well	Madison Lm	Water database lists 4 Worland Municipal wells:#1: 49-91-12NWSE; #2: 50-91-35SESE; #3: 49-91-1NWSW; #4: 49-90-18NWNW. Unclear which one was sampled

LEGAL LOCATION	Sr SITE ID		PRODUCING UNIT	NOTES
PENNSYLVANIAN / PERMIAN				
	P1	PBS	Phosphoria Lm	Spring discharges into Bighorn River from breakdown pile consisting of large pieces from the upper 100' limestone layer of the Phosphoria Lm.
55-95-3dca	P2	Clay Well	Tensleep Ss	
53-92-36ada	P3	Greybull Cemetary	Madison Lm, Tensleep Ss, Amsden Fm	Intended as a Madison well, improperly drilled so sources from Amsden, punching through into roughly top 100' of Madison Lm. Bottom depth 3250ft, producing from 2450-3250ft (800' section,) so main casing in Amsden Fm and Tensleep Ss
8S-28E-2 (Montana)	P4	Hillsboro Stream	Amsden Fm	Seepage zone in lower portion of the Amsden Fm, beneath the thick section of red shale. Spring discharges near the Hillsboro location in the Bighorn National Recreation Area.
see note	P5*	Tensleep Spring	Tensleep Ss	Map in Frost and Toner (in press) depicts Tensleep spring as located approximately 7 miles NE of the town of Hyattville
OTHER				
55-92-33cda	Flathead	Mayland-Leavitt Well	Flathead Ss	
43-94-31bcd	Thermopolis	Thermopolis	Paleozoic, undifferentiated	

LEGAL LOCATION	Sr SITE ID	SITE NAME	PRODUCING UNIT	NOTES
LOWER KANE AND HELLSPONT CAVES				
55-94-17adc	C1	Fissure Spring	Madison Lm	
"	C2	Upper Spring	Madison Lm	
"	C3	Lower Spring	Madison Lm	
55-94-17ada	C4	Hellspont	Madison Lm	
BIGHORN MOUNTAIN SAMPLES (unidentified sources)				
LOCATION	**SITE NAME**			
55-94-17adc	Bighorn River	Collected ~20cm from shore ~10m upstream of cave		
56-92-30ac	Five Springs Campground	Surface samples collected from stream though campground. Pump samples collected from hand pumps near parking area, which were allowed to flow for 5 minutes vefore collection.		
56-92-33	Overlook Spring	Sample collected from pipe just down hill from the overlook, parking area is entered from the west side, is on the SW side of 16A, and is marked as a "point of interest" on the Bighorn National Forest map.		
56-92-31bbb	Mountain Spring	Sample collected from pipe dishcarging to a surface spring near a dirt turn around. The road to the pipe turns south off os 16A very near the turnoff for the Five Springs Campground. The pipe runs uphill approximately 100m to where it taps the spring. A zone of seepage is apprent under the pipe. The location given is listed in the WRDS database as a Tensleep well, however, it is not certain that the pipe sampled is in fact this well.		
*	Madison Spring	Frost and Toner (2004)		
*	Snow	Frost and Toner (2004)		
*	Surface Flow	Frost and Toner (2004)		
*denotes sample collected by Frost and Toner (2004)				

a: Legal locations are based on Federal system of land subdivision. All locations have the format of three numbers potentially followed by up to three letters. The first number denotes the township, the second number denotes the range, and the third number denotes the section. The alphabetical designation denotes successive quarters of the section, which are lettered a, b, c and d in a counterclockwise manner starting with the northeast corner.

Appendix B: Goechemical analyses of Paleozoic water samples

#	LEGAL LOCATION	SAMPLE ID	SITE NAME	DATE	T(Wa) (C)	pH	ORP	DO (ppm)	Cond uS	TDS
MISSISSIPPIAN (Madison Aquifer)										
1	58-96-22bc	BHC-603-06	Crosby Well	6/11/2003	14.5	7.4	219	7.25	436	295
2	58-96-34cd	BHC-603-05	Cowley Mun. Well	6/10/2003	17.2	7.47	201	4.88	421	282
3	"	BHC-J02-012	Cowley Mun. Well	8/1/2002	17.2	7.38	240	-	408	281
4	55-94-17adb	KCW-A01-014	Salamander	8/2/2001	-	7.55	140	3.2	505	327
5	"	BHC-603-02	Salamander Spring	6/6/2003	17.2	7.59	195	3.31	483	325
6	"	BHC-J02-016	Salamander Spring	8/4/2002	17.4	7.52	195	-	466	322
7	55-94-28bd	BHC-J02-013	GP Gypsum Plant	8/1/2002	17.5	7.23	59	-	864	607
8	54-94-35*a	*d	Sheep Mtn	-	-	-	-	-	-	-
9	54-94-4ca	BHC-J02-007	Spence Oil #11	7/30/2002	-	-	-	-	865	609
10	54-94-4cd	BHC-J02-006	Spence Oil #12	7/30/2002	-	7.1	-	-	1204	859
11	54-94-5dd	BHC-J02-010	Spence Oil #69	7/30/2002	-	-	-	-	473	327
12	54-94-9ba	BHC-J02-008	Spence Oil #32	7/30/2002	-	-	-	-	687	478
13	54-94-9bb	BHC-J02-009	Spence Oil #56	7/30/2002	-	-	-	-	719	501
14	54-94-9ac	BHC-J02-005	Spence Oil #74	7/30/2002	-	-	-	-	492	341
15	53-91-26	BHC-603-12	Shell Well #2	6/12/2003	17.7	7.56	238	5.41	422	282
16	53-90-19bb	BHC-603-11	Shell Well #3	6/12/2003	15.4	7.57	219	4.38	463	313
17	49-89-6bd	*d	Hyattville City Well	-	-	-	-	-	-	-
18	*b	*d	Worland City Well	-	-	-	-	-	-	-
PENNSYLVANIAN / PERMIAN (Phosphoria, Tensleep, Amsden aquifers)										
19	55-94-9cc	BHC-J02-003	PBS	7/28/2002	13.2	7.17	-130	0.93	2233	1669
20	"	KCW-A01-015	PBS	8/2/2001	-	7.31	139	-	2441	1716
21	55-95-3dca	BHC-J02-015	Clay Well	8/3/2002	17.8	7.04	-56	-	3091	2375
22		BHC-603-04	Hillsboro Stream	6/9/2003	11.3	7.59	239	8.74	1159	811
23	53-92-36ada	BHC-603-13	Greybull Cemetary	6/12/2003	15.7	7.73	117	4.68	2548	1865
24	*c	*d	Tensleep Spring	-	-	-	-	-	-	-

#	F	Cl	HCO3	SO4	Na	K	Ca	Mg	CBE	SI				
	all major concentrations in ppm								(%)	Aragonite	Calcite	Dolomite	Anhydrite	Gypsum
MISSISSIPPIAN (Madison Aquifer)														
1	1.6	1	203	40	1	1	48	22	-0.8	-0.26	-0.11	-0.32	-2.35	-2.11
2	2.0	1	214	39	1	1	48	24	-0.4	-0.33	-0.18	-0.41	-2.37	-2.12
3	1.7	1	214	47	2	1	53	21	-1.6	-0.31	-0.15	-0.5	-2.25	-2
4	0.9	1	183	316	4	2	112	57	2.7	-0.31	-0.16	-0.36	-1.31	-1.06
5	0.4	1	239	55	4	2	53	24	-3.2	-	-	-	-	-
6	0.0	4	201	86	4	0	55	21	-6.3	-0.07	0.08	0.05	-1.99	-1.76
7	0.4	2	183	83	5	1	57	21	-0.9	-0.13	0.02	-0.16	-1.99	-1.75
8	0.5	2	202	81	4	1	63	25	2.7	-0.12	0.03	-0.09	-1.98	-1.73
9	0.6	3	237	43	4	1	51	23	-3.0	-	-	-	-	-
10	0.4	2	233	50	4	1	51	25	-1.8	-0.11	0.04	-0.02	-2.25	-2
11	2.3	10	369	204	21	18	99	43	-5.0	-	-	-	-	-
12	1.8	8	358	388	57	7	163	47	0.1	-	-	-	-	-
13	1.7	12	418	36	23	16	100	40	9.3	-	-	-	-	-
14	2.2	3	456	36	8	3	95	45	2.7	-	-	-	-	-
15	1.2	2	241	63	5	2	61	28	1.5	-	-	-	-	-
16	1.2	2	285	31	6	2	61	30	3.5	-	-	-	-	-
17	0.3	1	243	21	3	1	49	25	1.7	-0.07	0.07	0.1	-2.63	-2.39
18	0.2	1	228	13	3	1	39	22	-1.7	-	-	-	-	-
PENNSYLVANIAN / PERMIAN (Phosphoria, Tensleep, Amsden aquifers)														
19	0.8	33	241	1041	134	4	233	129	1.2	-0.17	-0.02	-0.1	-0.73	-0.48
20	0.0	48	238	1137	10	1	255	114	-14.2	0	0.15	0.13	-0.65	-0.4
21	0.0	12	169	1788	82	11	428	261	5.3	0.21	-0.07	-0.07	-0.41	-0.17
22	0.0	3	195	479	11	1	181	45	-1.6	0.14	0.3	0.15	-0.98	-0.73
23	2.6	9	62	1445	26	10	407	128	-0.9	0.03	0.18	0.08	-0.43	-0.18
24	0.2	1	280	11	3	2	56	20	-2.4	-	-	-	-	-

#	Si	Fe	Sr	Rb	U	Li	B	H2S	d18O
	ppm	ppm	ppm	ppb	ppb	ppb	ppb	ppm	
MISSISSIPPIAN (Madison Aquifer)									
1	3	0.00	0.22	1	12	5	22	-	-
2	4	0.00	0.23	1	5	4	20	-	-
3	4	0.00	0.22	1	5	4	10	0.0	-19.0
4	4	0.00	0.51	-	15	8	28	0.0	-19.6
5	4	0.00	0.50	1	16	9	523	-	-
6	4	0.01	0.49	1	17	7	21	-	-19.6
7	5	0.19	1.41	1	49	21	40	0.1	-19.9
8	-	-	-	-	-	-	-	-	-
9	4	0.01	2.51	16	0	130	95	14	-19.6
10	4	0.04	2.24	5	0	82	324	55	-19.7
11	4	0.02	0.78	2	21	14	33	4	-19.6
12	5	0.03	2.67	16	0	148	77	58	-19.7
13	5	0.02	3.09	3	0	23	42	22	-19.9
14	4	0.01	0.74	2	4	18	30	8	-19.3
15	4	0.00	0.46	1	3	8	25	-	-
16	4	0.00	0.47	1	2	7	21	-	-
17	-	-	-	-	-	-	-	-	-
18	-	-	-	-	-	-	-	-	-
PENNSYLVANIAN / PERMIAN (Phosphoria, Tensleep, Amsden aquifers)									
19	7	0.03	2.96	3	14	133	189	5	-18.5
20	6	0.01	1.84	-	12	97	168	0.6	-18.5
21	1	8.08	6.42	7	9	354	259	-	-21.8
22	6	0.00	2.20	1	4	18	91	-	-
23	4	0.16	8.34	7	53	161	246	-	-
24	-	-	-	-	-	-	-	-	-

#	LEGAL LOCATION	SAMPLE ID	SITE NAME	DATE	T(Wa) (C)	pH	ORP	DO (ppm)	Cond uS	TDS
OTHER AQUIFERS										
25	43-94-31bcd	BHC-J02-001	Thermopolis	7/24/2002	56 *i	-	-	-	-	-
26	55-92-33cda	BHC-603-03	Mayland-Leavitt Well	6/8/2003	31.2	8.58	-80	0.06	713	472
LOWER KANE CAVE										
27	55-94-17-adc	KCW-J03-08	Fissure Spring	6/14/2003	-	-	-	-	569	-
28	"	KCW-J02-006	"	8/4/2002	21.6	7.38	-86	-	561	387
29	"	KCW-D01-001	"	12/20/2001	19.9	7.19	-	0.6	611	-
30	"	KCW-A01-010	"	8/2/2001	22	7.3	-2	0	580	380
31	"	LKC-00-006	*g	8/14/2000	21.3	-	-	-	-	-
32	"	*e	*g	7/28/1970	23.5	6.8	-	0	695	-
33	"	KCW-J03-05	Upper Spring	6/12/2003	22.12	7.41	-278	0.05	562	-
34	"	KCW-J02-004	"	7/28/2002	21.9	7.42	-75	-	547	377
35	"	KCW-D01-002	"	12/20/2001	20.4	6.96	-	0.4	524	-
36	"	KCW-A01-001	"	7/28/2001	21.3	7.39	-80	0	577	379
37	"	KCW-01M-001	"	3/1/2001	21.9	7.36	-	1.4	-	0
38	"	LKC-00-007	"	8/15/2000	-	-	-	-	-	-
39	"	*e	"	7/3/1970	24	7	-	0	550	-
40	"	*e	"	7/3/1970	23.5	6.9	-	0	550	-
41	"	KCW-J03-12	Lower Spring	6/17/2003	21.5	7.23	-	-	562	377
42	"	KCW-J02-005	"	7/31/2002	21.7	7.26	-39	-	615	424
43	"	KCW-D01-005	"	12/20/2001	20.2	7.41	-151	0.1	539	-
44	"	KCW-A01-005	"	7/31/2001	22.1	7.22	-67	0	575	377
45	"	KCW-01M-005	"	3/1/2001	21.7	7.63	-	-	-	-
46	"	LKC-00-009	"	8/15/2000	22.8	6.94	-	2.7	-	-
47	"	*e	"	7/16/1970	23.5	7.25	-	0	*525*	-
48	"	*e	"	7/16/1970	23.5	7.1	-	0	*525*	-
49	"	*f	Lower Kane Cave*f	May-81	21	7.8	-	-	-	*478*

#	F	Cl	HCO3	SO4	Na	K	Ca	Mg	CBE	SI				
	all major concentrations in ppm								(%)	Aragonite	Calcite	Dolomite	Anhydrite	Gypsum
OTHER AQUIFERS														
25	3.4	247	622	568	191	39	301	66	0.3	-	-	-	-	-
26	1.9	22	154	146	146	3	7	1	3.3	0.02	0.16	-0.28	-2.6	-2.41
LOWER KANE CAVE														
27	0.9	4	201	116	7	2	76	24	1.1	-0.11	0.03	-0.11	-1.27	-1.54
28	0.9	4	201	110	7	2	83	30	8.5	-0.1	0.05	-0.05	-1.77	-1.54
29	1.5	6	224	166	8	-	72	26	-10.5	-0.35	-0.2	-0.56	-1.66	-1.42
30	0.5	4	209	115	6	0	68	23	-4.7	-0.24	-0.09	-0.34	-1.8	-1.57
31	1.1	5	214	156	7	2	89	27	-0.6	-	-	-	-	-
32	0.0	15	195	319	10	4	140	34	-1.0	-0.52	-0.38	-1.05	-1.2	-0.97
33	0.8	4	206	107	6	2	73	24	0.6	-0.1	0.05	-0.08	-1.81	-1.58
34	1.0	4	202	108	7	2	88	30	10.9	-0.03	0.12	0.07	-1.75	-1.52
35	1.0	5	212	143	6	-	76	26	-4.9	-0.56	-0.41	-1	-1.69	-1.45
36	0.6	5	211	110	6	0	70	23	-3.1	-0.14	0.01	-0.17	-1.81	-1.58
37	bdl	6	215	123	-	-	-	-	-	-	-	-	-	-
38	1.0	5	215	122	8	2	77	27	0.7	-	-	-	-	-
39	0.0	12	213	182	11	3	90	29	-2.4	-0.41	-0.27	-0.7	-1.54	-1.32
40	0.0	13	218	189	11	3	97	31	-0.5	-0.48	-0.34	-0.85	-1.51	-1.28
41	0.8	4	209	107	6	2	72	24	-0.4	-0.29	-0.14	-0.46	-1.82	-1.58
42	0.8	5	207	110	7	2	86	30	8.9	-0.19	-0.05	-0.24	-1.76	-1.52
43	1.2	7	215	144	5	-	73	25	-7.6	-0.13	0.02	-0.14	-1.7	-1.46
44	0.5	5	209	113	6	0	66	22	-5.8	-0.32	-0.18	-0.52	-1.82	-1.59
45	bdl	6	209	125	-	-	-	-	-	-0.51	-0.36	-0.87	-1.72	-1.49
46	0.9	5	213	124	7	2	82	28	3.2	-	-	-	-	-
47	0.0	13	218	195	11	3	96	32	-1.1	-0.14	0	-0.15	-1.5	-1.28
48	0.0	12	218	218	11	3	104	31	-2.1	-0.27	-0.12	-0.43	-1.43	-1.21
49	0.8	11	218	198	11	3	104	29	-0.8	-	-	-	-	-

#	Si	Fe	Sr	Rb	U	Li	B	H2S	d18O
	ppm	ppm	ppm	ppb	ppb	ppb	ppb	ppm	
OTHER AQUIFERS									
25	15	0.01	2.82	103	0	620	639	4.5	-18.7
26	6	0.00	0.12	3	0	52	167	0.1	-
LOWER KANE CAVE									
27	5	0.02	0.77	4	23	18	61	0.7	-
28	6	0.05	0.71	3	29	15	28	0.8	-19.8
29	5	0.01	-	-	26	18	572	-	-
30	5	0.03	0.74	-	24	16	39	0.4	-19.5
31	6	0.00	0.77	-	-	-	-	0.0	-19.8
32	17	0	1	-	-	-	-	5	-
33	4	0.00	0.72	4	24	14	35	-	-
34	5	0.03	0.71	3	26	18	30	0.9	-19.6
35	5	0.00	-	-	45	17	55	-	-
36	5	1.23	0.76	-	20	12	35	1.1	-19.5
37	-	-	-	-	-	-	-	0.7	-
38	6	0.01	0.75	-	-	-	-	0.6	-20.0
39	0	0	1	-	-	-	-	6	-
40	0	0	1	-	-	-	-	6	-
41	4	0.00	0.73	3	23	17	50	0.8	-
42	5	0.02	0.70	3	25	18	30	0.8	-19.7
43	5	0.00	-	-	33	17	461	-	.
44	5	0.02	0.75	-	23	16	40	0.5	-19.5
45	-	-	-	-	-	-	-	-	-
46	6	0.01	0.81	-	-	-	-	0.5	-20.0
47	0	0	1	-	-	-	-	5	-
48	0	0	1	-	-	-	-	5	-
49	-	-	-	-	-	-	-	-	-

#	LEGAL LOCATION	SAMPLE ID	SITE NAME	DATE	T(Wa) (C)	pH	ORP	DO (ppm)	Cond uS	TDS
HELLSPONT CAVE										
50	55-94-17-ada	BHC-J02-002	Hellspont	7/28/2002	19.1	7.38	-40	-	663	460
51	"	KCW-A01-013	"	8/2/2001	18.3	7.2	-13	-	718	472
52	"	LKC-00-012	"	8/15/2000	18.1	7.38	-	-	-	-
53	"	LKC-00-013	*h	8/15/2000	18.2	7.22	-	-	-	-
54	"	*e	"	8/4/1970	19.5	7.25	-	0	-	-
55	"	*e	*h	8/4/1970	19.5	7.1	-	0	-	-
BIGHORN MOUNTAIN SAMPLES (unidentified sources)										
56		BHC-603-01	Bighorn River	6/6/2003	16	8.36	176	8.49	785	553.6
57		BHC-J02-FS	Five Springs stream	8/7/2002	13	8.29	228		356	245.6
58		BHC-603-07	Mountain Spring	6/11/2003	9.3	7.65	243	8.74	618.6	425
59		BHC-603-08	Overlook Spring	6/11/2003	5.9	7.53	234	10	376.8	258.3
60		BHC-603-09	Five Springs pump	6/11/2003	6.8	7.75	220	8	351.5	240.2
61		BHC-603-10	Five Springs stream	6/11/2003	9	8.62	210		319.5	216
62		Frost & Toner (2004)	Madison Spring	-	-	-	-	-	-	-
63		Frost & Toner (2004)	Snow	-	-	-	-	-	-	-
64		Frost & Toner (2004)	Surface Flow	-	-	-	-	-	-	-

#	F	Cl	HCO3	SO4	Na	K	Ca	Mg	CBE	SI				
	all major concentrations in ppm								(%)	**Aragonite**	**Calcite**	**Dolomite**	**Anhydrite**	**Gypsum**
HELLSPONT CAVE														
50	1.3	9	214	161	9	3	90	32	1.6	-0.1	0.05	-0.08	-1.6	-1.36
51	0.7	9	212	181	9	0	81	28	-6.8	-0.34	-0.19	-0.59	-1.59	-1.34
52	0.9	12	212	188	10	3	92	32	-1.5	-0.12	0.03	-0.14	-1.54	-1.29
53	1.1	11	217	189	11	3	99	34	1.4	-0.24	-0.09	-0.39	-1.51	-1.27
54	0.0	19	236	275	15	4	122	32	-4.5	-0.1	0.05	-0.21	-1.3	-1.07
55	0.0	19	236	269	16	4	119	39	-1.4	-0.26	-0.11	-0.43	-1.33	-1.09
BIGHORN MOUNTAIN SAMPLES (unidentified sources)														
56	0	11	166	231	67	3	72	20	1.1	-	-	-	-	-
57	-	1	200	20	3	2	49	15	1.4	-	-	-	-	-
58	0	3	305	77	18	3	80	22	-1.3	-	-	-	-	-
59	0	1	230	17	1	2	66	11	1.1	-	-	-	-	-
60	0	2	210	16	4	2	52	14	1.9	-	-	-	-	-
61	0	1	203	9	2	1	54	10	0.8	-	-	-	-	-
62	0	0	115	3	2	1	21	9	-1.2	-	-	-	-	-
63	-	2	3	0	2	1	0	0	*14.1*	-	-	-	-	-
64	-	0	47	3	2	1	8	3	*-5.8*	-	-	-	-	-

#	Si	Fe	Sr	Rb	U	Li	B	H2S	d18O
	ppm	ppm	ppm	ppb	ppb	ppb	ppb	ppm	
HELLSPONT CAVE									
50	6	0.01	0.96	5	10	13	31	0.4	-19.6
51	5	0.01	1.04	-	8	30	58	1.2	-19.7
52	5	0.00	1.01	-	-	-	-	0.6	-20.1
53	5	0.00	1.10	-	-	-	-	1.2	-20.1
54	16	0	1	-	-	-	-	8	-
55	16	0	1	-	-	-	-	13	-
BIGHORN MOUNTAIN SAMPLES (unidentified sources)									
56	3.40	0.017	0.68789	1	7.09	37	111	-	-
57	2.084	0.003	0.093	0	0.459	6	47	-	-
58	3.14	0.001	0.26848	1	1.60	21	91	-	-
59	2.45	0.001	0.15256	1	0.68	8	46	-	-
60	2.58	0.004	0.1505	0	0.84	8	48	-	-
61	1.65	0.002	0.07253	0	0.31	4	29	-	-
62	-	-	-	-	-	-	-	-	-
63	-	-	-	-	-	-	-	-	-
64	-	-	-	-	-	-	-	-	-

a: Doremus (1986) lists 2 springs within Sheep Mountain at: 1) 54-94-35dbc and 2)54-94-35cdc.
b: The Wyoming Water database lists 4 Worland Municipal wells, located as folow: #1: 49-91-12NWSE; #2: 50-91-35SESE; #3: 49-91-1NWSW; #4: 49-90-18NWNW
c: Map in Frost and Toner (in press) shows the Tensleep spring located approximately 7 miles NE of the town of Hyattville
d: Sample from Frost and Toner (2004)
e: sample from Egemeier (1981)
f: sample from Doremus (1986). Location site for sample is not specified beyond Lower Kane Cave.
g: Sample take from Fissure Spring at time when it was not actively flowing, i.e. head level below lip of fracture opening.
h: Most samples at Hellspont are taken from the discharge point. Hellspont (spring) samples were taken at the actual spring in the cave.
i: Temperature of the spring was not measured in the field, this data point is taken from the park sign on site and the published values in Jarvis (1986), which are the same.

Appendix C: Strontium Analysis

#[a]	Site[b]	Location	[Sr][c]	$^{87}Sr/^{86}Sr$[d]	$^{87}Sr/^{86}Sr$[e]	$^{87}Sr/^{86}Sr$[f]	NBS
27	C1	Fissure Spring	0.77	0.710022	0.710018	0.710073	5
34	C2	Upper Spring	0.71	0.710028	0.710032	0.710035	3
33	"	Upper Spring	0.72	0.710051	0.710046	0.710102	5
37	"	Upper Spring	0.76	0.710124	(+/- .000018)		2
41	C3	Lower Spring	0.73	0.710009	0.710020	0.710009	4
45	"	Lower Spring	"	0.710108	(+/- .000008)		2
50	C4	Hellspont	0.96	0.710154	0.710157	0.710161	3
1	M1	Crosby Well	0.22	0.708907	0.708910	0.708907	4
1*	"	Crosby Well	"	0.708938	0.708936	0.708989	5
2	M2	Cowley Muni. Well	0.23	0.708940	0.708941	0.708940	4
2*	"	Cowley Muni. Well	"	0.708890	0.708900	0.708923	6
3	"	Cowley Muni. Well	0.22	0.708945	0.708954	0.708952	3
5	M3	Salamander Spring	0.50	0.709253	0.709256	0.709253	4
6	"	Salamander Spring	0.49	0.709241	0.709239	0.709248	3
7	M4	GP Gypsum Plant	1.41	0.708559	0.708577	0.708566	3
10	M5	Spence OIl Well #12	2.24	0.708404	0.708410	0.708411	3
14	M6	Spence OIl Well #74	0.74	0.709002	0.709008	0.709009	3
8	M7	Sheep Mtn Spring	0.87	0.709260	-	-	1
15	M8	Shell Well #2	0.46	0.709039	0.709041	0.709090	5
16	M9	Shell Well #3	0.47	0.708997	0.709004	0.709048	5
17	M10	Hyattville Municipal	0.495	0.708730	-	-	1
18	M11	Worland Municipal	0.284	0.709410	-	-	1
19	P1	PBS	2.96	0.708246	0.708255	0.708253	3
21	P2	Clay Well	6.42	0.708474	0.708480	0.708481	3
23	P3	Greybull Cemetary	8.34	0.708528	0.708533	0.708561	6
22	P4	Hillsboro Stream	2.20	0.707889	0.707891	0.707889	4
24	P5	Spring	0.42	0.712200	-	-	1
26	*Flathead*	*Mayland-Leavitt Well*	*0.12*	0.715972	0.715998	0.716006	6
*26**	*"*	*Mayland-Leavitt Well*	*"*	0.715987	0.715986	0.716039	5
25	Therm.	Thermopolis	2.82	0.715581	0.715589	0.715588	3
56	-	Bighorn River	0.69	0.709933	0.709933	0.709984	5
57	-	*Five Springs stream*	*0.09*	0.713041	0.713055	0.713048	*3*
58	-	Mountain Spring	0.27	0.713132	0.713144	0.713184	5
58*	-	Mountain Spring	"	0.713179	0.713185	0.713231	5
*59**	-	*Overlook Spring*	*0.15*	0.713583	0.713601	0.713616	*6*
*60**	-	*Five Springs pump*	*0.15*	0.714413	0.714424	0.714447	*6*
61	-	*Five Springs stream*	*0.07*	0.712582	0.712575	0.712634	*5*
*61**	-	*Five Springs stream*	*"*	0.712544	0.712559	0.712577	*6*
Rock	Phosphoria Lm (outcrop above PBS)		-	0.707220	-	-	7
Rock	Madison Lm (LKC)		-	0.708040	-	-	7
Rock	Madison Lm (Salamander)		-	0.707970	-	-	7

NBS STANDARDS		
1	Samples from Frost and Toner (2004)	
2	Run prior to this study on the UT-Austin TIMS	
3	3/28/2003	0.710243
4	7/28/2003	0.710250
5	8/22/2003	0.710199
6	8/25/2003	0.710217
7	-	-

a - Analysis ID# from Appendix B

b - Sr site ID

c - concentration in ppm

d - Rb corrected values

e - no Rb correction

f - ratios normalized to an NBS of 0.710250

* - denotes an unfiltered sample.

Notes: The highest blanks measured were 570 pg/ml for run #3 and 210 pg/ml for runs #4-6. Italicized samples contain concentrations of Sr that are less than 10X the Sr concentrations in the blank for that assessment, therefore the 87Sr/86Sr ratios may be impacted by signal from the blank.

Appendix D: PhreeqC Input Files

```
TITLE 1: Reaction of Upper Spring
water with Gypsum
-- Step 1 to SI -1.4
SOLUTION 1 Upper Spring (KCW-J03-05)
      units   mmol/kgw
      temp    25
      pH      7.41
      redox   S(6)/S(-2)
      Ca      1.821
      Mg      0.987
      Na      0.261
      Fe(2)   0.002
      Cl      0.121
      S(6)    1.114
      S(-2)   0.026
      C(4)    3.377
EQUILIBRIUM_PHASES
            Gypsum          -1.4
            Calcite   0
SAVE Solution 2
END
TITLE 2: Step 2 -- to SI of -1.2
USE Solution 2
EQUILIBRIUM_PHASES 1
            Gypsum          -1.2
            Calcite   0
SAVE Solution 3
END
TITLE 3: Step 3 -- to SI of -1.0
USE Solution 3
EQUILIBRIUM_PHASES 2
            Gypsum          -1.0
            Calcite   0
SAVE Solution 4
END
TITLE 4: Step 4 -- to SI of -0.8
USE Solution 2
EQUILIBRIUM_PHASES 3
            Gypsum          -0.8
            Calcite   0
SAVE Solution 5
END
TITLE 5: Step 5 -- to SI of -0.6
USE Solution 5
EQUILIBRIUM_PHASES 4
            Gypsum          -0.6
            Calcite   0
SAVE Solution 6
END
TITLE 6: Step 6 -- to SI of -0.4
USE Solution 6
EQUILIBRIUM_PHASES 5
            Gypsum          -0.4
            Calcite   0
SAVE Solution 7
END
TITLE 7: Step 7 -- to SI of -0.2
USE Solution 7
EQUILIBRIUM_PHASES 6
            Gypsum          -0.2
            Calcite   0
SAVE Solution 8
END
```

TITLE Inverse Model – Salamander spring to Upper spring (evolution within the Madison)

```
SOLUTION 1 Salamander Spring (BHC-603-02)
      units   mmol/kgw
      temp          17.2
      pe            0
      pH            7.59
      Ca            1.415
      Mg            0.863
      Na            0.20
      Fe(2)         3.58e-5
      Cl            5.64e-2
      S(6)          0.864
      S(-2)         0
      Alkalinity    2.994 as HCO3
SOLUTION 2 Upper Spring (KCW-J02-04)
      units   mmol/kgw
      temp          21.9
      pH            7.42
      pe            0
      redox         S(6)/S(-2)
      Ca            1.836
      Mg            1.111
      Na            0.259
      Fe(2)         4.835e-4
      Cl            0.124
      S(6)          1.124
      S(-2)         0.026
      Alkalinity    3.311  as HCO3
INVERSE_MODELING 1
      -solutions 1 2
      -uncertainty 0.1
      -range
      -balances
            Fe(2)   1.0
            Cl       0.2
            ph       0.1
      -phases
            Dolomite       dis
            Calcite
            Anhydrite
            CH2O
            Goethite
            Pyrite          pre
            Halite
PHASES
  CH2O
      CH2O + H2O = CO2 + 4H+ + 4e-
      -log_k  0.0
END
```

TITLE Forward Modeling of Salamander Spring to Upper Spring

```
SOLUTION 1 Salamander Spring (BHC-603-02)
      units   mmol/kgw
      temp    17.2
      pH      7.59
      Ca      1.415
      Mg      0.863
      Na      0.20
      Fe(2)   3.58e-5
      Cl      0.056
      S(6)    0.864
      S(-2)   0
      Alkalinity    2.994 as HCO3
EQUILIBRIUM_PHASES
          Dolomite          0.03
          Anhydrite         -1.80
          Calcite           0.08
          Halite            -9.17
          CH2O              -17.47
PHASES
  CH2O
      CH2O + H2O = CO2 + 4H+ + 4e-
      -log_k  0.0
END
```

TITLE Reaction Modeling of Salamder Spring to Upper Spring based on the results of Inverse Modeling

```
SOLUTION 1 Salamander Spring (BHC-603-02)
      units   mmol/kgw
      temp    17.2
      pH      7.59
      Ca      1.415
      Mg      0.863
      Na      0.20
      Fe(2)   3.58e-5
      Cl      0.056
      S(6)    0.864
      S(-2)   0
      Alkalinity    2.994 as HCO3
EQUILIBRIUM_PHASES
          Dolomite  0.00     1.88e-4
          Calcite     0.00     -3.60e-4
          Anhydrite 0.00     3.98e-4
          CH2O        0.00     5.20e-5
          Halite        0.00     6.76e-5
PHASES
  CH2O
      CH2O + H2O = CO2 + 4H+ + 4e-
      -log_k  0.0
END
```

TITLE Inverse Model – Upper Spring derived from a mixture of Salamander and PBS springs.

```
SOLUTION 1 Salamander Spring (BHC-603-02)
    units   mmol/l
    temp        17.2
    pH      7.59
    Ca      1.415
    Mg      0.863
    Na      0.20
    Fe(2)   3.58e-5
    Cl      0.056
    S(6)    0.864
    S(-2)   0
    Alkalinity   2.994
SOLUTION 2 PBS Spring (BHC-J02-
    units   mg/l
    temp        13.2
    pH      7.17
    Ca      233
    Mg      129
    Na      134
    Fe(2)   0.028
    Cl      33.3
    S(6)    1041
    S(-2)   5
    Alkalinity   241 as HCO3
SOLUTION 3 Upper Spring (KCW-J03-05)
    units   mmol/kgw
    temp    25
    pH      7.41
    redox   S(6)/S(-2)
    Ca      1.821
    Mg      0.987
    Na      0.261
    Fe(2)   0.002
    Cl      0.121
    S(6)    1.114
    S(-2)   0.026
    Alkalinity    3.377 as HCO3
INVERSE_MODELING 1
    -solutions 1 2 3
    -uncertainty 0.05
    -range
    -balances
        Fe(2)   1.0
                        Cl      0.1
        ph      0.1
    -phases
        Dolomite    dis
        Calcite     pre
        Anhydrite   dis
                CH2O
                Goethite
        Pyrite      pre
        Halite
PHASES
   CH2O
    CH2O + H2O = CO2 + 4H+ + 4e-
    -log_k  0.0
END
```

TITLE Inverse Model -- Upper Spring derived from an original mixture of Salamander Spring and Thermopolis Spring waters

```
SOLUTION 1 Salamander Spring (BHC-603-02)
    units   mmol/l
    temp    17.2
    pH      7.59
    Ca      1.415
    Mg      0.863
    Na      0.20
    Fe(2)   3.58e-5
    Cl      0.056
    S(6)    0.864
    S(-2)   0
    Alkalinity   2.994 as HCO3
SOLUTION 2 Upper Spring (KCW-J03-05)
    units   mmol/kgw
    temp    25
    pH      7.41
    redox   S(6)/S(-2)
    Ca      1.821
    Mg      0.987
    Na      0.261
    Fe(2)   0.001
    Cl      0.121
    S(6)    1.114
    S(-2)   0.026
    Alkalinity    3.377   as HCO3
SOLUTION 3      Thermopolis (BHC-J02-01)
    units   mmol/kgw
    temp            57
    pH      7.0
    Ca      7.515
    Mg      2.731
    Na      8.316
    Fe(2)   2.58e-4
    Cl      6.959
    S(6)    5.913
    S(-2)   0.13
    Alkalinity   9.933 as HCO3
INVERSE_MODELING 1
    -solutions 1 3 2
    -uncertainty 0.05
    -range
    -balances
        Fe(2)   1.0
                                Cl          0.1
        ph      0.1
    -phases
        Dolomite        dis
        Calcite
        Anhydrite
                CH2O
                Goethite
        Pyrite          pre
        Halite
PHASES
    CH2O
      CH2O + H2O = CO2 + 4H+ + 4e-
      -log_k  0.0
END
```

```
TITLE Forward Modeling of Salamder and Thermopolis springs mixture to Upper Spring
SOLUTION 1 Salamander Spring (BHC-603-02)
      units   mmol/l
      temp          17.2
      pH     7.59
      Ca     1.415
      Mg     0.863
      Na     0.20
      Fe(2)   3.58e-5
      Cl     0.056
      S(6)    0.864
      Alkalinity   2.994
SOLUTION 2     Thermopolis (BHC-J02-01)
      units   mmol/kgw
      temp          57
      pH     7.0
      Ca     7.515
      Mg     2.731
      Na     8.316
      Fe(2)   2.58e-4
      Cl     6.959
      S(6)    5.913
      Alkalinity   9.933
MIX 1
          1          .9485
          2          .0515
SAVE SOLUTION 3
END
USE SOLUTION 3
EQUILIBRIUM_PHASES
          Dolomite          0.03
          Anhydrite         -1.80
          Calcite            0.08
          CH2O              -17.47
          Halite            -9.17
PHASES
    CH2O
      CH2O + H2O = CO2 + 4H+ + 4e-
      -log_k  0.0
END
```

```
TITLE Reaction Modeling of Salamder and Thermopolis springs mixture to Upper Spring
SOLUTION 1 Salamander Spring (BHC-603-02)
      units   mmol/l
      temp          17.2
      pH      7.59
      Ca      1.415
      Mg      0.863
      Na      0.20
      Fe(2)   3.58e-5
      Cl      0.056
      S(6)    0.864
      Alkalinity   2.994
SOLUTION 2      Thermopolis (BHC-J02-01)
      units   mmol/kgw
      temp          57
      pH      7.0
      Ca      7.515
      Mg      2.731
      Na      8.316
      Fe(2)   2.58e-4
      Cl      6.959
      S(6)    5.913
      Alkalinity   9.933
MIX 1
          1          .9485
          2          .0515
SAVE SOLUTION 3
END
USE SOLUTION 3
EQUILIBRIUM_PHASES
          Dolomite          0.00              2.28e-4
          Calcite           0.00             -6.20e-5
          Anhydrite         0.00              1.62e-5
          CH2O              0.00              3.86e-5
          Halite            0.00             -3.26e-4
PHASES
  CH2O
      CH2O + H2O = CO2 + 4H+ + 4e-
      -log_k  0.0
END
```

REFERENCES

Agatston, R. S. (1954). Pennsylvanian and Lower Permian of Northern and Eastern Wyoming. AAPG Bulletin 38(4): 508-583.

Armstrong, S. C. and N. C. Sturchio (1997). Strontium Isotopic Evidence on the Chemical Evolution of Pore Waters in the Milk River Aquifer, Alberta, Canada. Applied Geochemistry 13(4): 463-475.

Banner, J. L. and M. Musgrove (1994). Tracing Ground-Water Evolution in a Limestone Aquifer Using Sr Isotopes: Effects of Multiple Sources of Dissolved Ions and Mineral-Solution Reactions. Geology 22: 687-690.

Banner, J. L., G. J. Wasserburg, P. F. Dobson, A. B. Carpenter and C. H. Moore (1989). Isotopic and Trace Element Constraints on the Origin and Evolution of Saline Groundwaters from Central Missouri. Geochimica et Cosmochimica Acta 53: 383-398.

Boyd, D. W. (1993). Paleozoic History of Wyoming. Geology of Wyoming: Geological Survey of Wyoming Memoir No. 5. A. W. Snoke, J. R. Steidtmann and S. M. Roberts: 164-187.

Bredehoeft, J. D., K. Belitz and S. Sharp-Hansen (1992). "The Hydrodynamics of the Big Horn Basin: A Study of the Role of Faults." AAPG Bulletin 76(4): 530-546.

Busby, J. F., L. N. Plummer, R. W. Lee and B. B. Hanshaw (1991). Geochemical Evolution of Water in the Madison Aquifer in Parts of Montana, South Dakota, and Wyoming. Washington, U.S. Geological Survey: 89.

Chaudhuri, S. (1969). The Isotopic Age of the Flathead Sandstone (Middle Cambrian), Montana. Journal of Sedimentary Petrology 39(1): 364-366.

Chaudhuri, S., V. Broedel and N. Clauer (1987). Strontium Isotopic Evolution of Oil-Field Waters from Carbonate Reservoir Rocks in Bindley Field, Central Kansas, USA. Geochimica et Cosmochimica Acta 51: 45-53.

Cooley, M. E. (1986). Artesian Pressures and Water Quality in Paleozoic Aquifers in the Ten Sleep Area of the Bighorn Basin, North-Central Wyoming. Reston, VA, U.S. Geological Survey: 54.

Crawford, J. G. (1940). Oil-Field Waters of Wyoming and Their Relation to Geological Formations. AAPG Bulletin 24(7): 1214-1329.

Crawford, J. G. (1964). Rocky Mountain Oil-Field Water, Geological Survey of Wyoming.

Dogramaci, S. S. and A. L. Herczeg (2002). Strontium and Carbon Isotope Constraints on Carbonate-Solution Interactions and Inter-Aquifer Mixing in Groundwaters of the Semi-Arid Murray Basin, Australia. Journal of Hydrology 262: 50-67.

Doremus, D. (1986). Groundwater Circulation and Water Quality Associated with the Madison Aquifer in the Northeastern Bighorn Basin, Wyoming. Department of Geology and Geophysics. Laramie, Univeristy of Washington: 81.

Egemeier, S. J. (1973). Cavern Development by Thermal Waters with a Possible Bearing on Ore Deposition, Stanford University: 88.

Egemeier, S. J. (1981). Cavern Development by Thermal Waters. National Speleological Society Bulletin 43: 31-51.

Engel, A. S., N. Lee, M. L. Porter, L. A. Stern, P. C. Bennet and M. Wagner (2003). Filamentous ‘Epsilonproteobacteria' Dominate Microbial Mats from Sulfidic Cave Springs. Applied and Environmental Microbiology 69(9): 5503-5511.

Engel A. S., L. A. Stern and P. C. Bennett (2004). Microbial Contributions to Cave Formation: New Insight into Sulfuric Acid Speleogenesis. Geology 32(5): 269-273.

Faure, G. (1998). Principles of Isotope Geology. New York, John Wiley & Sons: 589.

Frost, C. D. and B. R. Frost (1993). The Archaen History of the Wyoming Province. Geology of Wyoming. A. W. Snoke, Steidtmann, J.R., Roberts, A.M. Cheyenne, WY: 58-77.

Frost, C. D., B. N. Pearson, K. M. Ogle, E. L. Heffern and R. M. Lyman (2002). Sr Isotope Tracing of Aquifer Interactions in an Area of Accelerating Coal-Bed Methane Production, Powder River Basin, Wyoming. Geology 30(10): 923-926.

Frost, C. D. and R. N. Toner (2004). Strontium Isotopic Identification of Water-Rock Interaction and Ground Water Mixing. Ground Water 42(3): 418-432.

Henley, R. W., A. H. Truesdell, P. B. Barton, Jr. and J. A. Whitney (1984). Fluid-Mineral Equilibria in Hydrothermal Systems. In Reviews in Economic Geology, J. M. Robertson Ed. 1: 267.

Hennier, J. and J. H. Spang (1983). Mechanisms for Deformation of Sedimentary Strata at Sheep Mountain Anticline, Bighorn Basin, Wyoming. Thirty-Fourth Annual Field Conference 34: 96-111.

Hogan, J. F., J. D. Blum, D. I. Siegel and P. H. Glaser (2000). 87Sr/86Sr as a Tracer of Groundwater Discharge and Precipitation Recharge in the Glacial Lake Agassiz Peatlands, Northern Minnesota. Water Resources Research 36(12): 3701-3710.

Huntoon, P. W. (1985). Fault Severed Aquifers Along the Perimeters of Wyoming Artesian Basins. Ground Water 23(2): 176-181.

Huntoon, P. W. (1993). The Influence of Laramide Foreland Structures on Modern Ground-Water Circulation in Wyoming Artesian Basins. Geology of Wyoming: Geological Survey of Wyoming Memoir No. 5. A. W. Snoke, J. R. Steidtmann and S. M. Roberts: 756-789.

Jarvis, W. T. (1986). Regional Hydrogeology of the Paleozoic Aquifer System, Southeastern Bighorn Basin, Wyoming, with an Impact Analysis on Hot Springs State Park. Geology and Geophysics. Laramie, The University of Wyoming: 224.

Jastram, B. C. (1999). Structural Geology of the Sheep Mountain and Little Sheep Mountain Region, Bighorn Basin, Wyoming: Implications toward Hydrocarbon Occurences. Geology. Lafayette, The University of Louisiana at Lafayette: 100.

Katz, B. G. and T. D. Bullen (1996). The Combined Use of 87Sr/86Sr and Carbon and Water Isotopes to Study the Hydrochemical Interaction Between Groundwater and Lakewater in Mantled Karst. Geochimica et Cosmochimica Acta 60(24): 5075-5087.

Land, M., J. Ingri, P. S. Andersson and B. Ohlander (2000). Ba/Sr, Ca/Sr and 87Sr/86Sr Ratios in Soil Water and Groundwater: Implications for Relative Contributions to Stream Water Discharge. Applied Geochemistry 15: 311-325.

Lawson, D. E. and J. R. Smith (1966). Pennsylvnian and Permian Influence on Tensleep Oil Accumulation, Big Horn Basin, Wyoming. AAPG Bulletin 50(10): 2197-2220.

Libra, R., D. Doremus and C. Goodwin (1981). Occurence and Characteristics of Ground Water in the Bighorn Basin, Wyoming, Water Resources Research Institute, University of Wyoming.

Lowry, M. E. and G. C. Lines (1972). Chemical Analyses of Ground Water in the Bighorn Basin, Northwestern Wyoming, USGS, Water Resources Division: 16.

Montanez, I. P. and J. L. Banner (2000). Evolution of Sr and C Isotope Composition of Cambrian Oceans. GSA Today 10(5): 1-7.

Nickens, D., C. J. Fry, L. Ragatz, C. E. Bauer and H. Gest (1996). Biotype of the Purple Nonsulfur Photosynthetic Bacterium, Rhodospirillum. Archives of Microbiology 165(2): 91-96.

Parkhurst, D. L., and C. A. J. Appelo (1999). User's Guide to PHREEQC (Version 2): A Computer Program for Speciation, Batch-Reaction, One-Dimensional Transport, and Inverse Geochemical Calculations. U.S.G.S. Water-Resources Investigations Report 99-4259, p.312.

Picard, M. D. (1993). The Early Mesozoic History of Wyoming. Geology of Wyoming. A. W. Snoke, Steidtmann, J.R., Roberts, A.M. Cheyenne, WY: 210-249.

Plummer, L. N., J. F. Busby, R. W. Lee and B. B. Hanshaw (1990). Geochemical Modeling of the Madison Aquifer in Parts of Montana, Wyoming, and South Dakota. Water Resources Research 26(9): 1981-2014.

Rioux, R. L. (1958). Geology of the Spence-Kane Area, Big Horn County, Wyoming. Geology. Urbana, The University of Illinois: 182.

Rose, P. R. (1976). Mississippian Carbonate Shelf Margins, Western United States. Jour. Research U.S. Geol. Survey 4(4): 449-466.

Sando, W. J. (1976). Mississippian History of the Northern Rocky Mountains Region. Jour. Research U.S. Geol. Survey 4(3): 317-338.

Sando, W. J. (1988). Madison Limestone (Mississippian) Paleokarst: A Geologic Synthesis. Paleokarst. N. P. James and P. W. Choquette: 256-277.

Snoke, A. W. (1993). Geologic History of Wyoming within the Tectonic Framework of the North American Cordillera. Geology of Wyoming: Geological Survey of Wyoming Memoir No. 5. A. W. Snoke, J. R. Steidtmann and S. M. Roberts: 2-56.

Spencer, S. A. (1986). Groundwater Movement in the Paleozoic Rocks and Impact of Petroleum Production on Water Levels in the Southwestern Bighorn Basin, Wyoming. Geology and Geophysics. Laramie, WY, The University of Wyoming: 116.

Stone, D. S. (1967). Theory of Paleozoic Oil and Gas Accumulation in Big Horn Basin, Wyoming. AAPG Bulletin 51(10): 2056-2114.

Thomas, L. E. (1965). Sedimentation and Structural Development of Big Horn Basin. AAPG Bulletin 49(11): 1867-1877.

Toner, R. N. (2000). Sr and Pb Isotopic Investigations of Aquifer Systems in the Laramie and Bighorn Basins, Wyoming. Geology and Geophysics. Laramie, WY, The University of Wyoming: 141.

Western Water Consultants, I. and W. W. D. Commission (1982). Ground Water Development Feasibility Study, Town of Cowley. Laramie, WY.

Zelt, R. B., G. Boughton, K. A. Miller, J. P. Mason and L. M. Gianakos (1999). Environmental Setting of the Yellowstone River Basin, Montana, North Dakota, and Wyoming. Cheyenne, U.S. Department of the Interior. U.S. Geological Survey: 113.

The vita has been removed from the reformatted version of this document.